

Report Title: Novel Corrosion Sensor for Vision 21 Systems

Report Type: Technical Progress Report (Final)

Reporting Period Start Date: August 1, 2003

Reporting Period End Date: March 31, 2007

Principal Author: Heng Ban (Associate Professor)
Bharat Soni (Professor)

Date Report was Issued: April 2007

DOE Award Number: DE-FC26-03NT41807

Name and Address of Submitting Organization: University of Alabama at Birmingham
Department of Mechanical Engineering
1150 10th Avenue South
Birmingham, AL 35294-4461

DISCLAIMER

This report was prepared as an account of work sponsored by an agency of the United States Government. Neither the United States Government nor any agency thereof, nor any of their employees, makes any warranty, express or implied, or assumes any legal liability or responsibility for the accuracy, completeness, or usefulness of any information, apparatus, product, or process disclosed, or represents that its use would not infringe privately owned rights. Reference herein to any specific commercial product, process, or service by trade name, trademark, manufacturer, or otherwise does not necessarily constitute or imply its endorsement, recommendation, or favoring by the United States Government or any agency thereof. The views and opinions of authors expressed herein do not necessarily state or reflect those of the United States Government or any agency thereof.

ABSTRACT

Advanced sensor technology is identified as a key component for advanced power systems for future energy plants that would have virtually no environmental impact. This project intends to develop a novel high temperature corrosion sensor and subsequent measurement system for advanced power systems. Fireside corrosion is the leading mechanism for boiler tube failures and has emerged to be a significant concern for current and future energy plants due to the introduction of technologies targeting emissions reduction, efficiency improvement, or fuel/oxidant flexibility. Corrosion damage can lead to catastrophic equipment failure, explosions, and forced outages. Proper management of corrosion requires real-time indication of corrosion rate. However, short-term, on-line corrosion monitoring systems for fireside corrosion remain a technical challenge to date due to the extremely harsh combustion environment.

The overall goal of this project is to develop a technology for on-line fireside corrosion monitoring. This objective is achieved by the laboratory development of sensors and instrumentation, testing them in a laboratory muffle furnace, and eventually testing the system in a coal-fired furnace. This project successfully developed two types of sensors and measurement systems, and successfully tested them in a muffle furnace in the laboratory. The capacitance sensor had a high fabrication cost and might be more appropriate in other applications. The low-cost resistance sensor was tested in a power plant burning eastern bituminous coals. The results show that the fireside corrosion measurement system can be used to determine the corrosion rate at waterwall and superheater locations. Electron microscope analysis of the corroded sensor surface provided detailed picture of the corrosion process.

TABLE OF CONTENTS

DISCLAIMER	iii
ABSTRACT	iv
TABLE OF CONTENTS	v
LIST OF TABLES	vii
LIST OF FIGURES	viii
INTRODUCTION	2
Background and Significance	2
Current Knowledge and Technology	3
The Capacitance Sensor	4
Technical Issues and Challenges	5
Anticipated Benefits	6
Research Objectives and Scope	7
EXECUTIVE SUMMARY	8
EXPERIMENTAL	10
Sensor Principle	10
Sensor Design	11
<i>Substrate Material Selection</i>	11
Sensor Fabrication	13
<i>Sputtering Deposition Technology for Sensor Fabrication</i>	13
<i>Plasma Spray Technology for Sensor Fabrication</i>	14
Probe Design	14
Probe Temperature Control and Data Acquisition	15
Plant Measurement	15
RESULTS AND DISCUSSION	17
Laboratory Development and Testing	17
Plant Measurement Results	19
<i>Superheater Corrosion</i>	19
<i>Waterwall Corrosion</i>	20
Waterwall and Superheater Surface Temperature Estimation	22
Measurement Uncertainty Estimation	23
Corrosion Rate Change with Exposure Time	24
SEM Analysis and Metrology Calibration	24

CONCLUSIONS	26
REFERENCES	27
FIGURES	30

LIST OF TABLES

<u>Table</u>	<u>Page</u>
Table 1 Properties for BeO and Alumina (99.6 % Al ₂ O ₃)	11
Table 2 Chemical composition of the low carbon steel for coupon (%).	12
Table 3. Corrosion rate summary.....	21

LIST OF FIGURES

<u>Figure</u>	<u>Page</u>
Figure 1. A schematic diagram of capacitance sensor principle.....	30
Figure 2. A schematic diagram of equal potential lines for resistance sensor.....	31
Figure 3. Resistance change with metal thickness reduction.....	31
Figure 4. Thermal conductivity of BeO, Alumina (99.6%Al ₂ O ₃) and AlN.....	32
Figure 5. Design drawings of the the capacitance sensor.	32
Figure 6. A picture of the DC magnetron sputtering deposition system.	33
Figure 7. A schematic diagram for the laboratory experimental setup.....	33
Figure 8. Temperature control system for the probe.....	34
Figure 9. A pictures of wedged iron coating on the capacitance sensor.....	34
Figure 10. Resistance sensors (bottom) and sensor assembly (top).....	34
Figure 11. Temperature control system for the probe.....	35
Figure 12. Complete measurement system layout in the laboratory.....	35
Figure 13. Assembly drawing of the probe.....	36
Figure 14. Schematic diagram of probe installation.	37
Figure 15. Assembled corrosion probe	37
Figure 16. Power plant waterwall measurement.....	38
Figure 17. Corrosion probe inserted through the manhole at superheaters.	38
Figure 17. Corrosion at superheater location for coupon A.....	39
Figure 18. Corrosion at superheater location for coupon B.....	40
Figure 19. Corrosion with biomass co-firing (Coupon C).....	41
Figure 20. Corrosion in superheater for coupon D	41
Figure 21. Corrosion at waterwall location for 100% coal.....	42
Figure 22. Photo of ash deposition on the coupon inside the waterwall.....	42
Figure 23. Pictures of corrosion sensor after use.	43
Figure 21. SEM picture and EDS elemental analysis of ash deposit on sensor surface. ...	44
Figure 21. SEM analysis of corroded layer on sensor surface.....	45
Figure 25. SEM side view of the corroded layer on sensor surface.	46
Figure 26. SEM analysis of needles formed in ash deposit on sensor surface.	47
Figure 27. A corrosion model for the metal surface.....	46

INTRODUCTION

Background and Significance

Revolutionary sensor technology is a key component for DOE's approach for developing next generation energy plants that would have virtually no environmental impact. Relying on fossil fuels for a major share of our energy needs well into the 21st century and a diverse mix of energy resources, As the culmination of DOE power and fuels research and development directed at resolving energy and environmental issues, one of the focuses is to develop the critical technologies that underlie the components and subsystems ("modules") that are the building blocks of future energy plants. The key elements of the approach include: focusing on key technologies, stressing innovation and revolutionary improvements, producing early benefits, and emphasizing flexibility to meet market needs. One of the identified crosscutting technologies that are expected to be important, regardless of the actual configurations of future energy plants is the development of advanced sensors for highly integrated advanced energy systems.

Fireside corrosion is the external tube metal loss (wastage) caused by chemical reactions on water tubes exposed to the combustion environment in a furnace [1]. Corrosion is the leading mechanism for boiler tube failures [2, 3]. The direct economic cost of corrosion, through parts and labor to replace corroded equipment are often minor compared to the loss of production while the plant is under repair. For example, the cost of replaced power from the shutdown of a needed power plant can run into millions of dollars per day. Fireside corrosion typically occurs in high temperature, harsh combustion environment found in boilers and chemical recovery systems. The corrosion of boiler tubes can lead to the thinning of the tube reached more than 80% of the original thickness. Such excessive corrosion can lead to tube leakage or rupture, which can then lead to significant equipment damage and possible injuries to personnel, and in Kraft recovery boilers, smelt-water explosions.

Proper management and control of high temperature corrosion requires real-time information of corrosion rate [4]. Future trends in energy plant development tend to increase fireside corrosion due to introduction of technologies targeting emissions reduction, efficiency improvement, or fuel/oxidant flexibility. The availability of an on-line instrument capable of quantifying fireside corrosion rates would be a valuable new tool for plant operators who must meet environmental targets while minimizing the deterioration of valuable heat exchanger surfaces. Additionally, knowledge of localized corrosion rates provides critical information so that informed decisions can be made for maintenance and ongoing life extension of the plant [5-7].

This project attempts to develop high temperature corrosion sensors and associated measurement system for advanced power systems. The focus is the short-term determination of fireside corrosion in a combustion environment. A novel sensor concept was developed and examined previously, and the intent of this project was to develop a complete measurement system and evaluate its feasibility at the laboratory and pilot scale. The

investigation includes laboratory development of sensors, the probe and the measurement system, followed by the evaluation and improvement of the system in the laboratory, and the eventual testing of the complete system at a pulverized coal (PC) combustion furnace. The challenge of the proposed work is the design, fabrication and testing of the system that can function in a high temperature harsh combustion environment. The overall goal of the proposed research is to develop and prove the technology feasibility.

Current Knowledge and Technology

Current methods for corrosion measurement or monitoring fall into three main groups: downtime inspection, metal loss types, and electrochemical types [8-37]. The result of downtime inspection is of limited value for pro-active corrosion management because it provides only historical data. The simplest metal loss type is the weight-loss coupon, which is the most commonly used technique in corrosion research. A sample of the material of interest, of known weight, is exposed to the process for a known period. When it is removed, carefully cleaned and weighed, the change in weight is used to calculate the metal loss that may then be expressed as an annualized rate of loss (mils or millimeters per year). The coupon requires a relatively long exposure, for instance, 3 to 6 months, to the combustion process to yield accurate results. The constraints imposed by the time of exposure naturally limit the number of data points that can be obtained from a location, and ultimately do not detect process changes quickly.

Electrochemical techniques measure the corrosivity of an environment independent of actual material loss. Linear Polarization Resistance (LPR) is the most widely used technique of this type. It measures the DC current through the metal/fluid interface when the electrodes are polarized by a small electrical potential. As this current is related to the corrosion current, that in turn is directly proportional to corrosion rate, the method provides an instantaneous measurement of corrosion rate. This has advantages over metal loss methods, but is limited in the scope of its application by the requirement that the fluid be conductive, which in practice usually limits it to aqueous solutions. Other electrochemical techniques include Potentiostatic, Galvanostatic, Potentiodynamic, Galvanodynamic and AC Impedance Spectroscopy. None of these approaches have been successfully developed for field use as continuous monitors due to a variety of technical difficulties.

Electrochemical Noise (ECN) is a passive electrochemical technique that requires no polarizing current, but measures the naturally occurring electrochemical potential and current disturbances that result from corrosion. Electrical current noise is based on current variations between two nominally similar working electrodes, whereas potential noise is based on alterations between a working electrode and a stable, reference electrode. ECN is capable of giving accurate indications of general corrosion, pitting, and stress cracking when it is properly applied, but requires both expertise and complex data processing to be effective. Because ECN requires monitoring of very small signal fluctuations, this approach to corrosion monitoring is also affected by extraneous sources of signal noise in the plant. ECN is a relatively new technique and has applied the technology in coal combustion application by REI recently.

Metal loss type sensors can be combined with electrical measurements to determine the loss of metal and to provide an on-line monitoring capability. The most commonly used low-temperature corrosion probe is based on electrical resistance measurement. Because the electrical resistance of a current path increases as its cross sectional area is reduced, metal loss due to corrosion of the sample can be detected by an electrical resistance-measuring instrument. An Electrical Resistance (ER) sensor is often comprised of a sensing element that is basically a wire, strip or tube made of the alloy of concern, which is used to conduct the electric signal. When exposed to a corrosive environment, the cross-sectional area of the element is reduced. This increases the resistance of the sensing element, which can be measured and recorded as a function of time. Unlike electrochemical methods, ER sensors continue to function in the presence of non-conductive scales and are valuable tools for detecting under-deposit corrosion. As a simple and relatively inexpensive technique, ER is often the mainstay of a monitoring program in low-temperature applications, especially in the petroleum industry. In high-temperature combustion applications, however, ER sensors are significantly affected by instrumental and thermoelectric noise. The challenge is to minimize the persistent noise, whether due to thermal or electrical interference, in the power plant and combustion environment.

In summary, different corrosion monitoring technologies available for low-temperature applications are being adapted for on-line fireside corrosion monitoring. However, these technologies are either in development stage or create significant concerns for uncertainties or interferences inherent in the harsh combustion environment, which include high temperature, temperature fluctuations and ash deposition. It is necessary to develop a fireside corrosion monitoring system with demonstrated power plant operation and verifiable measurement result.

The Capacitance Sensor

A new sensor concept was developed and examined in the previous study. The concept is based on a new measurement principle that has not been previously applied for corrosion measurement. The technique uses a metal-loss type approach, which involves exposing a sensing element to a corrosive environment and measure the thickness decrease of the element as a function of exposure time. As all online approaches to corrosion measurement, the challenge is to measure a thickness change of the order of 1 micrometer or so without destroying or removing the element from the corroding environment. The new concept converts the thickness measurement to area measurement. The technique employs thin-film coating of the material to be corroded on a substrate. The thickness of the coating varies continuously, for instance, from 0 to 40 micrometers over a length of 4 cm. When the sensor element is exposed to the corrosive environment and corrodes away a layer of a certain thickness, the decrease in thickness will be proportional to the coating area recession or decrease. Thus, the design converts the depth (thickness) change of 1 micrometer to an equivalent length change of 1 mm, which is much easier to determine.

The change in size or area of the metal coating can be measured on-line by electrical capacitance. A thin ceramic plate substrate with metal coatings on both sides constitutes an electrical capacitor. The capacitance is a function of the overlapping area of the metal

coatings, and the thickness and dielectric properties of the ceramic. The change of capacitance is directly proportional to the change in the overlapping area of the metal coatings. The sensor design can include a front side coating area with linear thickness variation exposed to combustion environment, and a uniform-thickness backside coating not exposed to combustion environment. The decrease of coating area on the front side due to corrosion will be reflected proportionally by a decrease in capacitance.

This innovative concept represents a departure from existing approaches to metal loss type of corrosion monitoring technology. It can potentially result in a significant advancement in corrosion sensing technology. The ER method is currently under development for combustion environments. ECN or other electrochemical techniques may present problems in interpreting the data when there is ash or slag deposition on the sensor element. The new concept may be better suited for a suite of applications, including the combustion environment where ash deposition and temperature fluctuation are common and almost unavoidable.

Technical Issues and Challenges

Although the capacitance concept has shown promise, clear technical challenges remain. The obvious challenge, beyond the preliminary study, is to develop a system and prove its feasibility in laboratory, pilot combustor, and power plant testing. The capacitance or resistance technology has to be proven at a full-scale boiler before it can be developed into a commercial product. For corrosion monitoring in a combustion environment, proof-of-concept testing at coal-fired furnace is a necessary step. Therefore, the following technical issues must be addressed to further develop the concepts and the technology.

(1) Options for Sensor Design and Fabrication.

We need to have answers to questions such as: what is the best design to achieve high sensitivity and low cost, or what is the best initial element thickness (or slope). For example, the element needs to be thick enough to have a long service life, yet also thin enough to provide a high signal-to-noise ratio. These answers will have to come from research and development at the laboratory scale. The sensor designs need to take into account fabrication options. A compromise may have to be reached between an ideal design and practical requirements for fabrication. The designs will also have to be tested in coal-fired furnaces to see if they can survive and achieve the sensing objective.

(2) Complete Monitoring System Development and Improvement

The proof-of-concept step requires building of a complete system and demonstrating its feasibility at a full-scale furnace. There are many questions to be answered in designing and building the complete system, which needs to match the appropriate sensor designs from laboratory tests with robust probe design. A rugged, portable electronic measurement and control system that can function in the industrial environment need to be built. The measurement system also needs to automatically acquire and store data, and upload the data through (preferably) wireless communication.

(3) System Evaluation and Testing in a Coal Combustion Furnace

The corrosion monitoring system needs to be tested at a full-scale furnace to reveal areas that require improvement or modification. In addition, the probe and ancillary instrumentation need to be tested for long-term performance to determine the service life of the sensor. Such tests will provide information on the stability and long-term performance of the new technology for fireside corrosion monitoring.

Although in theory the change in sensor capacitance is proportional to its change in thickness, the degree of deviation from the linear correlation has to be experimentally determined. Such an evaluation and the data resulting from the evaluation may provide a more accurate estimation of error range and confidence level of the corrosion rate determined by the ER method.

(4) Calibration of Results with Metrology Analysis

The corrosion rate determined from the novel sensor needs to be compared to true metal-loss measurement, either on the same element or on a separate weight-loss coupon. Industry accepts the amount of metal loss measured by coupon exposure as an absolute and correct measure of corrosion averaged over a period of time. Calibration of the corrosion rate measured by the new method provides confidence in the quantitative result from the sensor. Such comparisons will ultimately verify the result of the new sensor for fireside corrosion measurement and promote the acceptance of the technology in industry.

Anticipated Benefits

The sensor and supporting measurement system developed by this project can be used in multiple end-use sectors to increase the overall efficiency of current and future energy plants. Having the availability of a real-time fireside corrosion monitor can help to bring about one or more of the following: (1) quick diagnosis of corrosion problems; (2) monitoring the effect of operating condition changes on corrosion; (3) providing advance warning of system upsets that could lead to corrosion damage; (4) determining the need to invoke process controls; (5) establishing a realistic inspection or maintenance schedule; and (6) an accurate estimation of the useful service life of equipment. Because fireside corrosion has a significant negative economic impact on energy plant availability, corrosion management can reduce such effects and increase the overall efficiency of the plant. The loss of electricity production due to plant downtime for repairing corroded waterwall tubes can run into millions of dollars per day. If the corrosion monitoring technology developed by this project leads to the reduction of downtime for an average of one day each year for each boiler that is monitored, the overall efficiency increase for that boiler is a fraction of one percent. However, the total amount of saving could be in hundreds of millions per year due to the large number of units in the U.S. that would benefit from the application of this technology. In addition to economics, the effects of corrosion can also lead catastrophic explosions that endanger life and safety, which is an especially serious concern for Kraft recovery boilers in the pulp and paper industry. This research can help to reduce such risks by providing a timely assessment of corrosion rates and can help operators determine the most efficient modes of operation. The increase in plant efficiency from corrosion management can directly reduce the emissions per unit of production. Since corrosion is an inherent process for metals exposed to a chemically reactive environment, corrosion

management and control is an important way to reduce its negative impact on plant availability for current and future energy systems.

Research Objectives and Scope

The overall goal is to develop an on-line fireside corrosion technology. This project is to design and build a system and prove its feasibility at a coal combustor. The specific objectives are to:

- (1) Develop the sensor and electronic measurement system;
- (2) Evaluate and improve the system in a laboratory muffle furnace; and
- (3) Evaluate and improve the system through tests conducted in a coal combustor.

The scope of work includes a comprehensive experimental program to be carried out in the laboratory and at a coal combustor. A corrosion monitoring system will be designed, tested, and improved in the laboratory and tested at coal combustor. The experimental effort focuses on designing and building a complete system including the sensor, temperature controlled probe, and electronic measurement and data acquisition. The system will be tested and improved through evaluations using a laboratory muffle furnace. A coal-fired combustor will be used to evaluate the technology in a coal combustion environment. Such evaluation is crucial because many technologies fail during this stage of development due to rapidly varying combustion conditions, the aggressive industrial environment, and high levels of ambient electrical noise. The technology will be evaluated to ensure that (1) it works in a combustion environment, (2) the result can be confirmed by metal-loss measurements, and (3) the system is rugged enough for the plant environment.

EXECUTIVE SUMMARY

Advanced sensor technology is identified as a key component for advanced power systems for future energy plants that would have virtually no environmental impact. This project intends to develop a novel high temperature corrosion sensor and associated measurement system for advanced power systems. Fireside corrosion should be properly managed with real-time corrosion rate information because it could lead to catastrophic equipment failure, explosions, and forced outages. However, short-term, on-line corrosion monitoring systems for fireside corrosion remain a technical challenge to date due to the extremely harsh combustion environment. The overall objective of this project is to develop a technology for short-term, on-line corrosion monitoring based on laboratory development and experiment, and coal-fired furnace testing.

The specific objectives of the project are to: (1) develop the sensor and electronic measurement system, (2) evaluate and improve the system in a laboratory muffle furnace, (3) evaluate and improve the system through tests conducted in a coal combustor. The scope of work includes an experimental program to be carried out in the laboratory and at a coal combustor. The on-line corrosion monitoring system to be developed includes the sensor, temperature-controlled probe, and electronic measurement and data acquisition. The system will be tested and improved through evaluations using a laboratory muffle furnace. A coal combustor will be used to evaluate and further improve the technology in a coal combustion environment. There are three main tasks in the project. The first task is to design and build a complete system during the first year. Task 2 is to evaluate and improve the system performance in a laboratory muffle furnace. Task 3 evaluates and improves the system in a coal combustor.

These tasks are successfully completed, namely, the development of the sensors, probes and the measurement systems in the laboratory, the testing of the system in a muffle furnace, and the testing of the system in a power plant. The completed work included the preparation and design of a corrosion probe, on which the corrosion sensor can be mounted. The first probe, which is slightly smaller in diameter, was redesigned with improvements to accommodate ceramic connectors for electrical connection. The probe temperature measurement and control was developed based on our experience, in addition to a probe temperature control system that was already available. They are portable and rugged, suitable for operation at ambient temperatures in a power plant environment. The probe temperature, or the temperature of the sensing element, is controlled with compressed air cooling. The electronic measurement with computer data acquisition was also developed in the laboratory. The data acquisition software was developed to allow the user to select data logging rate, the temperature for the sensor, and options for various measurement sequences. It was successfully tested to automatically log and save the data for days or weeks without the need for operator intervention. The probe temperature control was also tested in laboratory muffle furnace to control the air cooling parameters and fluctuation range of the probe temperature.

In addition to the capacitance sensor system, a development effort on the resistance sensor system is also pursued due the high cost of the capacitance sensor fabrication. The

resistance based system initially had difficulty in data processing due to persistent noise. Further investigation of the resistance sensor design led us to create a new sensor design that could minimize the noise. The advantage of this new design of resistance sensor is its significantly, more than 100 times, lower cost in comparison to the capacitance sensors. We can fabricate resistance sensor in the laboratory easily, whereas the capacitance sensors requires custom modification of the commercial sputtering facility, a job that sputtering service companies usually would not do. Also, because the sputtering coating of iron only has limited thickness, the resulting capacitance sensor cannot produce reliable corrosion rate data, although may be more appropriate for other applications. Therefore, we focused our testing effort at a power plant on the resistance sensor.

The plant measurements were conducted at two locations: waterwall and superheater, at 500 °C sensor temperature. The waterwall location was one floor above the biomass injection port of the tangentially-fired 65 MW boiler. The superheater location was in-between the primary and secondary superheaters. The switchgrass co-firing was maintained at 5% heating value of the overall fuel heating value. The results at the superheater location show that biomass co-firing has two scenarios regarding its impact on fireside corrosion. When a fresh coupon was exposed to biomass co-firing, the corrosion rate was about twice as much as that for 100% coal firing. On the other hand, if the fresh coupon was exposed to 100% coal firing first and biomass co-firing next, the corrosion rate for biomass co-firing was slightly less than that for coal. The waterwall corrosion rate for coal was similar to and less than that at the superheater location. Also, the waterwall corrosion rate appeared to be higher at higher boiler load for coal. The biomass co-firing did not produce meaningful results for waterwall.

Further analysis of the corroded sensor surface by SEM with EDS showed a more detailed picture of the corrosion process at the sensor surface. A corrosion product layer of a few to ten micrometers thick was formed on top of metal surface. The metal surface had a granular type of surface roughness of about one to two micrometers. The corrosion product layer also appeared to be granular, with a thin melt layer covering on top. Based on the findings, a three-layer model was proposed with metal at the bottom, corrosion product layer in the middle, and ash deposit layer at the top. The cracking and peeling off of the corrosion product layer exposed the metal to further corrosion.

EXPERIMENTAL

Sensor Principle

The principle of the novel capacitance sensor is based on the electrical capacitance technique, which has never been used for corrosion measurement. The sensor consists of a ceramic substrate with metal coatings on both sides, which forms a classical electrical capacitor, as shown in Figure 1. The capacitance of the sensor is a function of the overlapping area of the metal coatings, the thickness of the ceramic substrate and the dielectric constant of the ceramic. The front side coating exposed for corrosion has a linearly varying thickness, or wedge-shaped. When the sensor element is exposed to the corrosive environment and corrodes away a layer of a certain thickness in wedge-shaped coating, this thickness decrease will be reflected on and proportional to the coating area reduction. This design converts very small change in the depth (or thickness) to substantial change in length, which is much easier to measure. Therefore, any loss of the metal by corrosion will result in a reduction of the coating area. The change in the area of the metal coating can be measured by electrical capacitance, which is directly proportional to the change of the overlapping area of the metal coatings. The thickness reduction due to corrosion is therefore quantified by the capacitance change. The corrosion rate can be determined based on the decrease in electrical capacitance over the time. The capacitance is measured using a four-wire method, applying 100 kHz AC current and measuring the AC voltage drop across the capacitor to determine the impedance, which can be used to calculate the capacitance.

Another technique tested, the electrical resistance method also uses a sacrificial metal coupon exposed to the corrosive environment. The relative change of the coupon thickness is determined based on the measurement of the coupon DC electrical resistance change. Because the electrical resistance of a current path increases when the cross sectional area of the conductor is reduced, the metal loss due to corrosion can be detected by an electrical resistance-measuring instrument. The sensing coupon is made of a circular disk of the alloy of concern with four electrical connections. A DC constant current is applied through the two opposite electric connections and the voltage between the other two electric connections is measured, as shown in Figure 2, which is also a four-wire measurement similar to the capacitance measurement.

The corrosion of coupon material will reduce the thickness of the coupon, and lead to an increase of measured resistance or impedance. Since the electric current is maintained at constant, the voltage between the test poles 1 & 2 will increase as the thickness decreases. Figure 3 shows the theoretical relationship between the measured DC voltage and the coupon thickness in relative percentages for the resistance technique. Figure 3 was calculated using a commercial finite element package to model the geometry effect of a specific coupon size and the location of the four electric connections. The curve for partial corrosion was calculated to account for the fact that there is little corrosion on the rim of the coupon due to sealing o-ring. Figure 3 shows an approximate linear relationship when the change of resistance is not significant.

Sensor Design

Substrate Material Selection

The physical and chemical properties of the sensor substrate materials are important factors affecting the sensor design and performance. Since the sensor developed in this research will be used for corrosion monitoring in high temperatures and corrosive combustion environments, the substrate material needs to have properties of high thermal conductivity, low thermal expansion, good electrical insulation, corrosion-resistance and stability at high temperature environments.

The substrate of the sensor is a ceramic plate with high thermal conductivity and low thermal expansion coefficients. There are a few commonly used ceramic materials available for the sensor substrate. These materials include Beryllium Oxide (BeO), Aluminum Nitride (AlN) and Alumina (Al₂O₃). The comparisons of main properties of these materials are provided in Table 1 and Figure 4. Because of the presence of water vapor in combustion, AlN is not considered in this case.

Beryllium Oxide (BeO) is a ceramic material that combines excellent electrical insulating properties with high thermal conductivity. It is also corrosion resistant. Although beryllium oxide powders are toxic when inhaled or ingested, and the cost of machining is high, there are many applications that exploit its singular properties. BeO is a unique material for electrical and mechanical applications, which require dielectric property, mechanical strength and high thermal conductivity. It is particularly well suited for a heat sink and heat dissipation medium in integrated circuitry.

Therefore, BeO is distinguished by thermal conductivity comparable to that of electrical conductors, while retaining dielectric constant, loss factor and dielectric strength in the range of the most efficient electrical insulators. This unique combination of properties in conjunction with good mechanical strength and thermal shock resistance enable BeO to be the best substrate material of the sensor in this research.

Aluminum Oxide (Al₂O₃) or Alumina is the second choice for the sensor substrate although its thermal conductivity is not as high as BeO. The high volume resistivity, chemical stability at aggressive and high temperature environments, high dielectric constant coupled with low dielectric loss and excellent electrical insulation lead to its wide applications in electronics as substrates. More importantly, Alumina costs much less than BeO.

Table 1 Properties for BeO and Alumina (99.6 % Al₂O₃).

Property	BeO	99.6% Al₂O₃
<i>Electrical</i>		
Dielectric constant @1 MHz	6.7	9.8

Dielectric loss @1 MHz	0.0002	0.0001
Dielectric Strength (KV/mm)	>9.5	35
Electrical resistivity (Ohm-cm)	>10 ¹⁴	>10 ¹⁴
<i>Mechanical</i>		
Density (g/cm ³)	2.88	3.75
Youngs Modulus (GPa)	340	390
<i>Thermal Properties</i>		
CTE($\times 10^{-6}/^{\circ}\text{C}$) (25~400 $^{\circ}\text{C}$)	6.7	6.9
Thermal Conductivity (W/Mk)	290	30

Because the dielectric constant of the sensor substrate is the usually a function of temperature and there are temperature fluctuations during the measurement. It is important to determine the relationship between the dielectric constant and temperature because the measured capacitance becomes temperature-dependent through the dielectric constant of the ceramic substrate. A change in sensor capacitance could be caused by two reasons, corrosion of the front coating or sensor temperature change. To eliminate the capacitance change from the sensor temperature variations and obtain the corrosion rate, a temperature compensation technique is used to process test data based on measured sensor temperature and the relationship between the temperature and dielectric constant. The compensation can remove the influence of temperature variations on capacitance measurement.

For the resistance sensor, a specially designed holder was used as a sandwich structure for the sacrificial plate of low carbon steel 1010. This is a common carbon steel used for boiler tubes in small boilers and its chemical composition of which is shown in Table 2. High temperature ceramic adhesive was used to glue the sandwich structure together. Electrodes are spot welded on the metal plate, as well as the thermocouple for temperature control and measurement. Ceramic connectors were used to easy sensor replacement during the plant testing.

Table 2 Chemical composition of the low carbon steel for coupon (%).

Carbon, max	.25
Manganese, max	.90
Phosphorous, max	.025
Sulfur, max	.025
Nickel, max	.20
Chromium, max	.15
Molybdenum, max	.06

Sensor Fabrication

Sputtering Deposition Technology for Sensor Fabrication

The key for sensor fabrication is the forming a wedge-shaped front side coating to be exposed to combustion, with linear thickness variation. The sensor element design is shown in Figure 5. The backside coating not exposed to combustion has a uniform thickness and is relatively easy to make. The coating materials are different for the two coating deposition. Since backside coating should have no corrosion, it is better to select a material that does not corrode in air environment.

Sputtering deposition is a technique by which atoms and ions of Argon or other gases from the plasma bombard a target, thereby knocking atoms off of the target. These material atoms travel to a substrate where they are deposited and form a thin film. It is necessary to provide a uniform and abundant supply of ions over the surface of the target. This is achieved by maintaining a charge differential facilitating the movement of the sputtered atoms across the gap between the target and the substrate.

DC magnetron sputtering deposition technology was used for one type of the sensor coating deposition. The fabrication included the design and machining of accessory parts for substrate installation during the coating, target material preparation and the coating fabrication. A Denton DVI-SJ-24 multi-cathode DC/RF magnetron sputtering deposition system in the department, as shown in Figure 6, was utilized to deposit the iron coating on corrosion side and titanium coating on other side of the substrate. The DVI-SJ-24 is based on a “box coater” that provides easy access to substrates, sources, and instrumentation while maintaining excellent pumping characteristics. This system is designed to simplify the geometries necessary for the coordination of multiple source depositions. The system’s inherent flexibility allows for the operation of three sputter sources and the ability to heat, RF bias, and rotate the substrate. In a con-focal cathode arrangement, the cathodes are focused on a central area of the substrate table. Table rotation during sputtering permits co-deposition, provides continuous substrate exposure to the cathodes, and results in excellent coating uniformity. With this arrangement, the cathodes can be smaller than the substrate and still provides uniformity of the coating.

We used a slow moving shutter for the specific purpose of depositing the linearly increasing thickness on the front side for corrosion. A special substrate holder with mask was designed and machined to support the sensor substrate during the sputtering. The substrate holder was adjustable in x, y, z directions to keep the mask and substrate in the appropriate position. Since the coatings on the two side of the sensor consisted of different target materials, the deposition rate and sputtering time were different for the coating on two sides. To achieve the required coating slope, experimental coatings were conducted to provide information on deposition rates. The needed exposure time of the substrate in plasma and shutter moving speed were calculated before the sputtering operation. The wedge-shaped coating was deposited by gradually moving the shutter over the coating area of the substrate during the sputtering. The area with longest exposure time had maximum coating thickness. The deposited coating had a gradual linearly changing thickness.

Low carbon steel 1010 was used as target materials to create wedge-shaped coatings. It took 7.5 hours for this deposition to complete, with total 45 steps along total length of 15

mm at 10-minute interval for each step. The maximum coating thickness measured by the profilometer was about 1.7 μm , because deposition rate for this material is very low. The whole process was extremely labor intensive because of the slow moving shutter, at the speed of about 1 inch per 7.5 hours, was manually operated moving stage with controls through the high vacuum chamber. Later, as the sputtering system was not available in the department due to the departure of a faculty member, the fabrication was done at a NASA facility through a technical collaborator. No commercial sputtering service company is able to fabricate our design for a limited number of pieces with reasonable cost.

For the backside coating, all unmasked area of the substrate had the same exposure time and the sensor holder rotated continuously during the sputtering. Since Titanium has a relatively higher deposition rate than low carbon steel 1010, the backside coating thickness achieved 2 μm during 1.5 hours of the deposition.

Plasma Spray Technology for Sensor Fabrication

Plasma spray process is basically the spraying of molten or heat softened material onto a surface to form a coating. Material in the form of powder is injected into a very high temperature plasma flame, where it is rapidly heated and accelerated to a high velocity. The hot material impacts on the substrate surface and rapidly cools down forming a coating. Such a plasma spray process carried out correctly is called a "cold process" (relative to the substrate material being coated) as the substrate temperature can be kept low during processing avoiding damage, metallurgical changes and distortion to the substrate material.

A plasma spray system in Plasma Process Inc., in Huntsville, Alabama was tested to fabricate the front and back side coatings. The front side wedge-shaped coating thickness varies from the thinnest to the thickest of 50 μm over a total length of 61mm. The backside coating has a uniform coating thickness of 100 μm . The target material was a low carbon steel "Atomet 95". In addition, a layer of Titanium coating was sprayed around the holes for electrical connection of the sensor. The purpose of Titanium was to prevent the coating oxidation (or corrosion) at electrical connection areas.

The linear thickness change is not guaranteed because it is a manual spray gun operation. Our sample is too small and it is almost impossible to produce a linear slope of thickness change. For our sensor, such non-linear thickness variation is detrimental to the metal loss measurement because the measured capacitance is not proportional to the corrosion anymore. Qualitatively, manual plasma spray can generate a coating thick on one side and thinner on the other side. The deviation from the linear thickness change can only be determined by the measurement of each sensor. We did not pursue further on the plasma spray technique for the fabrication of the capacitance sensor.

Probe Design

The probe for the application in coal-fired furnace was re-designed to accommodate the ceramic connectors for the sensor element. The requirement for the probe includes

mounting of the sensor element at the end, the temperature control of the sensor element with compressed air cooling, and the flange mount for insertion to the combustor. The existing probe is shorter and slightly smaller in diameter. The new probe is longer, which can be used to access superheater section of the boiler. The new design incorporated features for more ruggedness and future applications in power plants.

Probe Temperature Control and Data Acquisition

The temperature control system and the data acquisition systems were developed. We previously used this temperature control system in pilot furnace experiments and had good experience with it. It was proved to be rugged and precise for the similar furnace probe applications. Our original temperature control system can control the probe temperature precisely. However the size of the control cabinet is large and not as convenient. Both systems would be evaluated in our experiments.

The computer data acquisition with a LCZ meter was developed. The 4-wire measurement technique was applied to measure capacitance, similar to the resistance measurement. One pair of leads supplied test current to the sensor and a separate pair of leads made the voltage measurement. The method can prevent the voltage drop in current carrying wires from affecting the voltage measurement. The 4-wire method were also arranged to eliminate the impedance from the electrical leads as source of error, and thus improved the measurement accuracy. The data can be converted to corrosion rate information on a continuous online basis. An OMEGA thermometer/controller connected to a thermocouple transfers the temperature of the sensor element to the computer. Data acquisition software was developed to perform automatic data collection by the computer to obtain the test data from the SR175LCR meter and thermometer respectively. The rate of data acquisition could be adjusted by program. The data acquisition computer could acquire and display the measured capacitance and temperature of the sensor on real time basis, and the measurement results were programmed to be automatically saved every four hours for further data processing and analysis. The data acquisition software can run continuously until it receives the stop command.

For the resistance method, the four-wire measurement technique with a constant DC current source was used with a high precision digital voltmeter. A measurement of the resistance takes several steps. First the voltage is measured without applying the current. The reading is the background noise to be subtracted from the voltage signal with current on. Then the current is turned on and the voltage is measured. The same procedure is then applied to a standard resistor. The sensor resistance is comparative obtained from the known standard resistor. Such a procedure can remove significant noise, including the thermocouple effect from the wiring.

Plant Measurement

The plant has two tangentially-fired boilers of 65 MW each. The primary fuel is pulverized Eastern U.S. bituminous coal. The corrosion rate measurement was performed on

unit #2, which had switchgrass co-firing. Switchgrass was separately milled and burned by direct injection above the coal burners into the furnace at 5% heating value of the overall fuel heating value. The corrosion measurement was carried out at two locations of the boiler. One location was on the waterwall corner above the burners, and the other in between the primary and secondary superheaters.

During a measurement campaign, the boiler load was held constant at 540,000 lb steam per hour (approximately 65 MW), or 320,000 lb/hour. Switchgrass was burned from early morning (typically 6-6:30 am) to afternoon (typically 3-4 pm) on test days. The remaining time was on coal only. The composite fuel, fly ash, and bottom ash were sampled daily during the campaign (typically five days). In addition, the plant CEM and boiler load data are available.

At the start of each campaign, a fresh coupon is installed and the probe is inserted into the furnace. The cooling air is initially at full flow rate and then on PID control based on the coupon temperature. Computer data acquisition records the coupon temperature and coupon resistance data with time stamp at every few seconds. The data file is automatically saved in every four hours into the hard drive, which is usually downloaded daily for the monitoring of coupon resistance change. The data is then processed to generate coupon corrosion rate. The operation is also pictured and the probe inside the furnace is photographed from a port on the other side of the furnace corner. The used coupons were carefully pictured and stored for future analysis on the residue layer on the surface. The used coupons can also be cleaned and measured for thickness change.

RESULTS AND DISCUSSION

Two types of sensors based on the capacitance or resistance method, as well as the corresponding measurement systems, were developed in the laboratory. Both systems worked well in the laboratory muffle furnace, where the temperature and air environment are not as harsh as the coal flames and ash deposits. However, the coating thickness of the capacitance sensor was limited by the sputtering method; the capacitance sensor could not function well in the coal combustion environment. The resistance sensor, on the other hand, was made at a much lower cost and worked well in the coal combustion environment. The power plant experiments with the resistance sensor showed interesting results for a boiler with biomass co-firing with an eastern bituminous coal. Analysis of the samples showed the detailed mechanism of the fireside corrosion process.

Laboratory Development and Testing

The tasks for the first two years were to design and build the corrosion sensor, probe and measurement system, and test in a muffle furnace in the laboratory. These goals were successfully achieved with the development of two types of sensors and measurement systems. The completed work also included the preparation and design of a second corrosion probe for more flexible plant test. The schematic diagram for the laboratory experimental setup for the capacitance probe is shown in Figure 7. The schematic for the resistance system is very similar to the capacitance system, as shown in Figure 13.

The wedge-shaped coating of the sensor element is shown in Figure 9. The picture shows the front of the sensor with the wedge coating, where the right side of the coating is thicker and the left side is thinner. Four connection bolts are also shown in the picture. Figure 8 shows the resistance sensor and how the sensor is mounted on the tip of the probe. The resistance sensor, after many versions of design, has a sandwich structure and a supporting ring. Four connectors are welded on the sensor piece. A hollow screw cap is used to tightly press the supporting ring of the sensor on the probe tip. For quick sensor change, the connectors are plugging-in type of ceramic thermocouple connectors.

The probe temperature measurement and control components were developed based on our experience in pilot and plant furnaces, shown in Figure 11. The existing probe temperature control system that was already developed has a cabinet. These two control systems are rugged and suitable for operation in a power plant environment. The probe temperature, or the temperature of the sensing element, is controlled with compressed air cooling. These temperature control units have been tested in a muffle furnace in the laboratory and in a coal-fired furnace. Both functioned well as designed. Both can control the sensor temperature for extended period without the need for intervention, and the temperature data are automatically logged into the computer.

The electronic measurement with computer data acquisition was also developed and tested successfully in the laboratory. For capacitance, the laboratory setup for the probe,

temperature and measurement system is shown in Figure 12. A muffle furnace is used and the sensor end of the probe is inserted into the muffle furnace. The compressed air cooling, and temperature control system is connected. A desktop computer or a laptop computer can be used for data acquisition and control. The data acquisition software was developed to allow the user to select data logging rate, the set temperature for the sensor, and options for various measurement sequences. In the muffle furnace test, the system automatically logged and saved data for days or weeks without the need for operator intervention.

For power plant measurement, two air-cooled probes were designed and fabricated. The design of the probe is shown in Figure 14, and the schematic probe installation is shown in Figure 14. The sacrificial sensor coupon (diameter 43 mm, sandwich structure with ceramic and a metal holder) is installed at the end of the probe, which can be inserted into the furnace and exposed to the combustion environment. Figure 14 is a picture of the assembled probe, ready to be inserted into the superheater location. In our experiment, the view port or manhole on the furnace wall were modified for the probe insertion. The probe tip, where the sensor is mounted, is about flush with the water tubes. Compressed air is used to cool the coupon to a constant temperature. The air-conditioned instrument cabinet with computer data acquisition, and the installed probe on the view port on the waterwall, are shown in Figure 14. Figure 147 is close-up picture of the probe inserted through a manhole at the superheater location. A door of the manhole was modified with a connection flange for the probe insertion.

While both capacitance and resistance systems performed well in the muffle furnace in the laboratory, however, the fabrication of the capacitance sensor turned out to be very difficult and costly. Initially, we used the sputtering system available in the department. We modified the system to enable a graduate student to operate manually the slow moving shutter in 8 hours of sputtering time for one side of the sensor substrate. The procedure is labor intensive and requires special modification of the sputtering system. Later, the sputtering system was not available in the department anymore, and the sensor fabrication was done in a similar system at NASA through a collaborator. When the NASA system is down, we looked for commercial sputtering companies to fabricate the sensor. But no commercial sputtering service company is able to fabricate our design at a reasonable cost. Furthermore, the sputtering deposition of iron is very slow, less than $2 \mu\text{m}$ per 8 hours. Ideally, the sensor should have a coating of a linear thickness variation of a 0-40 μm slope on the front side. Thicker coating minimizes the effect of initial higher corrosion rate of a fresh metal surface. The corresponding sputtering time, however, would be 176 hours for one side of the substrate, making the fabrication process extremely costly.

As the fabrication of the capacitance sensor turned out to be difficult, the experiments on the resistance sensor system made significant progress. The resistance based system was previously tested under industrial support and had difficulty in data processing due to persistent noise. Our further investigation of the resistance sensor design led us believe that problems could be solved by a new design of the sensor element. Another advantage of the new design of resistance sensor is its significantly lower cost in comparison to the capacitance sensors. The cost of the capacitance sensor is hundreds times more than the resistance sensor without mass production facility. We can fabricate resistance sensors in the laboratory easily, whereas making the capacitance sensors requires custom modification of the commercial sputtering facility, a high cost job that many sputtering service companies

would not consider. Therefore, using the similar temperature control, data acquisition, and high temperature probe, we focused the power plant experiments on the new type of resistance sensor.

We have gained significant experience at a coal-fired power plant through the interaction with plant operators and preliminary testing of the resistance sensor and measurement system. The experience led to design modifications for the practical constraints in a plant environment. Based on our experience in the pilot-scale furnace and the power plant, it was concluded that it is easier to directly conduct power plant test because the plant operates all the time, and have less changes in operation condition. We decided to focus on power plant trials in the final phase of the project, instead of pilot-scale furnace testing. Power plant testing of the system can also accelerate the pace of bringing the technology to practical application by demonstrating the measurement system at full-scale. Therefore, we focused effort on the testing of the resistance-based system at a coal-fired power plant.

The result of plant tests indicated that the system could determine metal corrosion rate in a relatively short period. The data was verified with metrology measurement. It should be noted there were many lessons learned from the unique plant environment. For instance, the AC power at the plant is not always stable and could be quite noisy, which caused unexpected software shutdowns and fluctuations in recorded data. The moisture content of the compressed air is sometimes high and caused cooling system problems. The dust in the plant environment has caused the computer failures. The boiler workers for the superheater repair knocked down the data acquisition equipment and damaged some parts. The boiler repair, probably the use of power tools, generated noises in the data. The probe in the superheater location was one time totally buried under fly ash due to soot blowing. Unlike relative clean laboratory, there are many unexpected factors that can affect the measurement result. Diagnosing and solving these problems that are unique in plant environment, we have improved the measurement system and had successful measurement campaigns.

Plant Measurement Results

Superheater Corrosion

There were four coupon measurements finished with good results at the superheater location. Two coupons started with 100% coal burn first, then was exposed to biomass co-firing. The other two coupons started with biomass co-firing, then 100% coal. It was found that the response of coupon resistance was dependent on whether the coupon was first exposed to the biomass co-firing or 100% coal firing. For a fresh coupon, the corrosion rate for biomass co-firing is twice as much as that for 100% coal. If the fresh coupon is first exposed to 100% coal firing for about 10 hours, then to biomass co-firing, the corrosion rate for biomass co-firing is in a range similar to or slightly below that for 100% coal firing.

Coupon A: 100% coal first, then biomass

During this test, the load was held at 530,000 lb/hr during day time. (0-10, and 24-34 hr), and it was not held constant during other times (night time). The probe was inserted at 6:27 am. The coupon resistance and temperature change are shown in Figure 18. The raw data for resistance and temperature are shown in (a) and (b), and (c) shows the resistance after noise filtering and temperature compensation. From the resistance change, the corrosion rates of coupon were obtained, 13.9 $\mu\text{m}/\text{day}$ in the coal-burn period (0~10 hr), and 9.9 $\mu\text{m}/\text{day}$ during the biomass burned period (24~34 hr), as showed in Fig. 3c.

Coupon B: 100% coal first, then biomass

Different from coupon A, the constant steam load of 530,000 lb/h was held all the time during this campaign. The measurement started at 16:26 pm. The coupon resistance and temperature change are shown in Figure 18. From the resistance change, the corrosion rates of coupon were calculated to be 14.8 $\mu\text{m}/\text{day}$ for the coal-firing period (0~14 hr), and 7.2 $\mu\text{m}/\text{day}$ for the biomass co-firing period (14~24 hr). These corrosion rates are quite similar to the previous results for coupon A, which are 13.4 and 9.9 $\mu\text{m}/\text{day}$, respectively. After biomass co-firing, the corrosion rate for 100% coal is 5.7 $\mu\text{m}/\text{day}$. This rate is smaller than that for 100% for the first 0-14 hours.

Coupon C: Biomass first

The biomass burn started at about 6:30 am, and the corrosion probe was put into the boiler at 9:38 am. The steam load was held at constant 530,000 lb/h. The coupon resistance and temperature changed are shown in Figure 18.

The corrosion rate of the coupon was calculated from first 7 hour data, when it is all biomass co-firing on the fresh coupon. The rate is 27.3 $\mu\text{m}/\text{day}$. This number is about twice as much as that for 100% coal firing on a fresh coupon.

Coupon D: Biomass first

This measurement was a repeat for the previous coupon C. The steam load was held at constant 530,000 lb/h. The fuel was biomass co-fired with coal. The coupon resistance and temperature change are shown in Figure 21. The corrosion rate of coupon was obtained as 28.2 $\mu\text{m}/\text{day}$, which is close to the previous result of coupon C, 27.2 $\mu\text{m}/\text{day}$. This result confirms that for biomass co-firing, the corrosion rate is about double that for 100% coal firing on a fresh coupon.

Waterwall Corrosion

Coupon E: 100% coal firing at low load

During this campaign, the steam load of boiler was held at 320,000 lb/h during the day from 6:00 am to 4:00 pm, and the load was not held constant at night. The fuel was

100% coal. The coupon resistance is shown in Figure 22. From the resistance change, the corrosion rate was calculated to be 7.24 $\mu\text{m}/\text{day}$ for the first 20 hrs. This result can be used to compare with the corrosion rate for a higher steam load to show the effect of load on corrosion rate.

Coupon F: Biomass first, then 100% coal

The corrosion rate in the coal burning period was about 9.11 $\mu\text{m}/\text{day}$ (from 10 to 24 hr). The raw data had many spikes, which correspond to the use of power tools by the construction or repair workers at the time of the measurement. These spikes were mostly filtered out. In general, the data at waterwall location have more noise and fluctuation in comparison to the data from the superheater location.

Coupon G: 100% coal first, then biomass

In the case of 100% coal burning, the corrosion rate in the first 14 hours was 17.3 $\mu\text{m}/\text{day}$. Because the high fluctuation of the data in the first 14 hours, the corrosion rate calculation has a high uncertainty level. After 24 hours, the fuel was shifted to 100% coal again. The sensor resistance kept increasing, and the corrosion rate was obtained at 10.9 $\mu\text{m}/\text{day}$ from the resistance change of 32~64 hour.

Table 3 summarizes the results of the successful measurements. The superheater measurement has confident results on the comparative rates on a fresh coupon for biomass co-firing and 100% coal, where the biomass has about double the corrosion rate. However, if the coupon has exposed to 100% coal firing first for about 10 hours, then the corrosion rate for biomass co-firing is lower than that for either 100% coal or biomass co-firing on the fresh coupon.

For waterwall, the measured data have more noise and fluctuations. The corrosion rate of 100% coal firing appeared to be similar, but smaller than that for the superheater. The boiler load also seems to have a slight influence on the corrosion rate: higher corrosion rate for higher steam load.

Table 3. Corrosion rate summary

No	Location	Fuel sequence	Steam (lb/h)	Corrosion rate ($\mu\text{m}/\text{day}$)	
				100% Coal	Biomass
A	Superheater	100% coal Biomass+coal 100% coal	530,000	13.9 (0-10 hr)	9.9 (24-34 hr)
B	Superheater	100% coal Biomass+coal 100% coal	530,000	14.8 (0-14 hr) 5.7 (24-40 hr)	7.2 (14-24 hr)

C	Superheater	Biomass+coal	530,000		27.2 (1-6.5 hr)
D	Superheater	Biomass+coal	530,000		28.2 (1-7hr)
E	Waterwall	100% coal	320,000	7.24 (0-20hr)	
F	Waterwall	Biomass+coal 100% coal	530,000	9.11 (10-24 hr)	
G	Waterwall	100% coal Biomass+coal 100% coal	530,000	17.3* (0-14 hr) 10.9(32-72 hr)	

* high uncertainty

Waterwall and Superheater Surface Temperature Estimation

For all the results, the coupon temperature was set at 500 °C. The reason for the set temperature selection was mostly based on the previous experience at the plant. If the temperature is too low, it requires a longer exposure period to obtain confident corrosion rate data. At the time, the temperature of the waterwall was measured by an IR thermometer, and 500 °C was selected by the team. However, the true metal surface temperature for the waterwall and superheater is lower than 500 °C. Therefore, the true corrosion rate for the waterwall and superheater should be lower than the measured value reported in this project.

The waterwall and superheater surface temperature on the furnace side is estimated here to provide guidance for the correct interpretation of the corrosion results. The given boiler data include: saturated pressure (gauge): 875 psig (6.03 MPa), steam temperature: 860 °F (460 °C) at steam load 500,000 lb/hour. The conductivity of carbon steel, based on the handbooks, is 45 W/m-°C at 300 °C (572 °F), and 42 W/m-°C at 400 °C (752 °F). The estimated heat flux on the waterwall is about 0.2 MW/m² (based on Steam), and the estimated thickness of the waterwall is 5 mm. The saturated water inside the waterwall can be found from the steam table at 278 °C (532 °F). Therefore, the outside surface temperature of the waterwall is

$$t_{waterwall} = t_{sat} + \frac{q}{k} \delta = 278 + \frac{0.2 \times 10^6}{45} \times 0.005 = 300 \text{ } ^\circ\text{C} \quad (572 \text{ } ^\circ\text{F})$$

For the primary superheater, the parameters are: the steam temperature of secondary super heater, 460 °C (860 °F); the steam temperature of primary super heater, 373 °C (703 °F). The outside surface temperature is about 30 °C higher than the steam temperature, and for the measurement location in between the primary and secondary superheater,

$$t_{\text{Superheater}} = 373 + 30 = 403 \text{ }^{\circ}\text{C} \quad (757^{\circ}\text{F})$$

Therefore, the corrosion rate for the true metal surface should be assessed at about 300 °C for the waterwall and 400 °C for the superheater. The set temperature of the measurement is 200 °C and 100 °C higher than these estimated metal surface temperatures, respectively. The measured corrosion rates should be much higher than the true corrosion rate because of the higher set temperatures. More experiment on the temperature effect on the corrosion rate in plant conditions would provide answers and correlations to predict the corrosion rate at different temperatures. There are reports on laboratory studies on temperature effect on corrosion. But we did not find any report on the temperature effect on fireside corrosion for power plant experiments.

Measurement Uncertainty Estimation

The measured data has high noise and high fluctuation levels. The noise is averaged and filtered out mostly. The fluctuation is still quite significant. Currently, we do not have a thorough understanding for the reasons for these fluctuations. Further study in a base-load unit, or a unit with minimum or no change of operation conditions, is needed to establish the understanding of the reasons for the fluctuations. However, based on our experiments and experience from previous measurements, the fluctuations seem to correlate with the changes of boiler load, and CEM data.

In general, the coupon resistance is highly dependent on coupon temperature. Because the resistance is measured for the whole coupon surface, the temperature distribution on the whole coupon surface should be ideally held at a constant value. In reality, the temperature distribution on the coupon surface can vary significantly. For instance, in the pilot combustor experiment, the temperature at differently locations of the coupon surface can vary above 10 °C, based on IR camera measurement, with the air cooling to the set temperature. The thermocouple that measures the coupon temperature is weld on the center of the coupon and is used for coupon temperature control. The automatic control can only ensure the center of the coupon is at the set temperature. The temperature in other areas on the coupon, on the other hand, is dependent on factors such as corrosion product formation and ash deposition. A very thin layer of ash can change the radiative properties of the surface and thus heat flux to the coupon. The temperature in the area is then changed. The speculation is that the fluctuation, i.e., the dependence of coupon resistance on many operational and other factors, has significant contributions from the non-uniform temperature distribution on the coupon surface. As shown in Figure 23, the ash deposition on the sensor surface increases with time at the waterwall location. In the future, some type of soot blowing mechanism should be incorporated into the probe system to minimize the effect of ash deposition.

The overall uncertainty in corrosion rate is mostly controlled by the fluctuations of the resistance data. The instrument measurement uncertainty of resistance and time contribute almost nothing to the overall uncertainty. The uncertainty for each measurement

can be analyzed individually based on the data, which is a time consuming task. However, it can be roughly estimated that the corrosion results have about 20-30% uncertainty level.

Corrosion Rate Change with Exposure Time

It is generally believed that the corrosion is faster initially, and slows down when a layer of corrosion product establishes and functions as a diffusion barrier. The corrosion rate of the fresh coupon is higher for the first half hour, as evidenced by the data curve. Usually there is an initial jump of the resistance in the data curve, which is more apparent in Figures 18 & 19. To eliminate such effect, the calculation of corrosion rates excluded the data for the first half hour.

Currently, there is no detailed understanding on exactly how long this initial period is and when the corrosion reaches steady-state in the literature. Generally, the nature of the corrosion and corrosion product or deposit on the surface would determine the length of the initial period. Our observation of the first half hour is primarily based on the data collected, and it should be good for the data being analyzed. There may still be slight decrease of corrosion rate after the first half hour, which is not possible to assess from the data measured in this study. Ideally, we would want data for extended time, two weeks for instance, under constant conditions. Then we can assess exactly how much time is needed to establish steady-state corrosion.

Further expanding the thought of initial transition period and steady-state corrosion, we can compare the corrosion rates for different conditions, such as different fuel, load, or other operational parameters. It would be an interesting topic itself to see whether the first half hour data can be used to assess the relative corrosion rate of boiler different conditions. More time-dependent corrosion experiments are needed to establish such a technique for assessing relative corrosion rate quickly. The issue of corrosion rate changes with time and how the measured data would be a worthy research topic following this study.

SEM Analysis and Metrology Calibration

There are obvious color differences in the ash deposit or corrosion product on the coupon surface for biomass co-firing and 100% coal firing, as shown in coupon pictures in Figure 24. The analysis of the coupon surface by SEM with EDS was performed to determine the morphology and composition of the deposit.

The coupons were also be measured by metrology method to determine the average thickness of the metal loss. This type of measurements was performed in previous studies and the result was consistent with the electrical resistance method. In other words, if the furnace electrical resistance measurement indicates 1 mil metal loss, the value can be confirmed by micrometer measurement in the laboratory. To perform such measurement, the ASTM surface cleaning procedure or similar method has to be used to remove the deposit from the surface. Because all the current coupons are preserved for further SEM and/or

chemical analysis, the metrology measurement of the coupon thickness were only done for a few samples, and the result were quite consistent with the resistant method.

Figure 25 is an SEM picture of the ash layer on the sensor surface, with EDS analysis of the elements. The sensor was used at the waterwall location. The spherical particles in the picture are typical coal fly ash particles. The estimated average diameter of the particle is smaller than typical fly ash particles collected at the electrostatic precipitator. The ash deposit also appears to have attached to larger bulging irregular-shaped base. The elements found in the EDS analysis are common fly ash components.

The SEM picture of Figure 26 focused on the part of the sensor surface that is free of ash deposit. In the picture, there appear to be a thin layer attaching to the rough surface, with a few ash spheres here and there. The EDS analysis indicates that the thin layer is mostly made of iron and oxygen, whereas the rough base is mostly iron. The result indicates that the thin layer is likely the corrosion product. The rough base is the fresh metal surface after the thin layer peeled off. The sensor surface is then further tilted to allow a side view of the corrosion product, as shown in Figure 27. The rough metal surface has granular type of roughness dimension on the order of 1-3 μm . The corrosion product layer has a thickness of about 5-10 μm . The top of the corrosion layer appear to have a melted substance, and the bottom of the layer is more granular.

Based on the SEM analysis of the sensor surface, we can form the picture of metal corrosion on the sensor surface, as shown in Figure 28. Such a model is helpful in establishing the detailed description of the complex interactions and reactions among gas-melt-solid phases.

A type of interesting ash morphology is observed in the SEM analysis, shown in Figure 29. Among the typical spherical ash particles, clusters of needle type of structure were noticed in the picture. This type of structures is not seen in coal fly ash collected in the electrostatic precipitators. The EDS analysis showed somewhat different elemental composition from fly ash particles. It could be the unique environment near the sensor surface that caused the formation of some type of crystals.

CONCLUSIONS

Two corrosion monitoring systems were designed and built in the laboratory, and successfully tested in a muffle furnace. The difficulty and high cost of capacitance sensor fabrication led us to focus our effort on resistance sensors. Full-scale power plant measurements indicated that the system can determine the corrosion rate for waterwall and superheater tubes. The results at the superheater location show that biomass co-firing has two scenarios regarding its impact on fireside corrosion. When a fresh coupon is first exposed to biomass co-firing, the corrosion rate for biomass co-firing is much higher than the case when the coupon is first exposed to 100% coal firing and then biomass co-firing. The waterwall corrosion rate for 100% coal firing is similar to, but smaller than that for the superheater location. Also, the waterwall corrosion rate appeared to be higher at higher boiler load for coal. SEM with EDS analysis provided a detailed picture of the corrosion on the sensor surface. A three-layer corrosion model was proposed with metal at the bottom, corrosion product layer in the middle, and ash deposit layer at the top. The cracking and peeling off of the corrosion product layer exposed the metal to further corrosion

REFERENCES

- [1] Harb, J. N. and Smith, E. E., 1990, "Fireside Corrosion in PC-fired Boilers," *Progress in Energy and Combustion Science*, **16**, No. 3, pp.169-190.
- [2] Dooley, B. and Chang, P., 2000, "The Current State of Boiler Tube Failures in Fossil Plants," *Power Plant Chemistry 2000*, **2**, No. 4.
- [3] Cultler, A. J. B., Flatley, T. and Hay, K. A., 1980, "Fireside Corrosion in Power-station Boilers," *Combustion*, **12**, pp. 17-25.
- [4] Kane, R. D., 2002, "Corrosion Monitoring for Industrial and Process Applications," *Corrosioneering, Newsletter, InterCorr International, Inc., Houston, Texas USA*.
- [5] Natesan, K., Purohit, A. and Rink, D. L., 2001, "Fireside Corrosion of Alloys for Combustion Power Plants," Argonne National Laboratory, 9700 South Cass Avenue, Argonne, IL 60439.
- [6] Natesan, K., 2001, "Fireside Corrosion of Alloys for Combustion Power Plants," Advanced Research Materials Program, Work Breakdown Structure Element ANL-4, Under Contract w-31-109-Eng-38.
- [7] Natesan, K. and Kraus, C., 2000, "Corrosion Performance of Structure Alloys and Coatings in Presence of Deposits," *Proc. 15th Ann. Conf. on Fossil Energy Materials*, Knoxville, TN, USA.
- [8] Viswanathan, R. and Bakker, W. T., 2000, "Materials for Boilers in Ultra Supercritical Power Plants," *Proceeding of 2000 International Joint Power Generation Conference*, Miami Beach, Florida.
- [9] Farrell, D. M. and Robbins, B. J., 2000, "Online Corrosion and Thermal Mapping of Industrial Plants by Non-intrusive Means," Rowan Technologies Ltd, UK, *Corrosion 2000*.
- [10] Jaske, C. E., Beavers, J. A. and Thompson, N. G., 1995, "Improving Plant Reliability Through Corrosion Monitoring," *Fourth International Conference on Process Plant Reliability*, Houston, Texas, USA.
- [11] ASTM Standard: G96-90 (2001) e1 Standard Guide for On-line Monitoring of Corrosion in Plant Equipment (Electrical and Electrochemical Methods), 2002 ASTM International, West Conshohocken, PA.
- [12] ASTM Standard: G1-90 (1999) e1 Standard Practice for Preparing, Cleaning and Evaluating Corrosion Test Specimens, 2002 ASTM International, West Conshohocken, PA.

- [13] Blough, J. L. and Seitz, W. W., 1996, "Fireside Corrosion Testing of Candidate Superheater Tube Alloy and Cladding Phase II Field Testing," Technical Report, Livingston, NJ: Foster Wheel Development Corporation, ORNL/SUB/93-SM401/01.
- [14] Weele, S. V. and Blough, J. L., 1990, "Literature Search Update • Fireside Corrosion Testing of Candidate Superheater Tube Alloys, Coating and Cladding," NJ: Foster Wheel Development Corporation. FWC/FWDC/TR-90-11.
- [15] Weele, S. Van and Blough, J. L., 1991, "Literature Search Update•Fireside Corrosion Testing of Candidate Superheater Tube Alloys, Coating and Cladding," NJ: Foster Wheel Development Corporation. ORNL/SUB/89-SA187/02.
- [16] Hurley, J. P. and Weber, G. F. et al, 2000, "Engineering Development of Coal-fired High-Performance Power Generation Systems Phase II and Phase III," Corrosion Testing to Support the Development of Advanced, High-performance Coal-fired Power Systems, Combustion 2000.
- [17] Davis, K. A., Green, G. C., Linjewile, T. and Harding, S., 2001, "Evaluation of an On-line Technique for Corrosion Characterization in Furnaces," *Joint International Combustion Symposium*, AFRC/JFRC/IEA, Kauai, HI.
- [18] Farrell, D. M. and Robins, B. J., 1998, "Online Monitoring of Furnace Wall and Superheater Corrosion in Power Generation Boilers," VTER Technical Paper, CSS 98, 39th corrosion Science Symposium, 8th Sept. 98, University of Northumbria at Newcastle, U.K.
- [19] Jaske, C. E. and Shannon, B. E., 2002, "Inspection and Remaining Life Evaluation of Process Plant Equipment," *Proceedings of the Process & Power Plant Reliability Conference*.
- [20] Farrel, D. M. and Robins, B. J., 2002, "On-line Corrosion Mapping Using Advanced Electrical Resistance Techniques," UK NDT 2002 Conference.
- [21] Seth, V. K., and Sagues, A. A., 1983, "Use of a Continuously Monitoring Corrosion Probe in a Fluidized Bed Combustor," Paper 38, Corrosion 83, NACE, Houston.
- [22] McKenzie, M. and Vassie, P. R., 1985, "Use of a Weight Loss Coupons and Electrical Resistance Probes in Atmosphere Corrosion Tests," *British Corrosion Journal*, **20**, No. 3, pp. 117-124.
- [23] Haynes G. S. and Baboian R., 1983, "Laboratory Corrosion Test and Standards," ASTM Special Technical Publication 866, Texas Instruments, Incorporated, Philadelphia.
- [24] Gareau, F. S, 1988, "Remote Corrosion Monitoring Using an Interactive Data Acquisition and Transfer System," Paper 107, Corrosion 88, NACE, Houston.

- [25] Bergstrom, D. R., 1981, "Case Histories- Electrical Resistance Probes Control Corrosion in Chemical System," *Materials Performance*, **20**, No. 9, pp.17-21.
- [26] Davis, C. J., James, P. J. and Pinder, L. W., 1997, "Combustion Rig Studies of Fireside Corrosion in Coal-fired Boilers," *Corrosion 97*, New Orleans, Louisiana, USA.
- [26] Nelson, W. and Cain, C., Jr., 1960, "Corrosion of Superheaters and Reheaters of Pulverized Coal-fired Boilers and Gas Turbines," *Transactions of the ASME, Journal of Engineering for Power*, **7**, pp. 194-204.
- [28] Hladky, K. and Dawson, J. L., 1982, "The Measurement of Corrosion Using Electrochemical Noise," *Corrosion Science*, **22**, No. 3, pp. 231-237.
- [29] Eden, D. A., Hladky, K., John, D. G. and Dawson, J. L., 1986, "Electrochemical Noise-Simultaneous Monitoring of Potential and Current Noise Signals from Corroding Electrodes," Paper 274, *Corrosion 86*, NACE, Houston.
- [30] Magaino, S., 1988, "Corrosion System Noise Analysis," *Corrosion Engineering*, **37**, No. 11, pp. 629-635.
- [31] Roberge, P. R., Beauudon, R. and Sastri, V. S., 1989, "Electrochemical Noise Measurement for Field Applications," *Corrosion Science*, **29**, No. 10, pp. 1231-1233.
- [32] Farrel, D. M., 1989, "Electrochemical Noise Processes," *Proceeding from UK Corrosion 89*, Vol. 3, Blackpool, pp. 93-107.
- [33] Butcher, D. W., 1983, *On-Line Monitoring of Continuous Process Plants*, Ellis Horwood, Ltd., UK. and John Wiley & Sons, Inc., USA.
- [34] Eden, D. A., Rothwell, A. N. and Dawson, J. L., 1991, "Electrochemical Noise for Detection of Susceptibility to Stress Corrosion Cracking," Paper 444, *Corrosion 91*, NACE, Houston, USA.
- [35] Hlladky, K. and Dawson, J. L., 1981, "The Measurement of Localized Corrosion Using Electrochemical Noise," *Corrosion Science*, **21**, No.4, pp. 317-322.
- [36] Eden, D. A. et al., 1985, "Electrochemical Noise Measurement and Their Applications to Coated Systems," *Division. of PMSE, Papers 1985*, Vol. 53, ACS, pp. 388-390.
- [37] Farrel, D. M., Scott, F. H., Rocchini, G. and Golombo, A., 1992, "Influence of Electrochemical Processes on High Temperature Corrosion Reactions in Combustion System," *Materials at High Temperature*, **10**, No. 1, pp. 11-19.

FIGURES

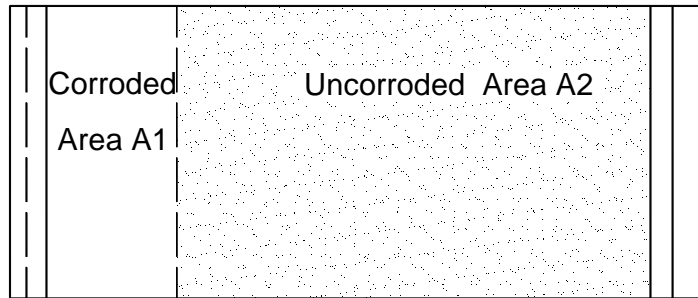
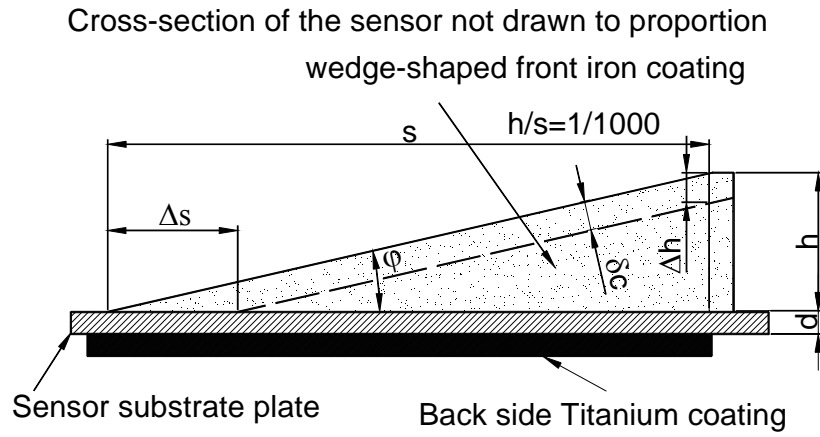


Figure 1. A schematic diagram of capacitance sensor principle.

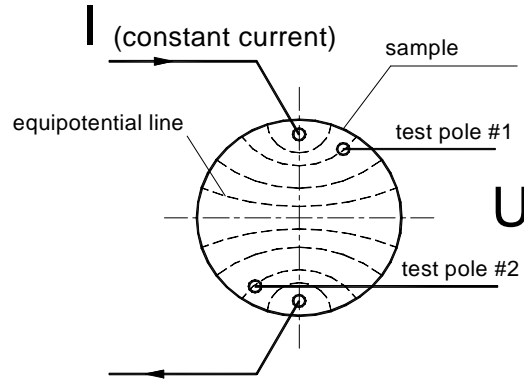


Figure 2. A schematic diagram of equal potential lines for resistance sensor.

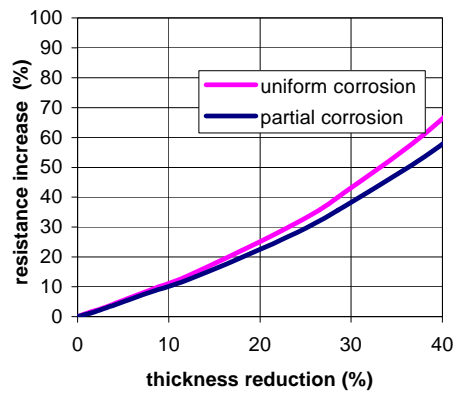


Figure 3. Resistance change with metal thickness reduction

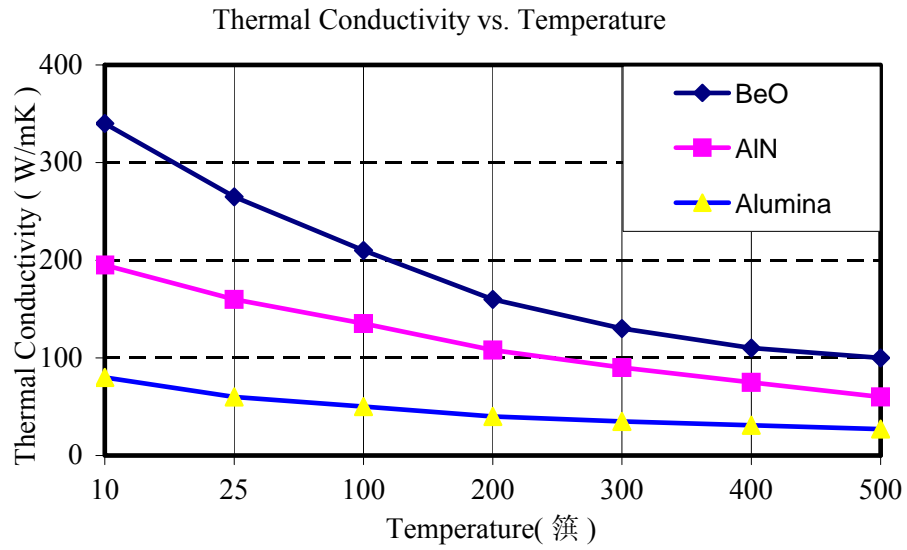


Figure 4. Thermal conductivity of BeO, Alumina (99.6%Al₂O₃) and AlN.

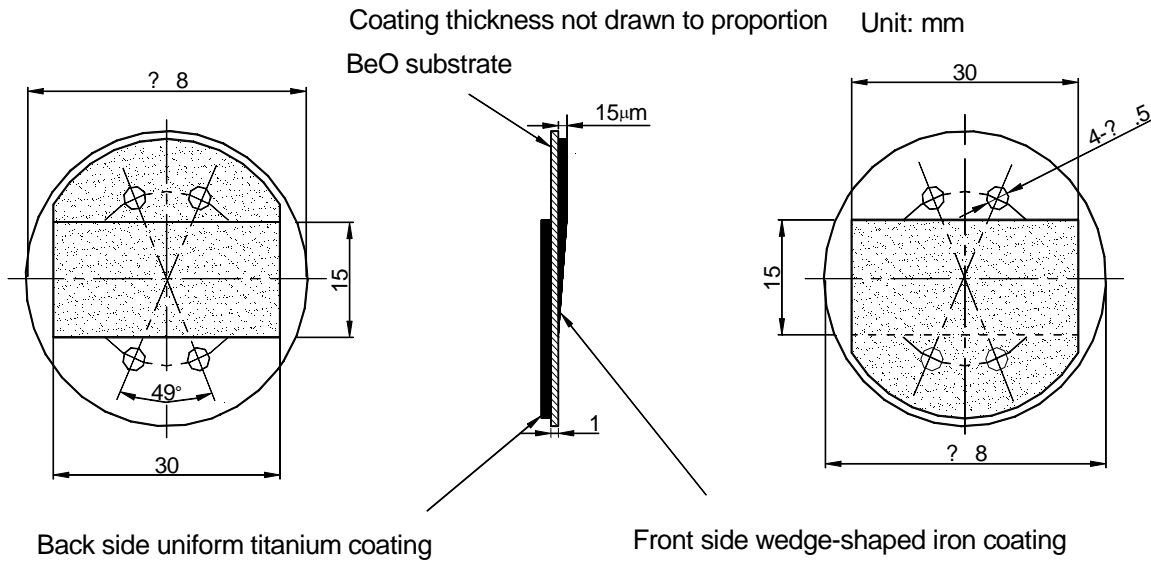


Figure 5. Design drawings of the the capacitance sensor.



Figure 6. A picture of the DC magnetron sputtering deposition system.

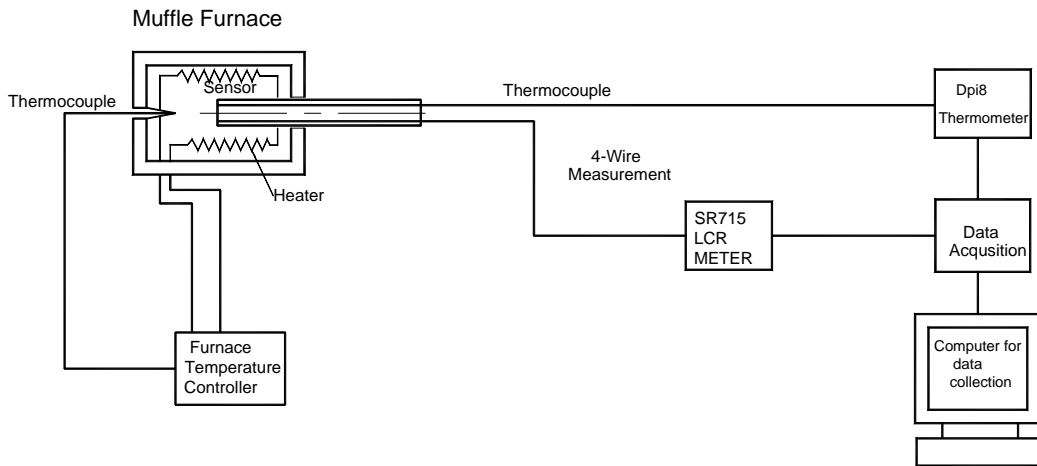


Figure 7. A schematic diagram for the laboratory experimental setup.

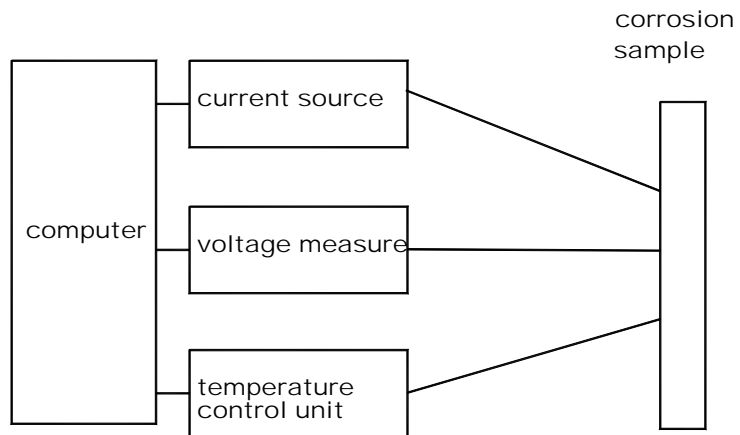


Figure 8. Temperature control system for the probe.



Figure 9. A pictures of wedged iron coating on the capacitance sensor.



Figure 10. Resistance sensors (bottom) and sensor assembly (top)



Figure 11. Temperature control system for the probe.

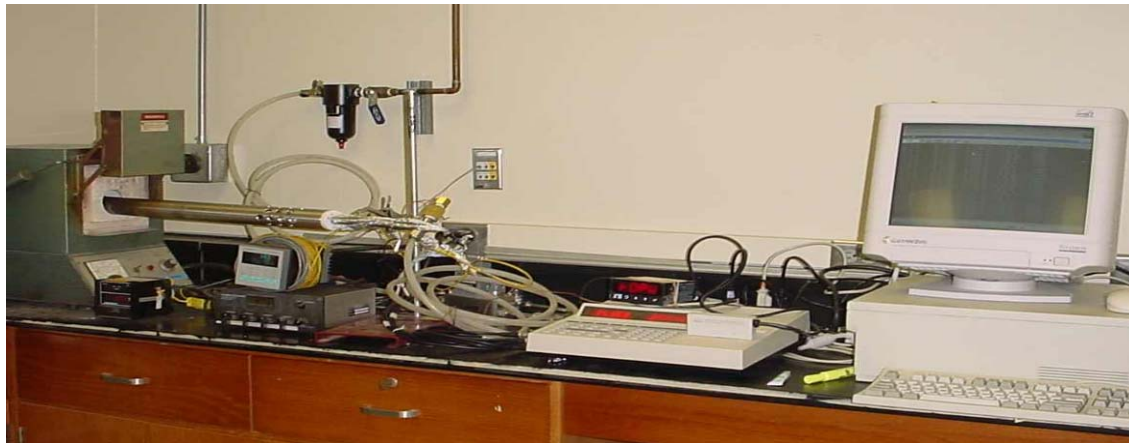


Figure 12. Complete measurement system layout in the laboratory.

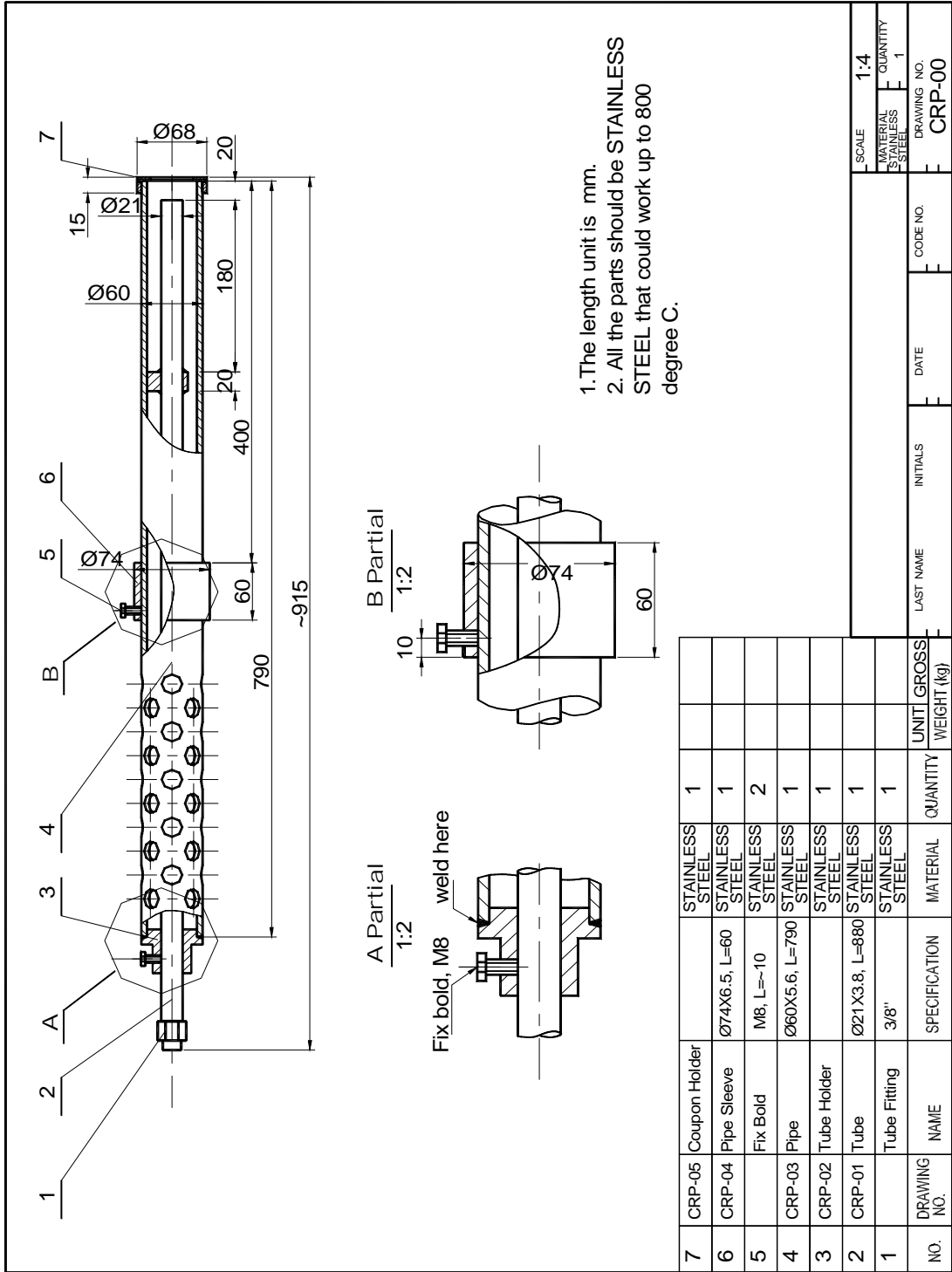


Figure 13. Assembly drawing of the probe.

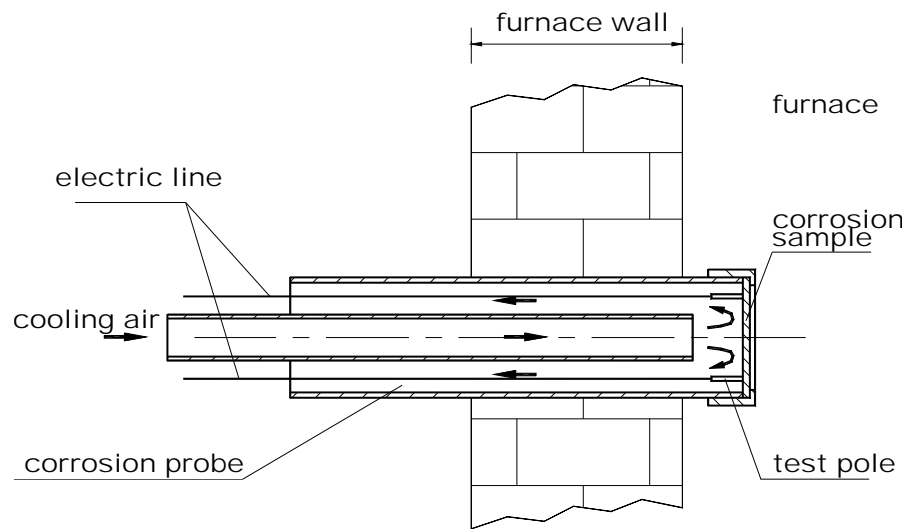


Figure 14. Schematic diagram of probe installation.



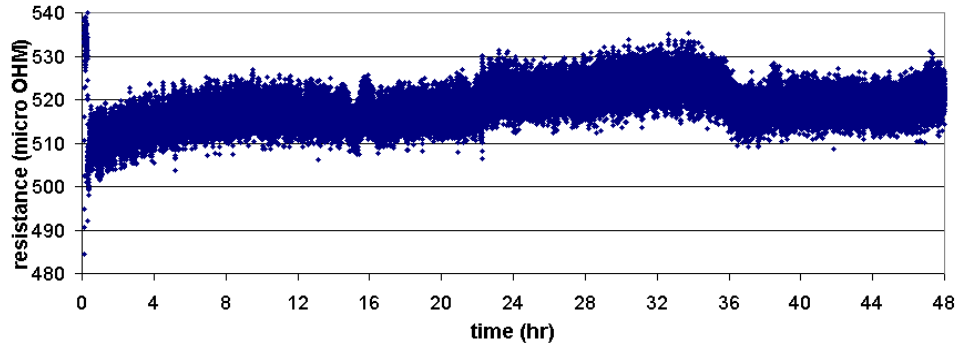
Figure 15. Assembled corrosion probe



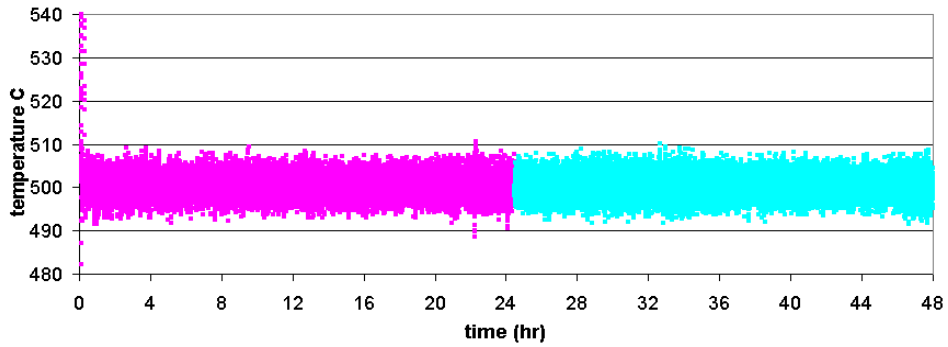
Figure 16. Power plant waterwall measurement.



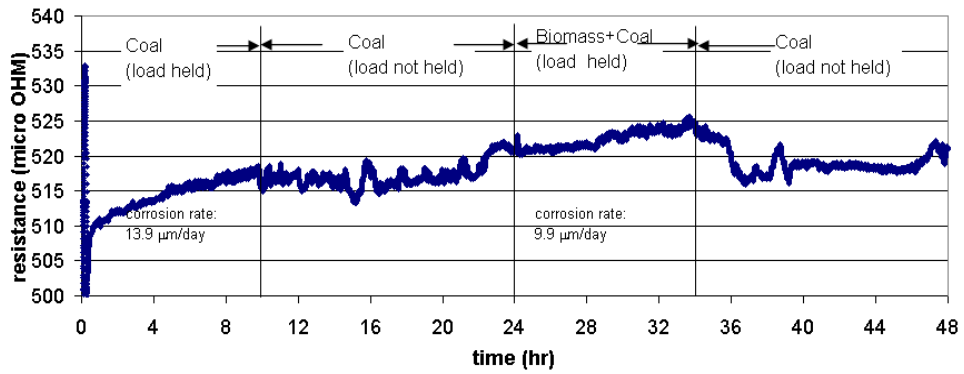
Figure 17. Corrosion probe inserted through the manhole at superheaters.



(a) Coupon resistance raw data

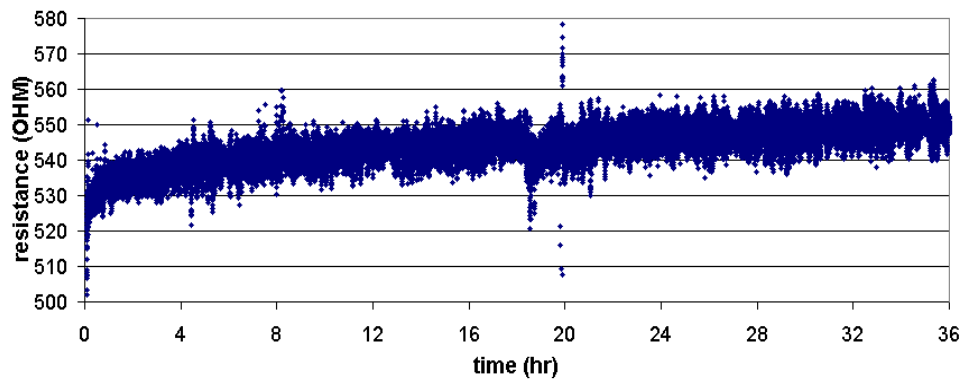


(b) Coupon temperature test result

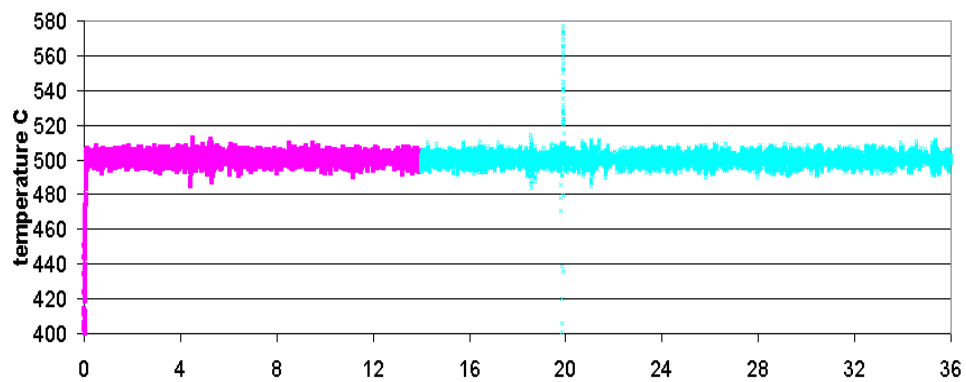


(c) Coupon resistance after noise filtering and temperature compensation

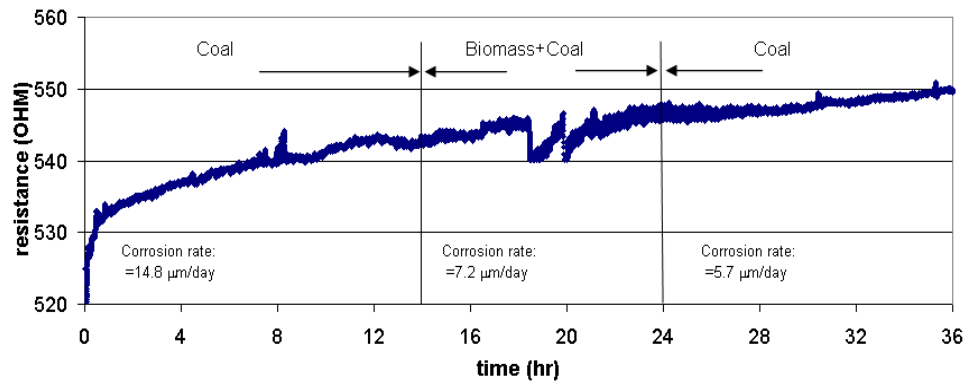
Figure 18. Corrosion at superheater location for coupon A



(a) Coupon resistance test result



(b) Coupon temperature test result



(c) Coupon resistance after filtering and compensation

Figure 19. Corrosion at superheater location for coupon B

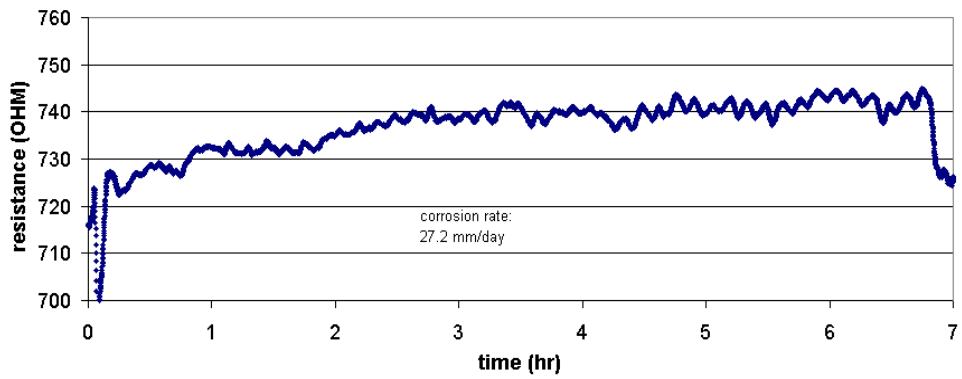


Figure 20. Corrosion with biomass co-firing (Coupon C).

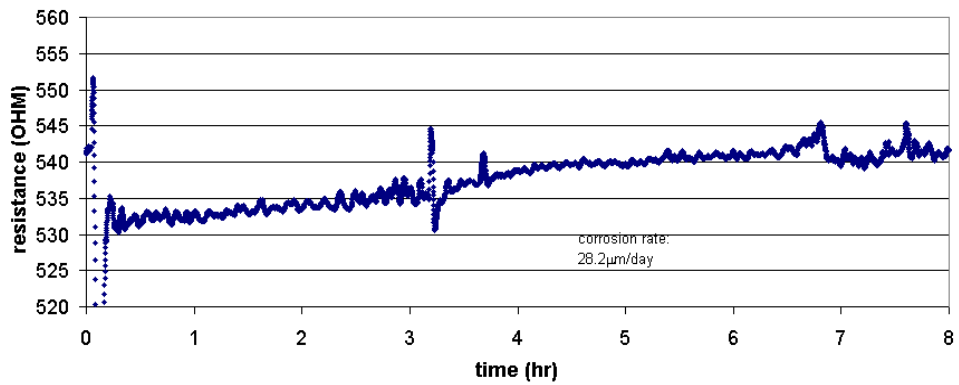


Figure 21. Corrosion in superheater for coupon D

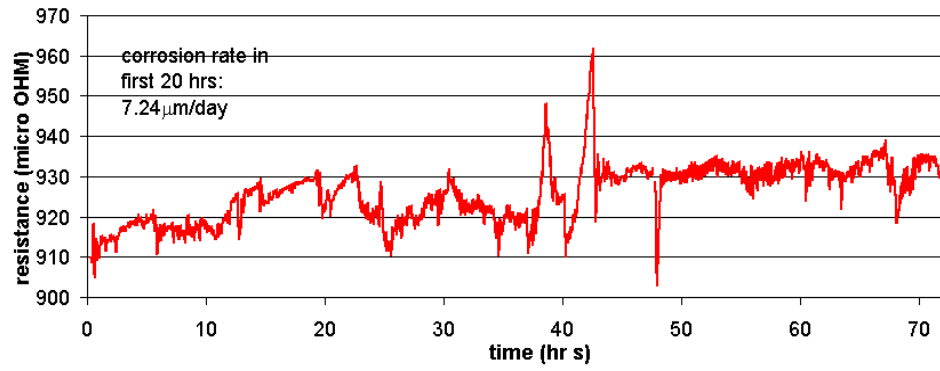


Figure 22. Corrosion at waterwall location for 100% coal.

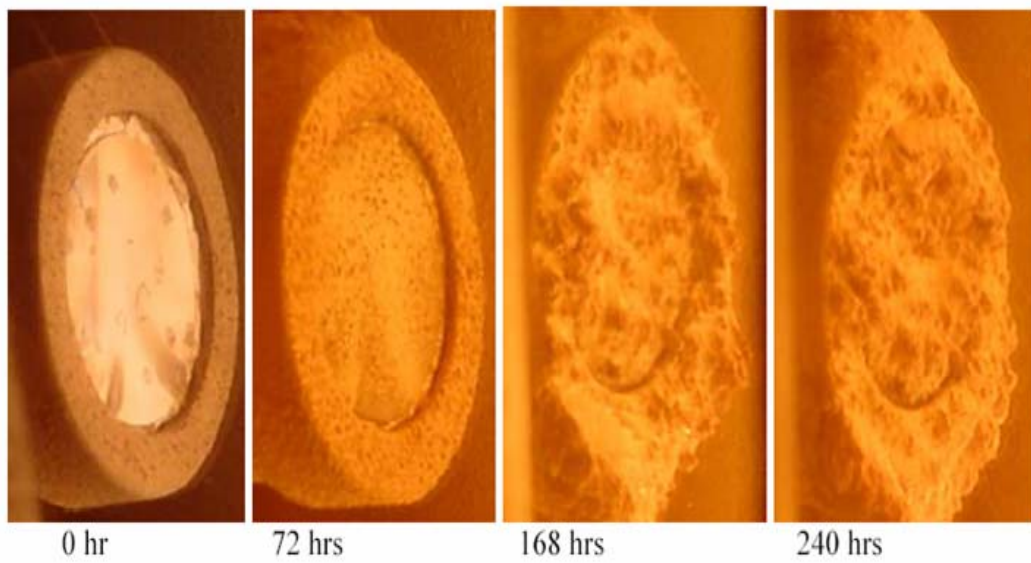


Figure 23. Photo of ash deposition on the coupon inside the waterwall



coupon after test at water wall 160 hr
(coal)



coupon after test at waterwall, 28 hr
(biomass, then coal)



coupon after test at superheater, 50 hr
biomass

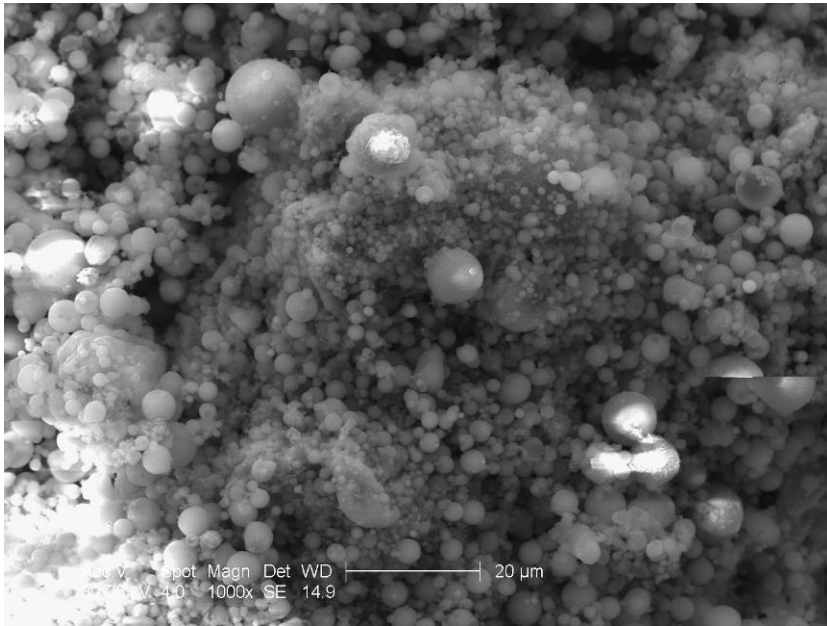


coupon after test at superheater, 8 hr
coal then biomas



coupon after test at super heater, 110 hr
(biomass, then coal)

Figure 24. Pictures of corrosion sensor after use.



C:\Archive\Ban\Waterwall Coal #2 Area Scan.spc

Label A:

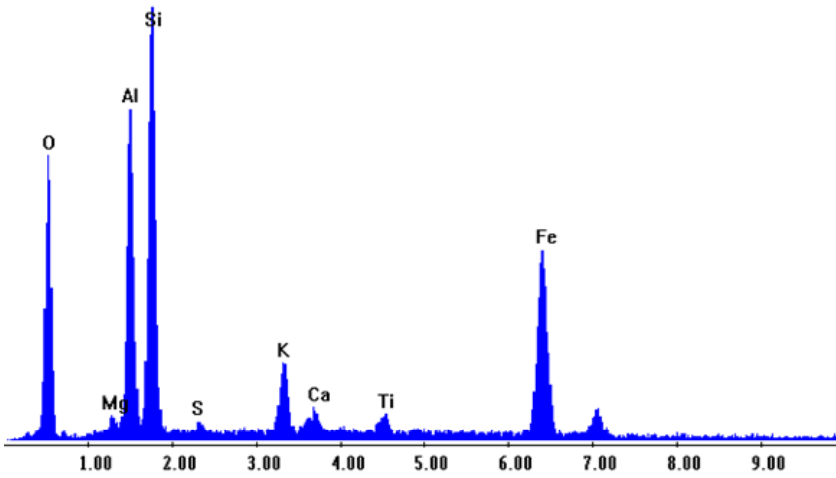
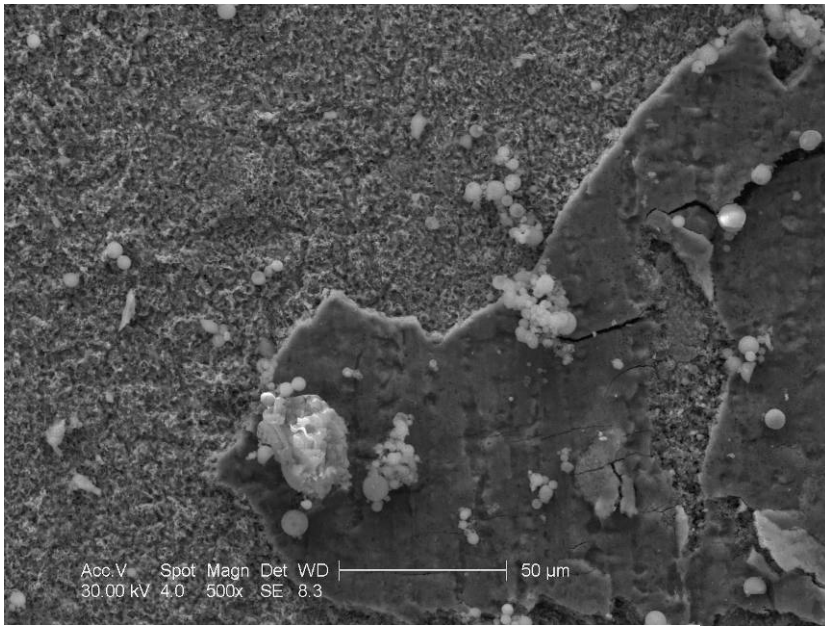
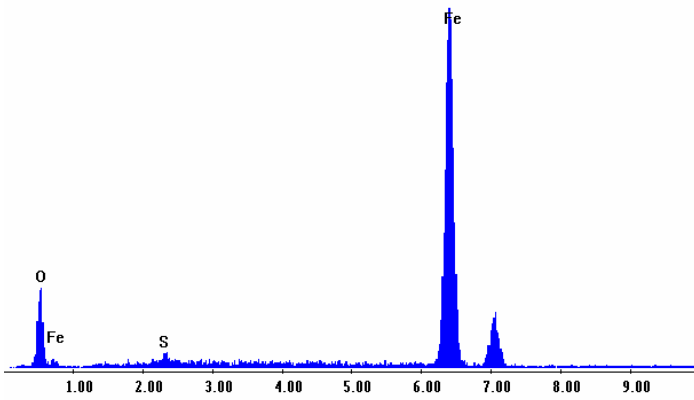


Figure 25. SEM picture and EDS elemental analysis of ash deposit on sensor surface.



C:\Archive\Ban\Waterwall Coal #2 Upper Substrate.spc

Label A:



C:\Archive\Ban\Waterwall Coal #2 Lower Substrate.spc

Label A:

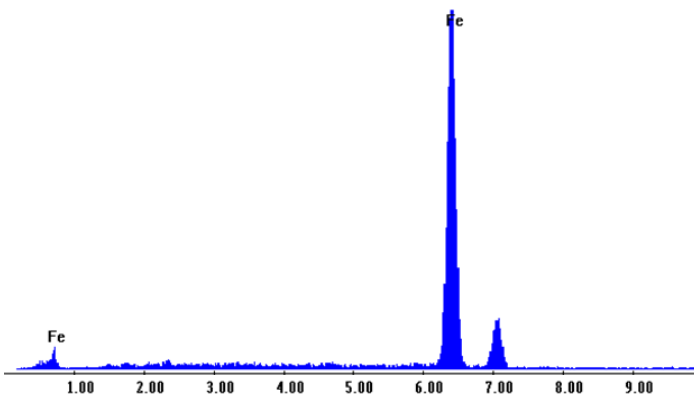


Figure 26. SEM analysis of corroded layer on sensor surface.

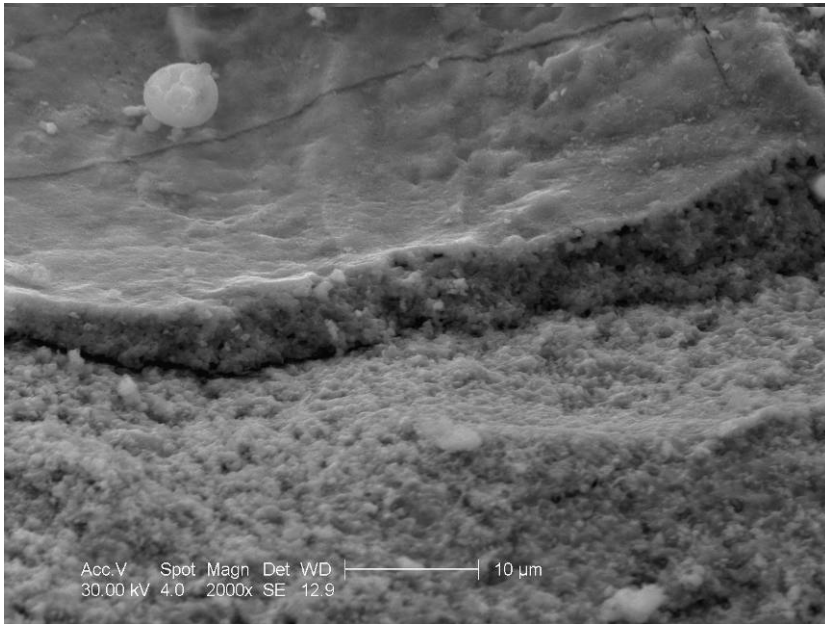


Figure 27. SEM side view of the corroded layer on sensor surface.

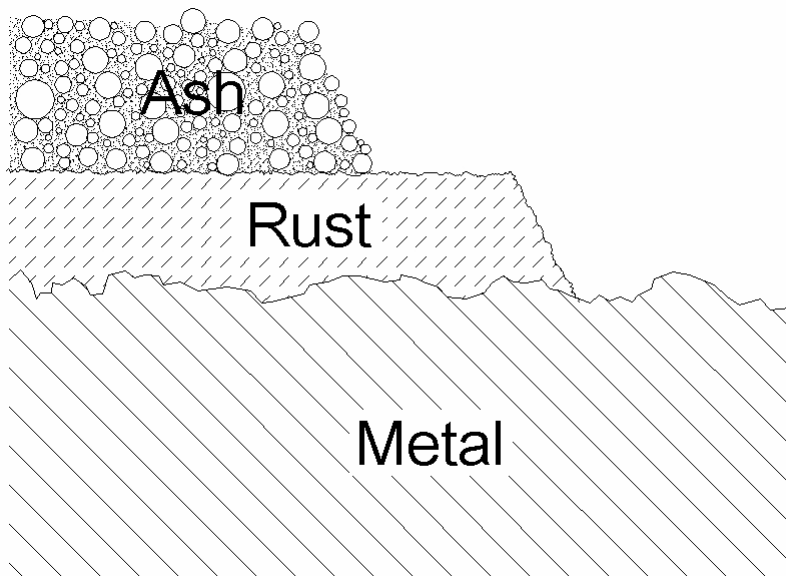
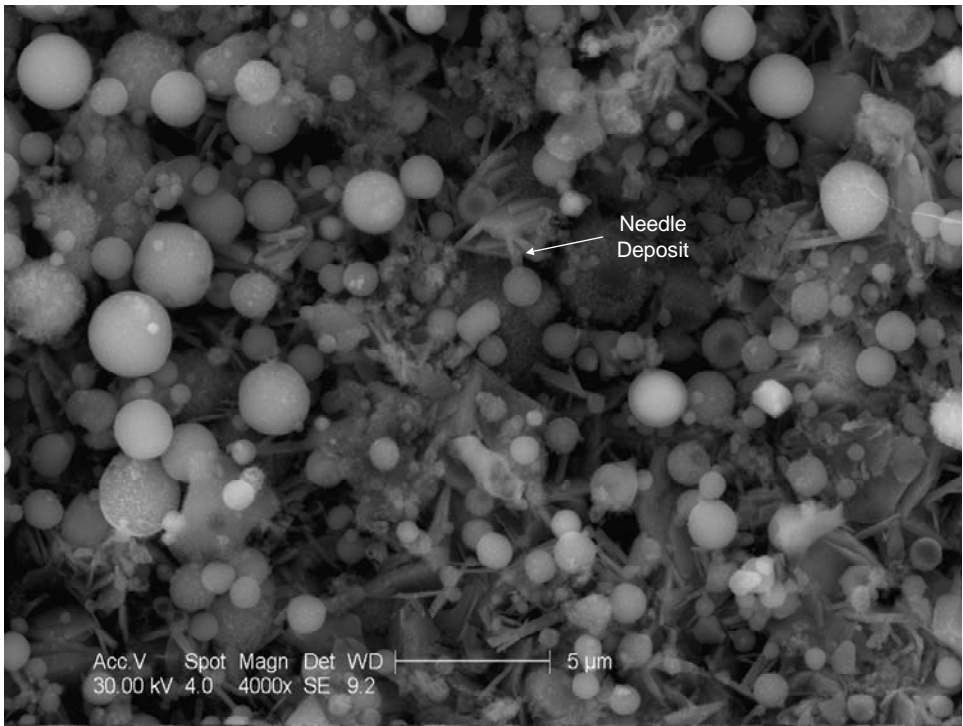


Figure 28. A corrosion model for the metal surface.



C:\Archive\Ban\Superheater Coal #5 Needle.spc

Label A:

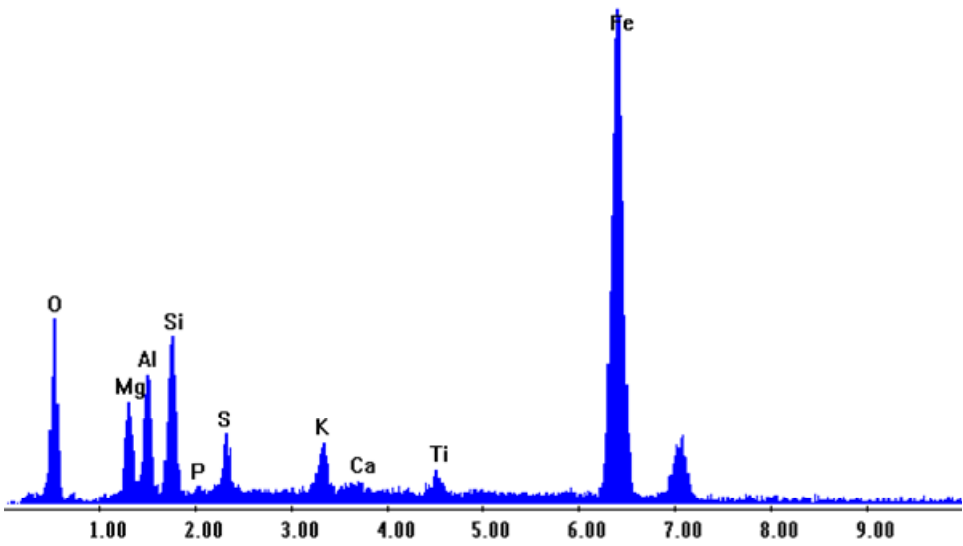


Figure 29. SEM analysis of needles formed in ash deposit on sensor surface.

Publications and Presentations

DE-FG2603NT41807 “Novel Corrosion Sensor for Vision 21 Systems”

PI: Bharat Soni, PhD

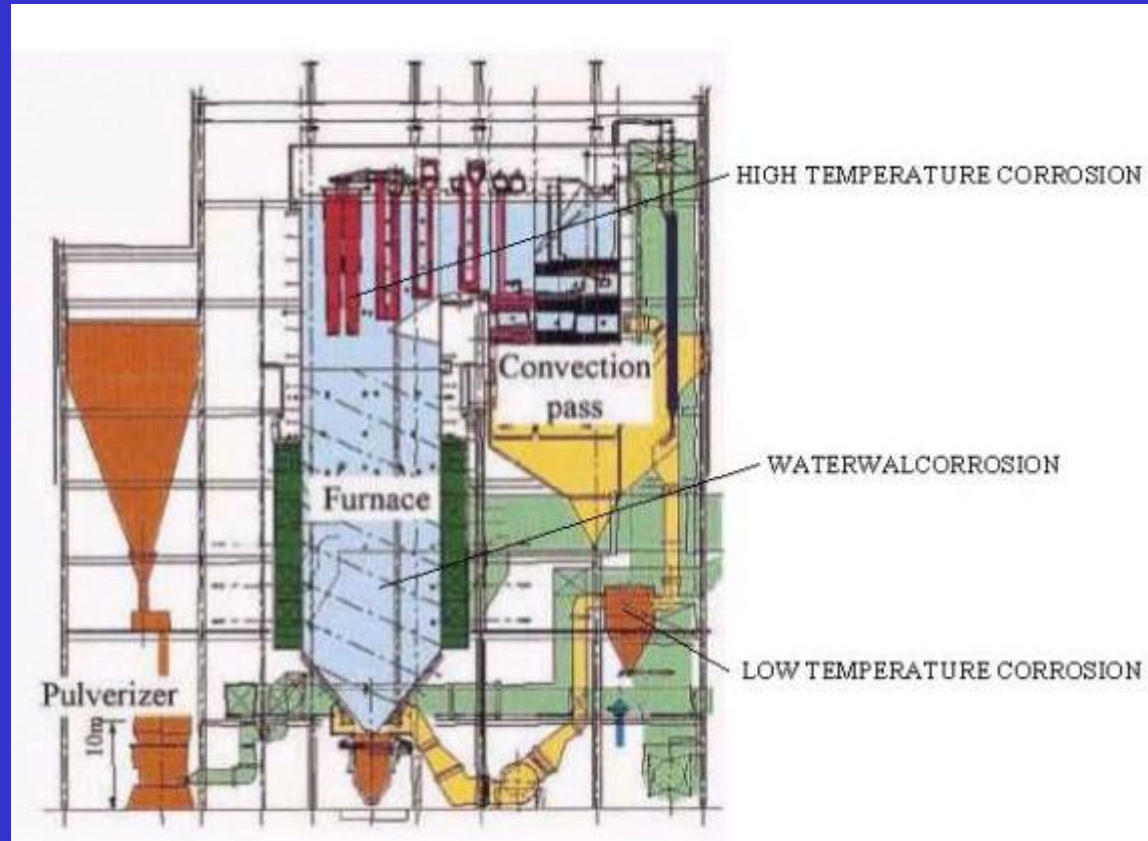
1. Zuoping Li, Heng Ban, Bochuan Lin, A Novel Sensor for Fireside Corrosion Monitoring, Proceedings of the Twentieth International Pittsburgh Coal Conference, 11 pages, 2003
2. Bochuan Lin, Heng Ban, and Arun Mehta, Plant Test of an On-line Fireside Corrosion Monitor, Proceedings of the 29th International Technical Conference on Coal Utilization & Fuel Systems, ISBN No.0-932066-29-05, Library of Congress Card Catalog No.86-06147, Coal Technology Association, Vol. 1, pp.489-496, 2004.
3. B. Lin, H. Ban, C. Boohaker, and B. Zemo, Waterwall and Superheater Fireside Corrosion Measurement, Southern Electric Exchange Annual Conference, Orlando, FL, 2006.
4. US-UK Energy Collaboration Workshop, Oak Ridge, Tennessee, 2006
5. Presentation at Gadsden Steam Power Plant, 2006.

A Novel Sensor and Measurement System for Corrosion Monitoring in Combustion Environments

Zuoping Li, Bochuan Lin & Heng Ban

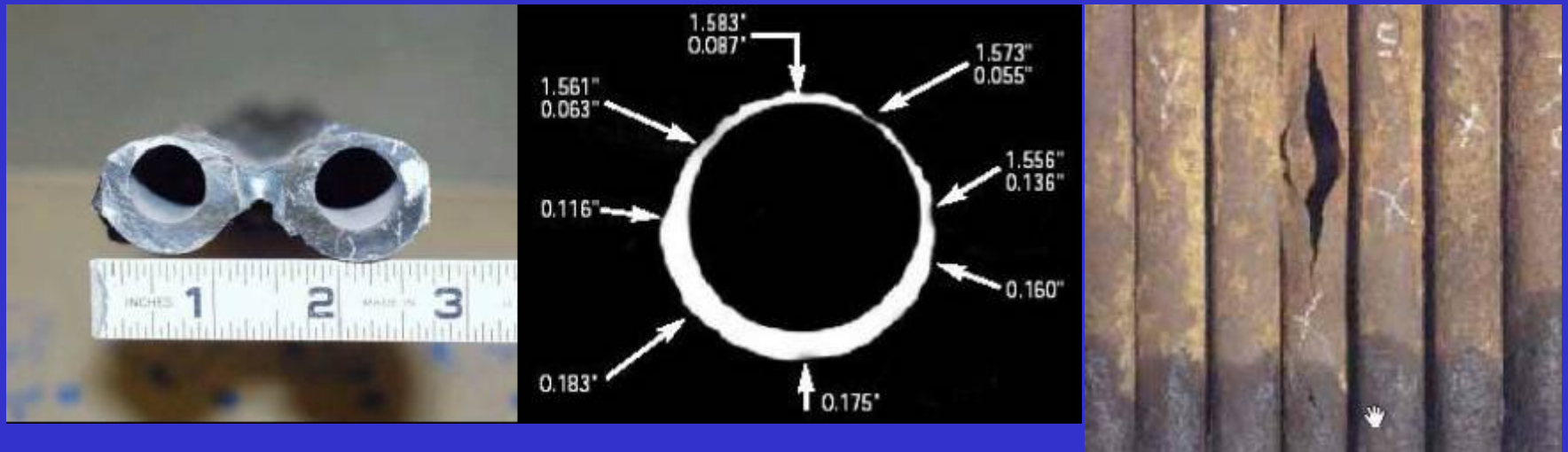
Department of Mechanical Engineering
University of Alabama at Birmingham

Fireside Corrosion



Fireside corrosion is a continuing concern, especially in low emission combustion mode and using opportunity fuels. Corrosion cost electric utilities \$6.9 billion/yr in USA (NACE).

Boiler Tube Failure Due to Fireside Corrosion



Tube failure is the leading cause of boiler shutdowns

Why Corrosion Monitoring

- Diagnoses of corrosion problems
- Advanced warning of system upsets leading to corrosion damage
- Execution of the process control
- Determination of inspections and /or maintenances
- Estimation of the equipment lifetime

Corrosion Monitoring Methods

- Off-line, non-continuous measurement
 - Visual Inspection
 - Radiography (X-Ray)
 - Ultrasonic Testing
 - Weight-loss Coupon
- On-line, continuous measurement
 - Electric Resistance (ER) Technique
 - Electrochemical Noise (ECN) Technique

Challenge

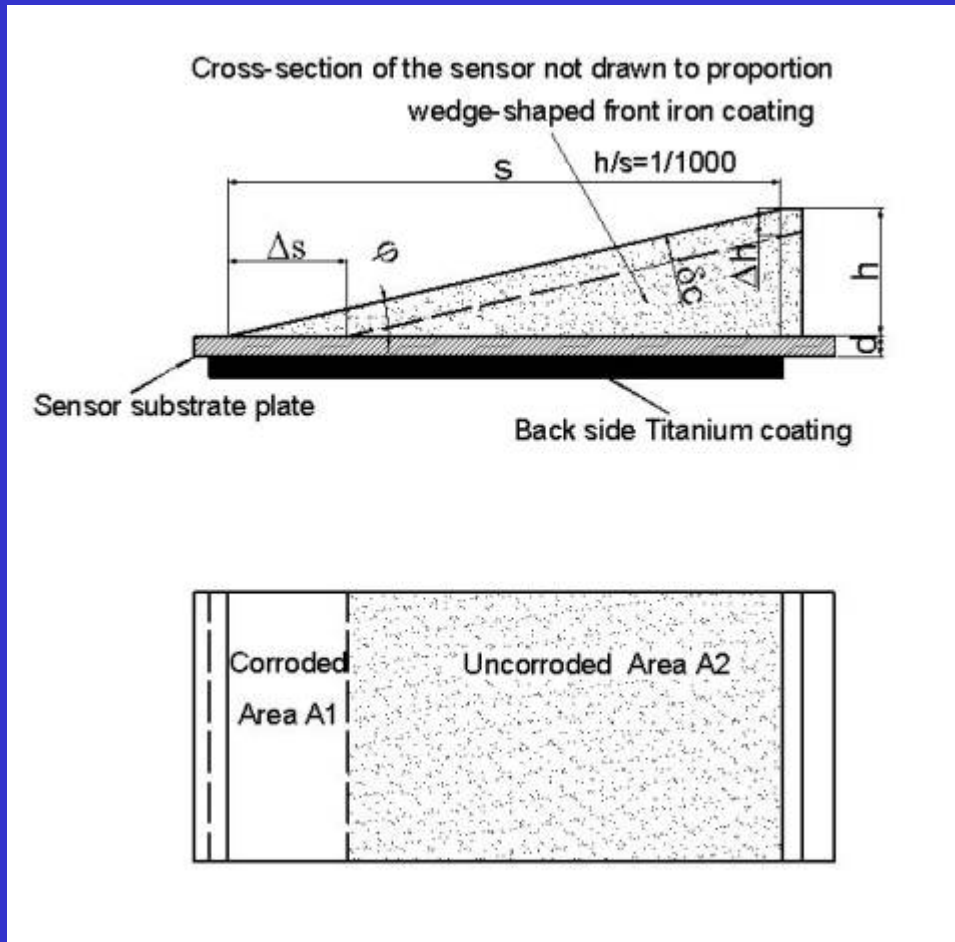
- Off-line measurement made during scheduled or forced outages is unable to get instantaneous corrosion information.
- Online-line continuous measurement is still underdevelopment
- Challenge: to measure corrosion rate in one shift (8 hours)

Objectives

- To examine the feasibility of the new sensor concept in the laboratory.
- To investigate options for sensor design and fabrication.
- To obtain information on measurement uncertainty.

Principle of Novel Sensor

corrosion->area->capacitance



$$C = \frac{\epsilon S}{d}$$

Corrosion rate R is:

$$R = \frac{\Delta C \times d}{\epsilon} \frac{h}{(t - t_0) \sqrt{s^2 + h^2}}$$

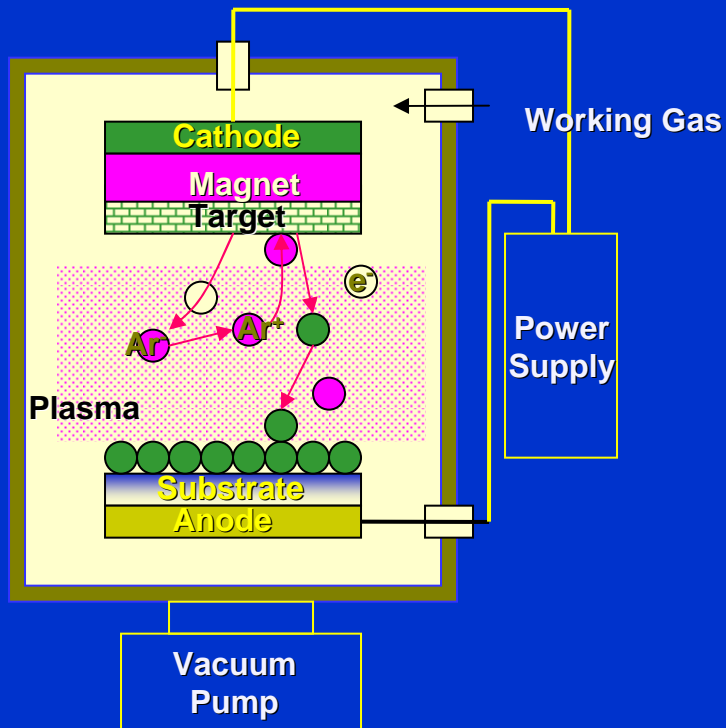
$$R = \frac{\Delta C \times d}{\epsilon} \frac{h}{(t - t_0) s} \quad (\text{since } h \ll s)$$

Fabrication Method

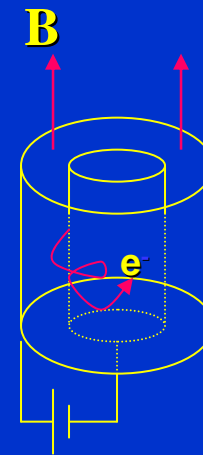
- Magnetron Sputtering Deposition Technology
- Plasma Spray Technology

Sputtering Deposition Process

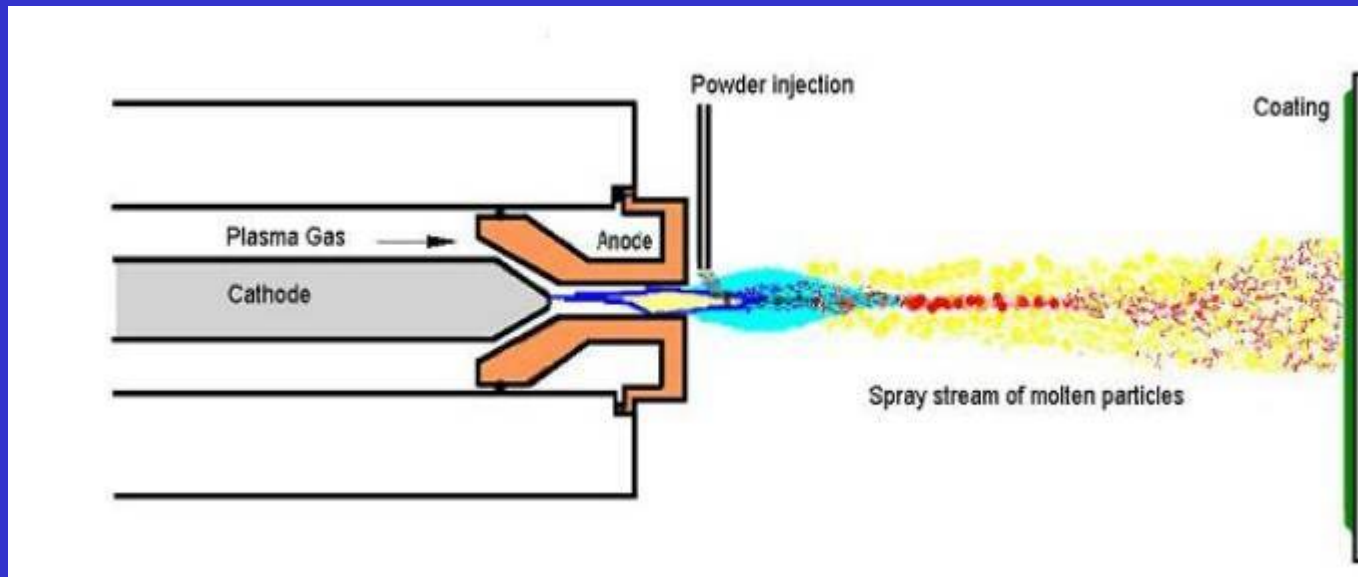
Magnetron Sputtering Deposition System



Cylindrical Magnetrons



Plasma Spray Process

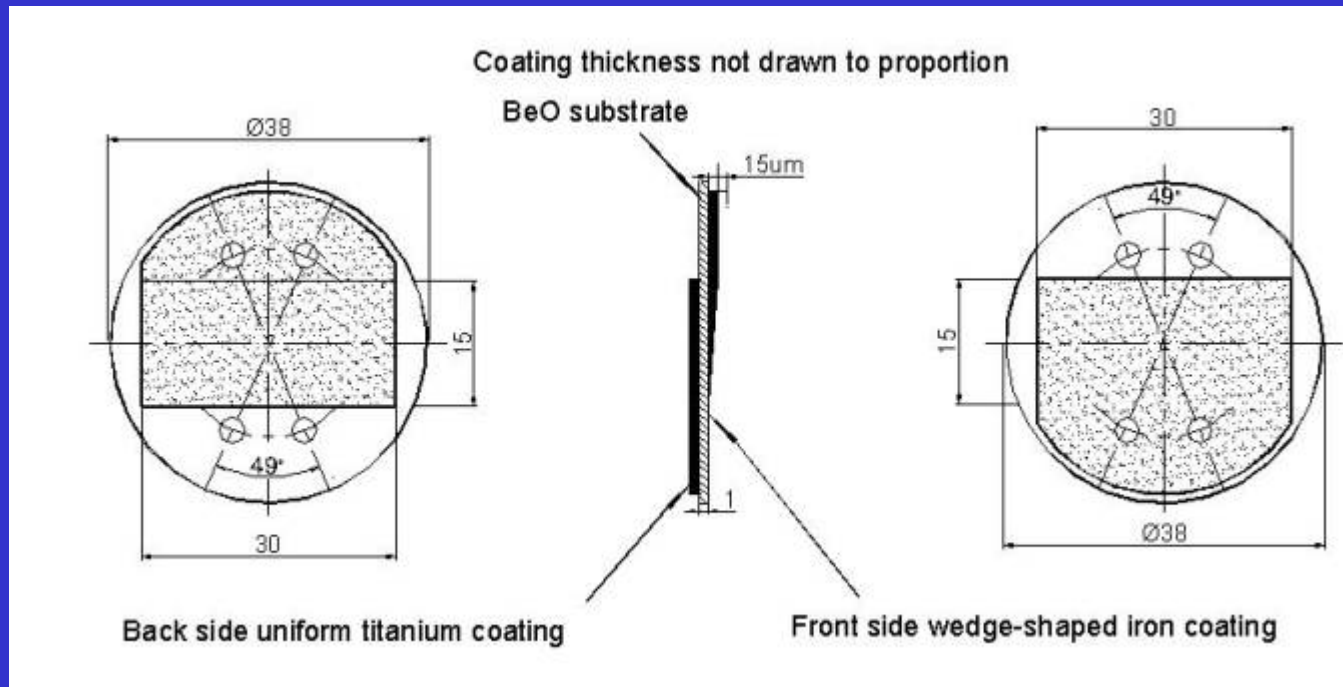


Substrate Materials Selection

- BeO
 - High thermal conductivity
- Alumina (Al_2O_3)
 - High dielectric constant

Novel Sensor Design

Sensor Type 1



Sputtering Deposition for Sensor



DC Sputtering System



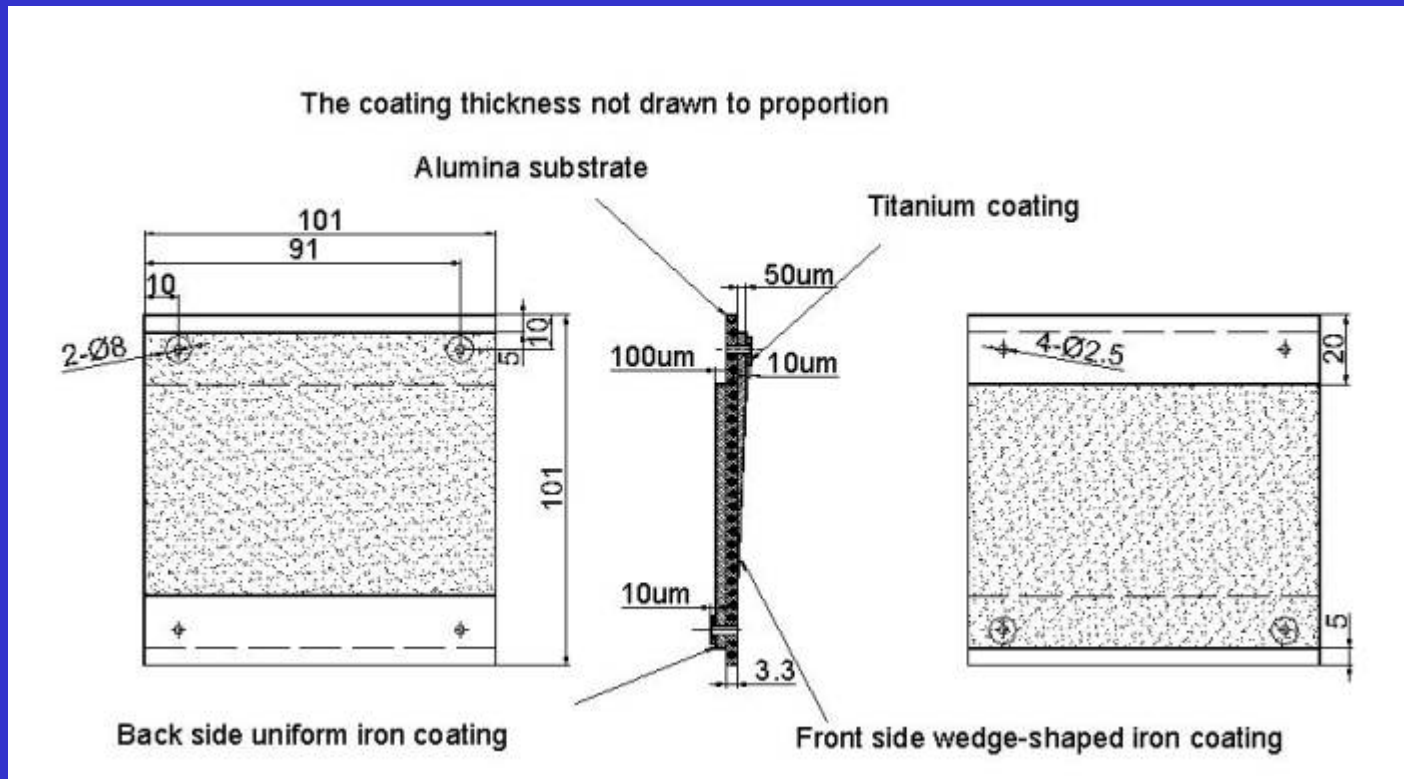
Wedge-shaped Coating



Backside coating

Novel Sensor Design

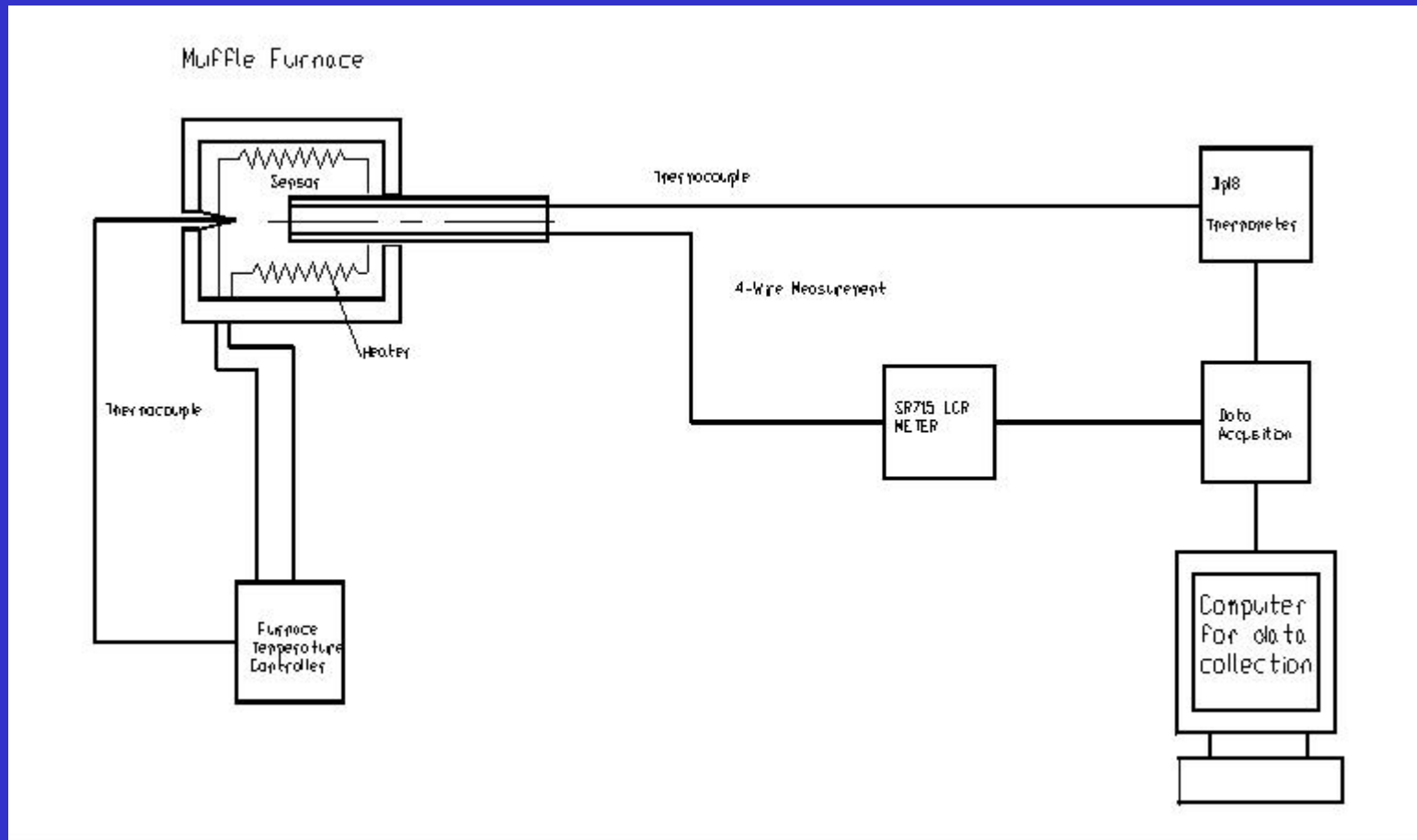
Sensor Type 2



Experimental Setup

1. Muffle Furnace: up to 1000 °C
2. Furnace temperature control: +/- 2 °C
3. Programmable temperature control for the corrosion probe
4. LCR meter (programmable)
5. Data acquisition software and the computer

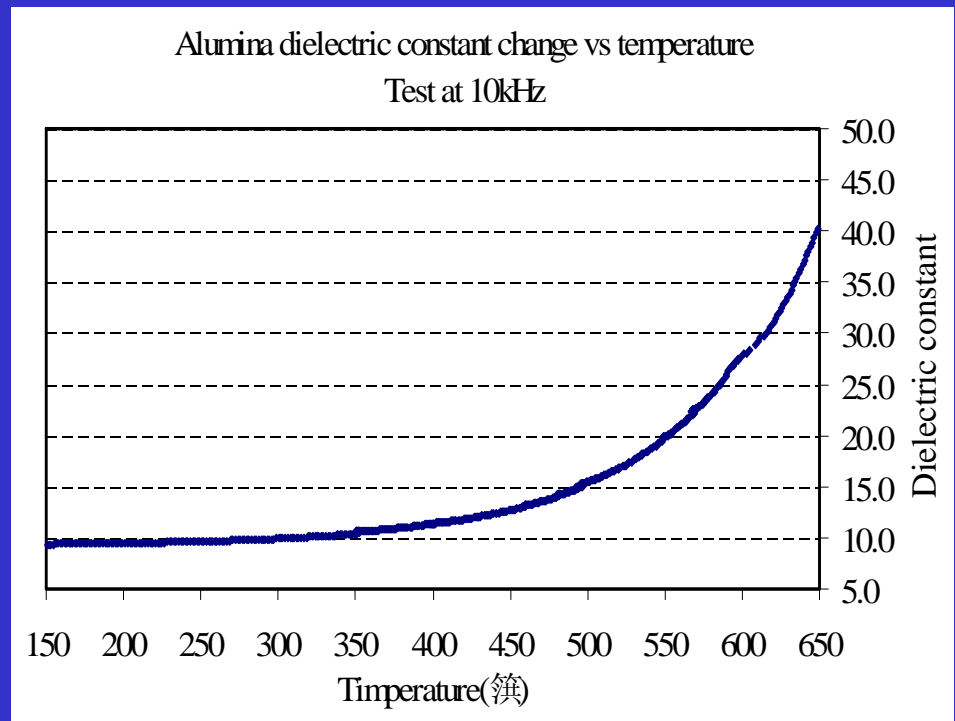
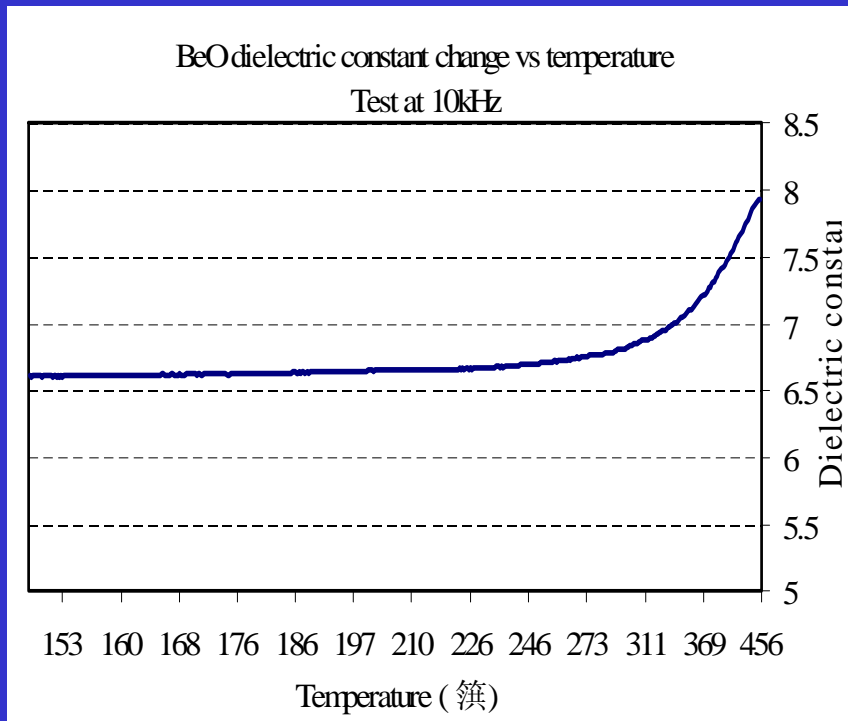
System Diagram



System Picture

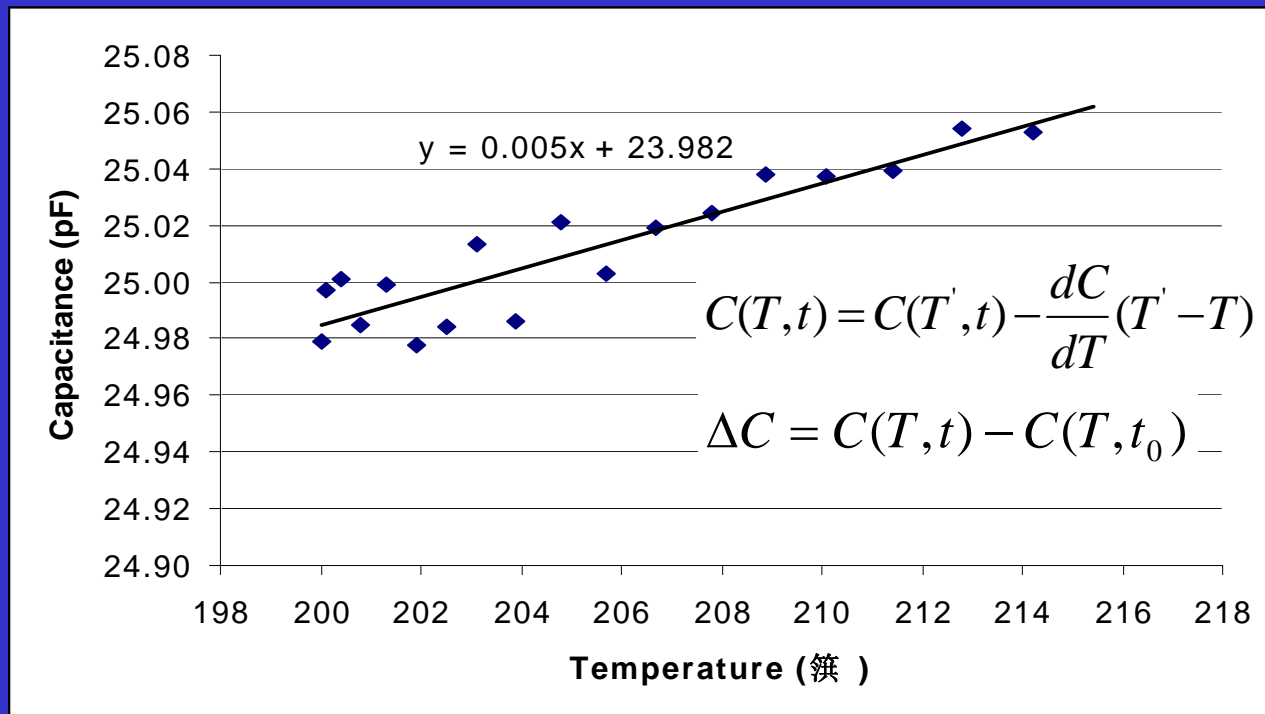


Substrate Dielectric Constant



Reported dielectric constant at 25°C @1MHz: 6.5~6.7 for BeO and 9.3~ 9.8 for Alumina(99.6% Al_2O_3). High temperature values are not available.

Temperature Compensation for Corrosion Rate Calculation

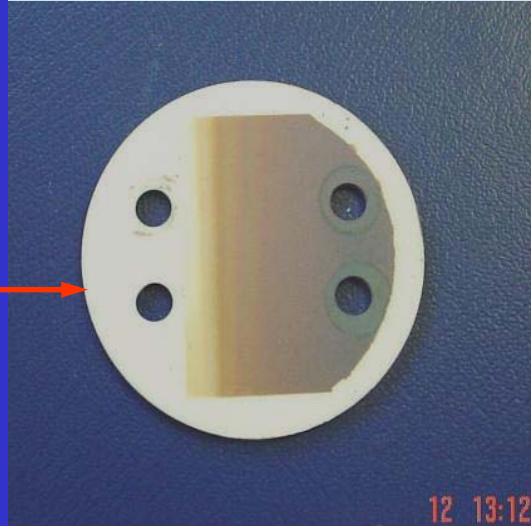


Corrosion Test Results- Sensor Type1

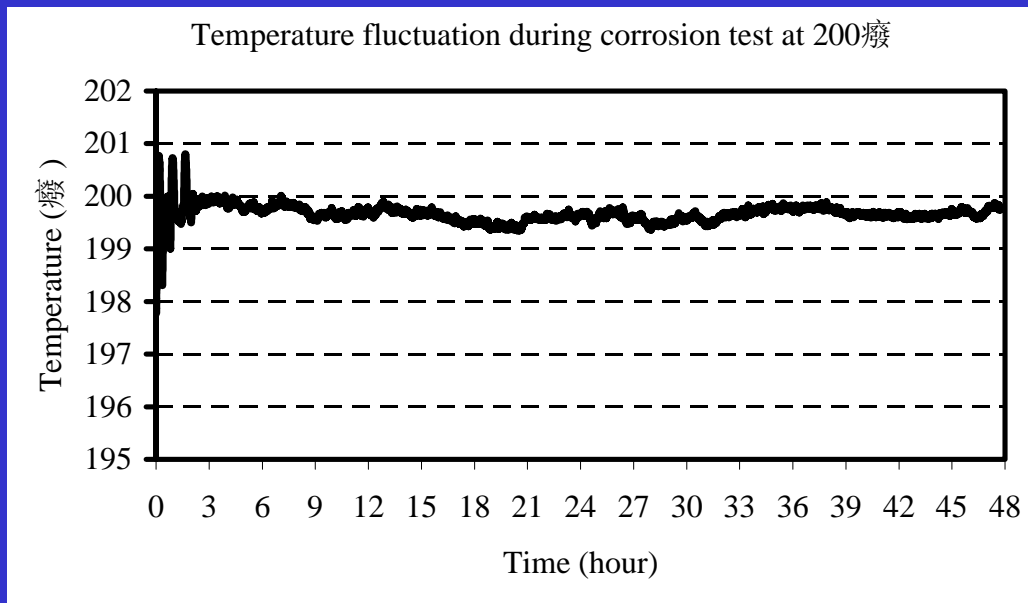
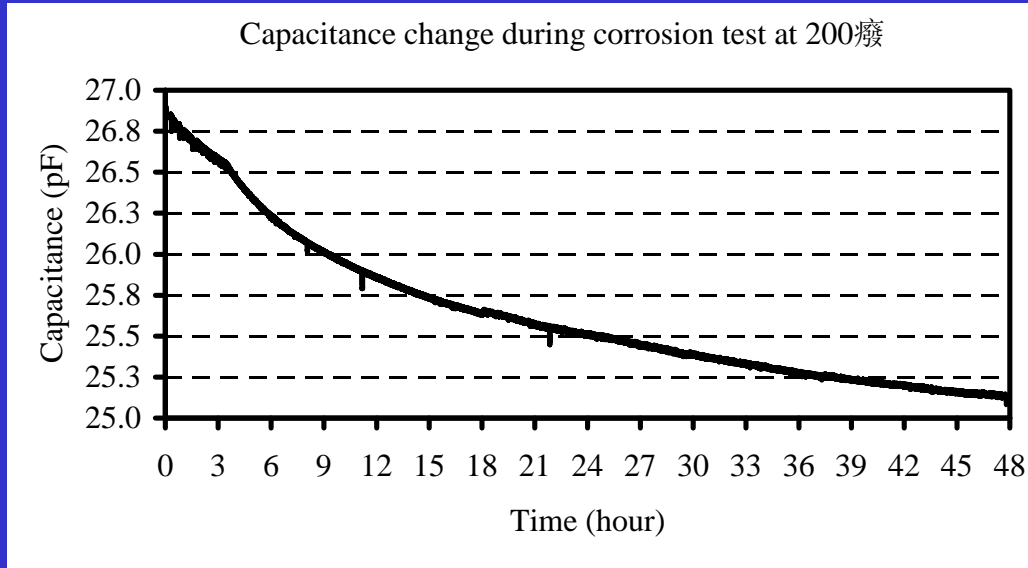
Before corrosion



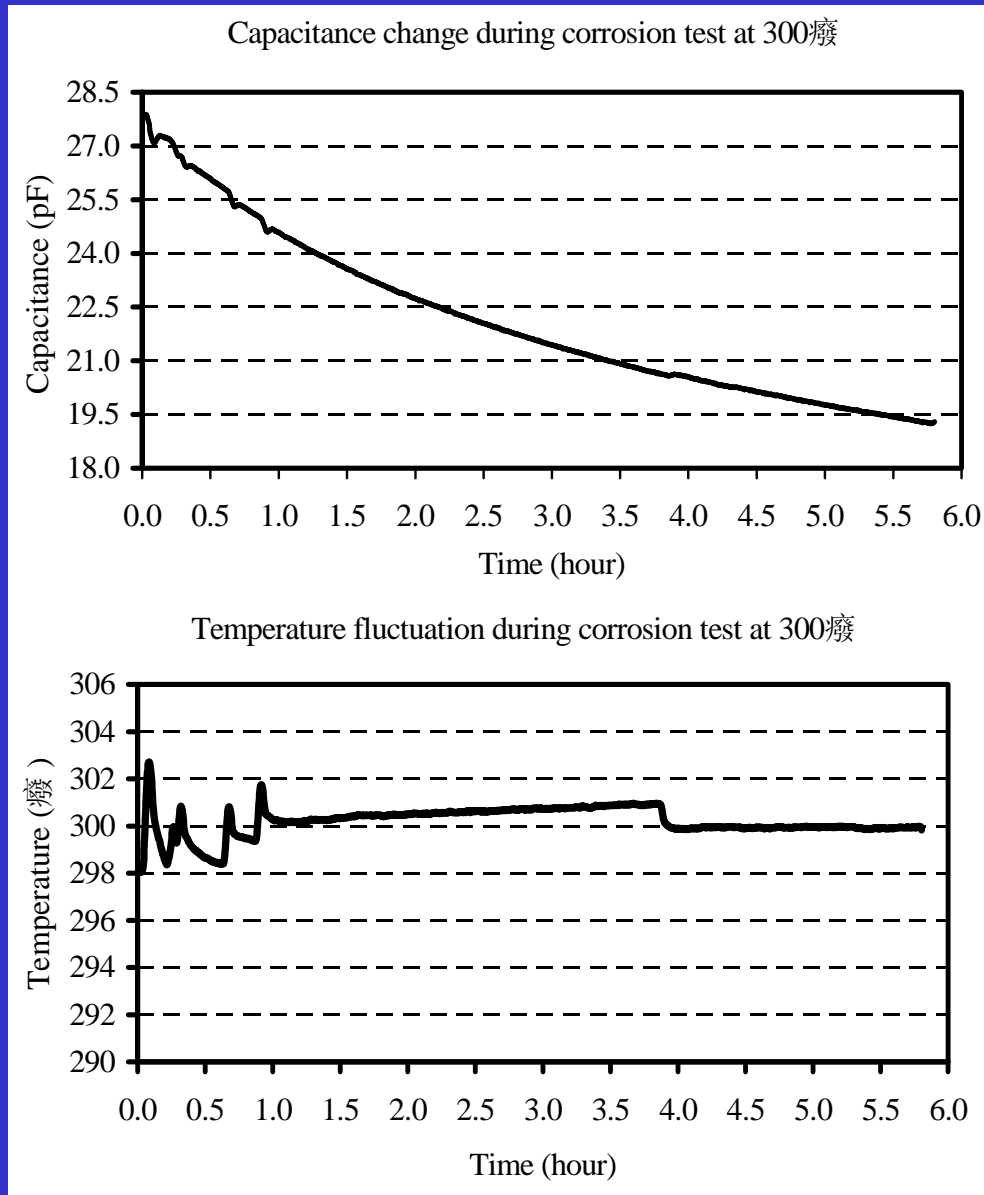
After corrosion



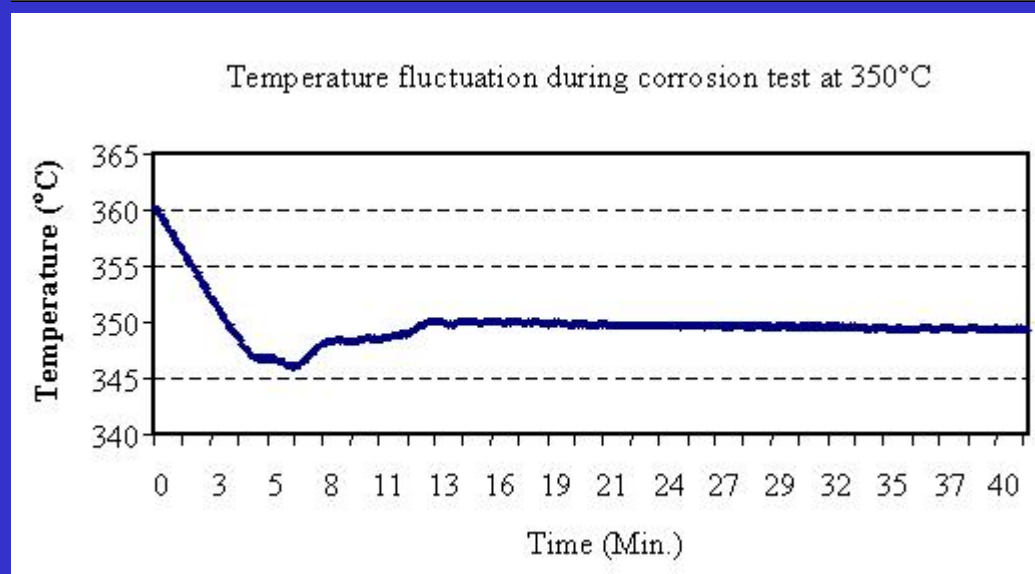
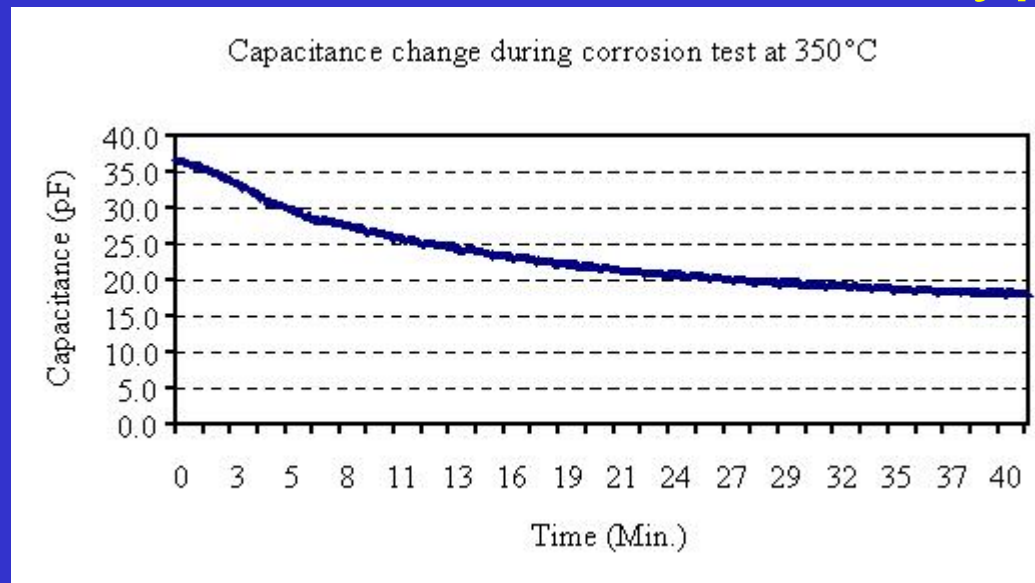
Corrosion Results - Sensor Type 1



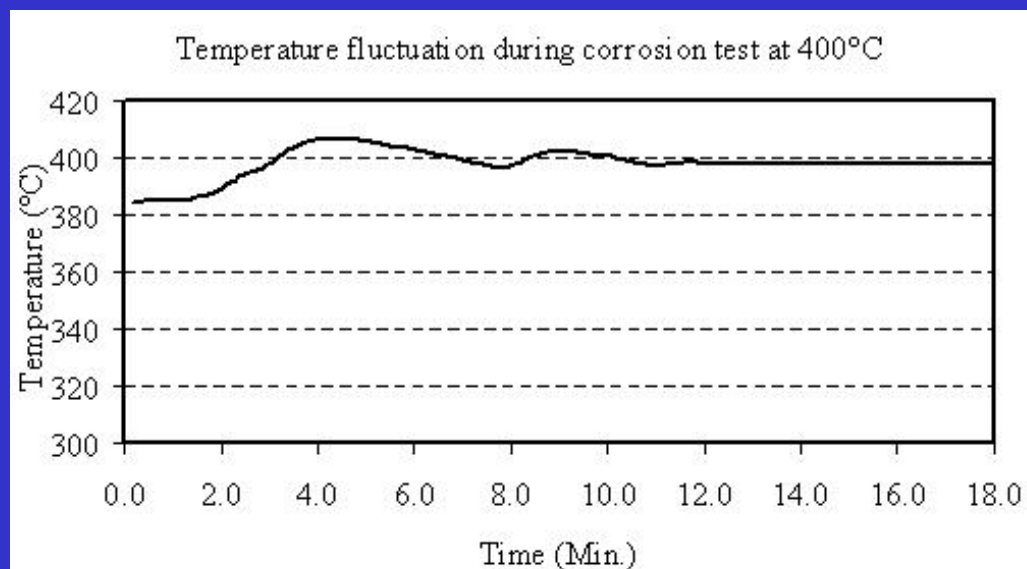
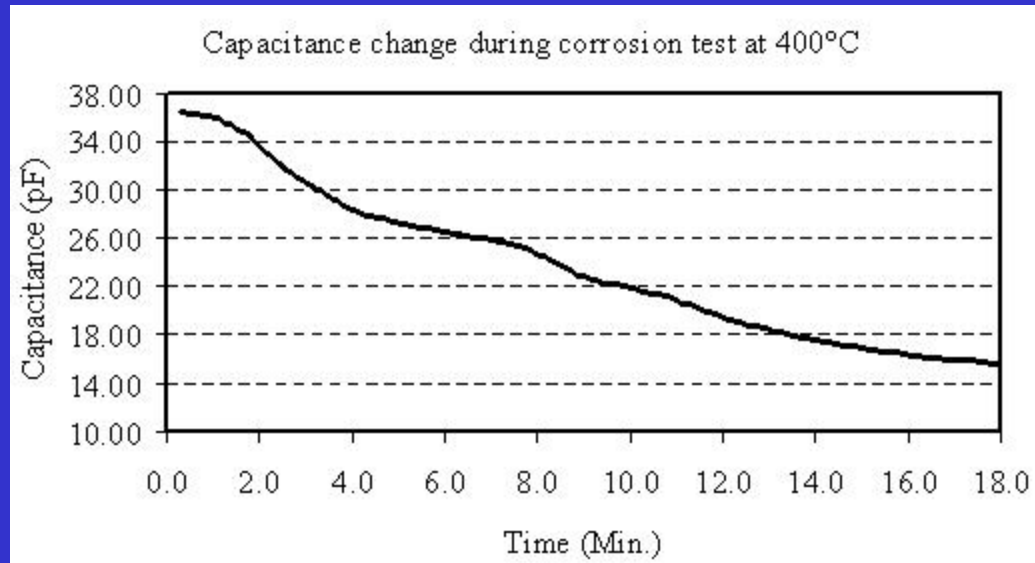
Corrosion Results --Sensor Type 1



Corrosion Results --Sensor Type 1



Corrosion Results --Sensor Type 1



Corrosion Results –Sensor Type 2

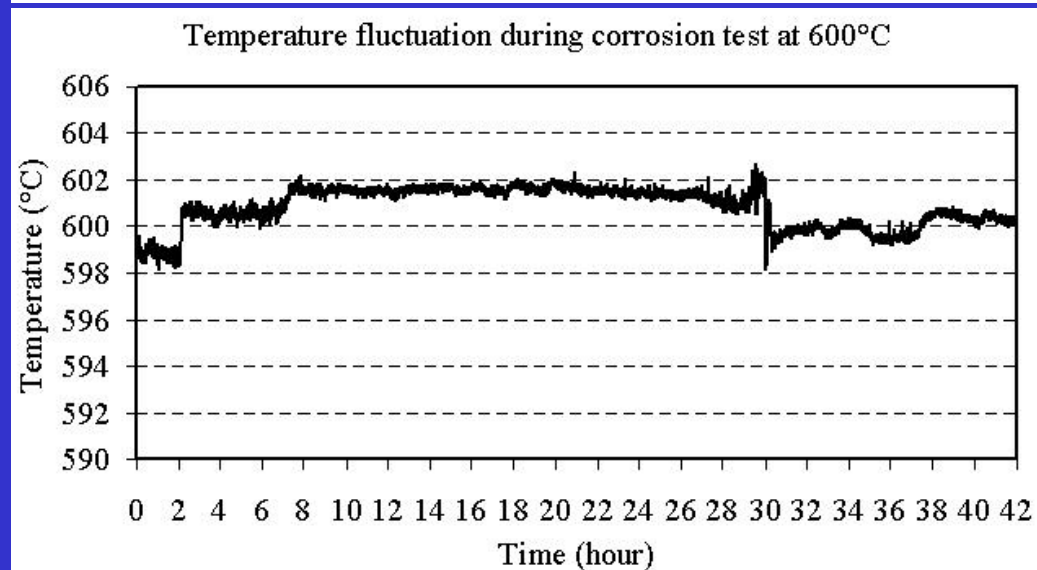
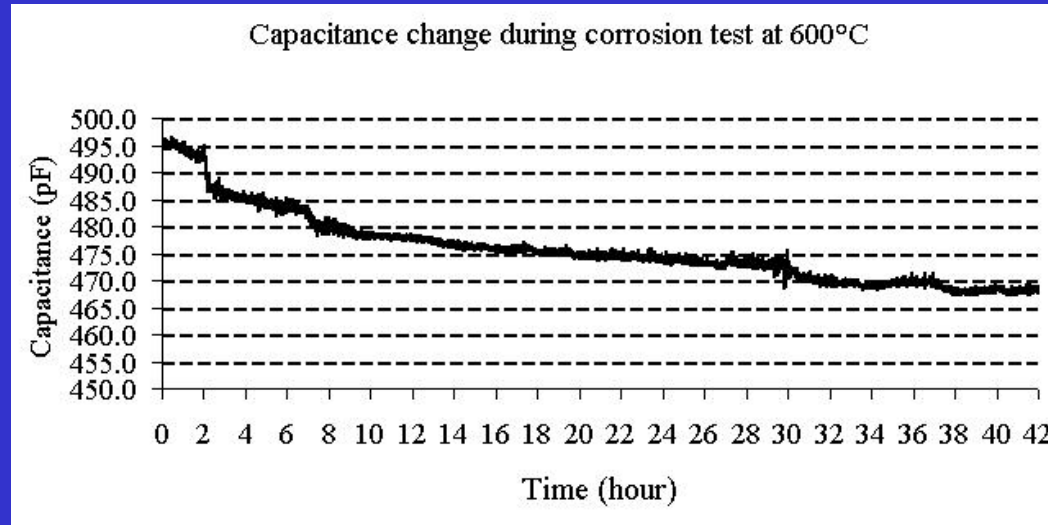


Before corrosion

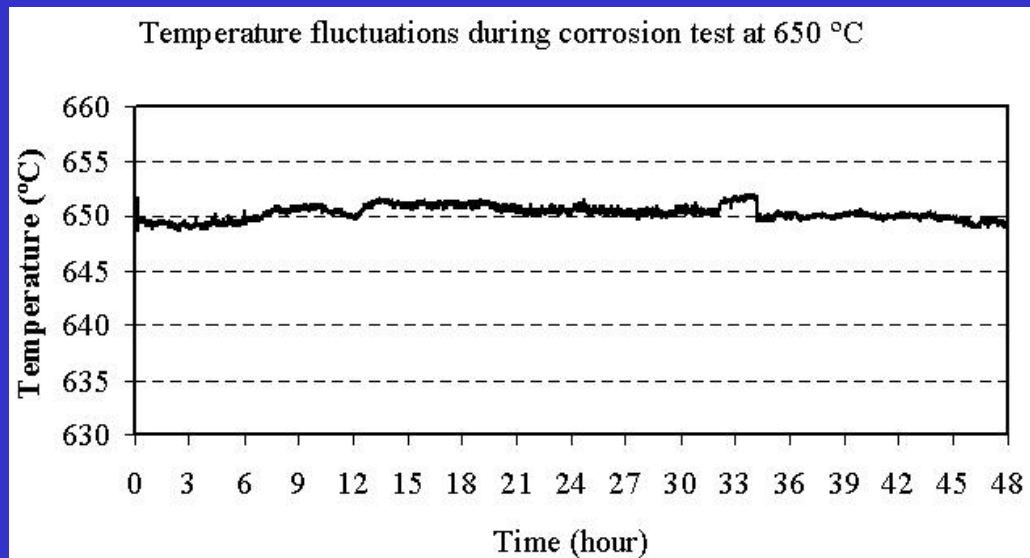
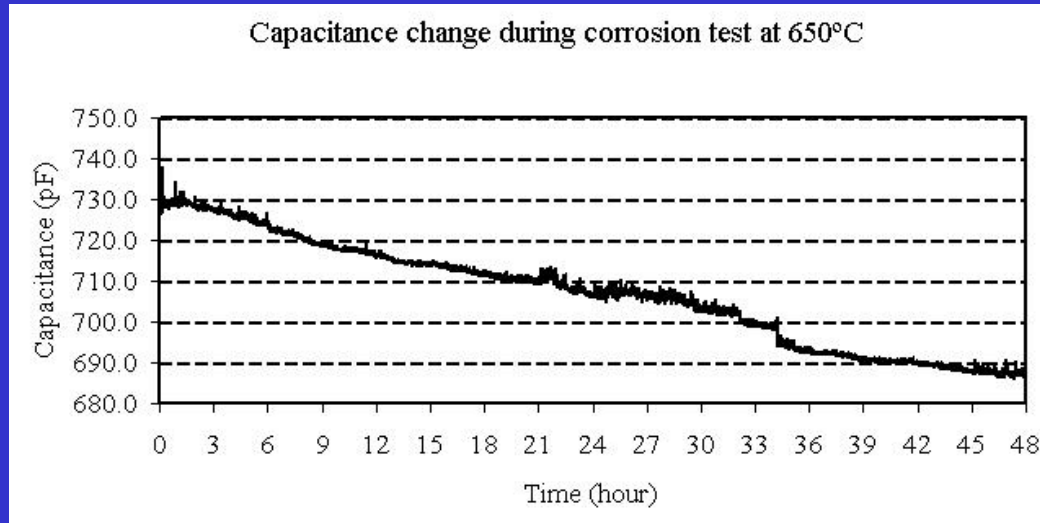


After corrosion

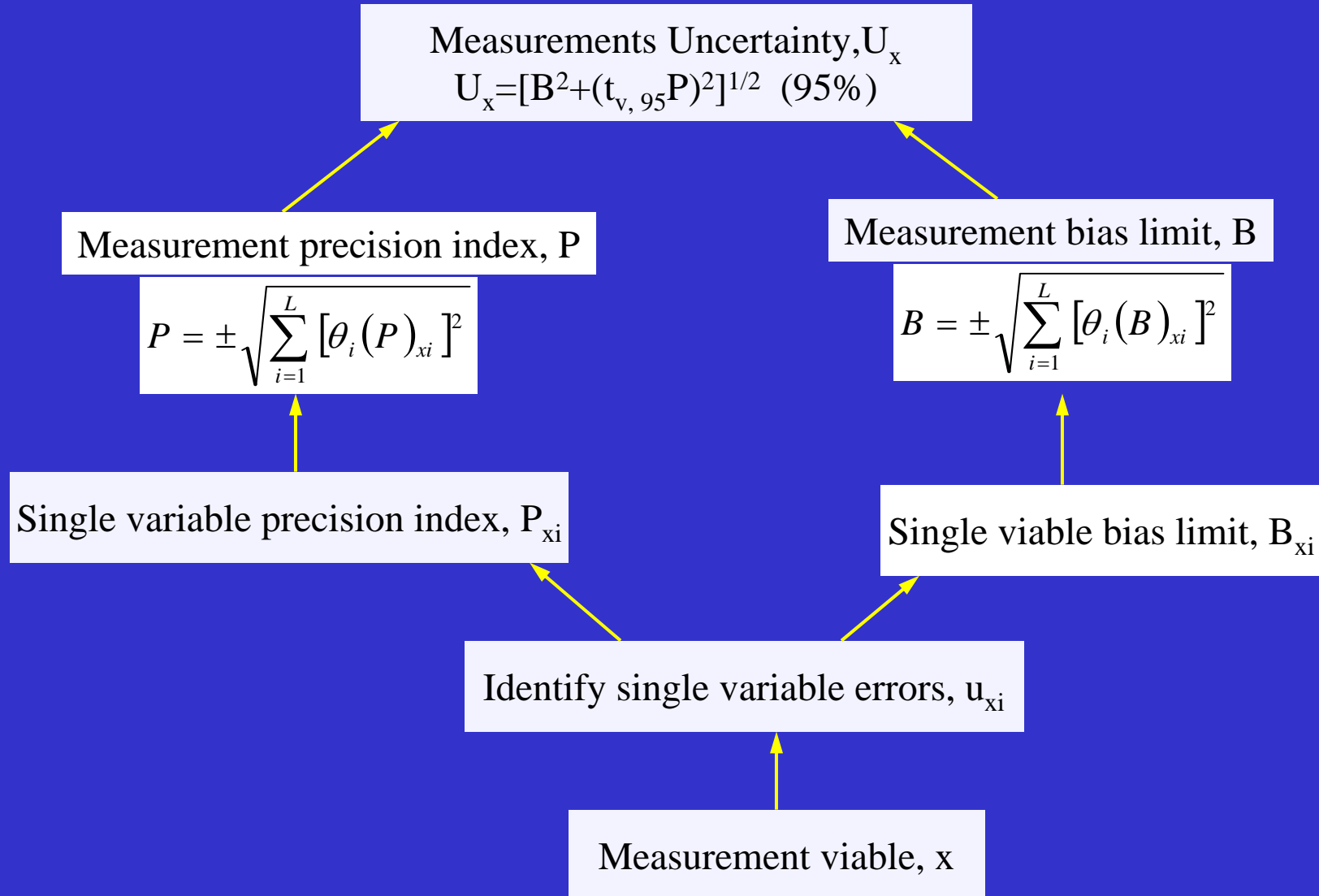
Corrosion Results—Sensor Type 2



Corrosion Results—Sensor Type 2



Uncertainty Analysis



Uncertainty for Corrosion Rate

$$R = f(\Delta C, \varepsilon, d, h, s, t) = \frac{\Delta C \times d}{\varepsilon} \frac{h}{t \times s}$$

$$\bar{R} = \frac{\bar{\Delta C} \times \bar{d} \times \bar{h}}{\bar{\varepsilon} \times \bar{t} \times \bar{s}}$$

$$P_R = \sqrt{\left[\frac{\partial R}{\partial \Delta C} (P)_{\Delta C} \right]^2 + \left[\frac{\partial R}{\partial \varepsilon} (P)_{\varepsilon} \right]^2 + \left[\frac{\partial R}{\partial d} (P)_d \right]^2 + \left[\frac{\partial R}{\partial h} (P)_h \right]^2 + \left[\frac{\partial R}{\partial s} (P)_s \right]^2 + \left[\frac{\partial R}{\partial t} (P)_t \right]^2}$$

$$B_R = \sqrt{\left[\frac{\partial R}{\partial \Delta C} (B)_{\Delta C} \right]^2 + \left[\frac{\partial R}{\partial \varepsilon} (B)_{\varepsilon} \right]^2 + \left[\frac{\partial R}{\partial d} (B)_d \right]^2 + \left[\frac{\partial R}{\partial h} (B)_h \right]^2 + \left[\frac{\partial R}{\partial s} (B)_s \right]^2 + \left[\frac{\partial R}{\partial t} (B)_t \right]^2}$$

$$u_R = \sqrt{B_R^2 + (t_{v,95} P_R)^2}$$

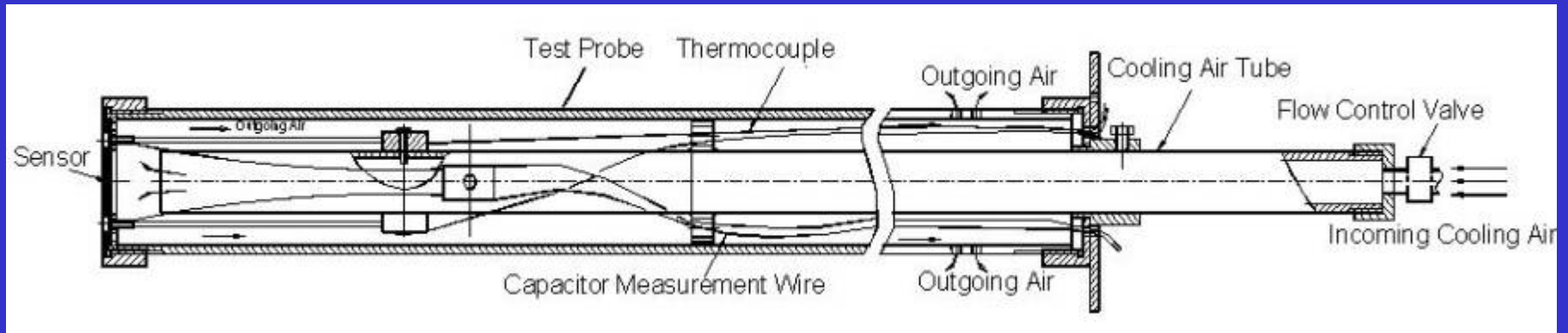
Result with Uncertainty:

$$R' = \bar{R} \pm u_R \quad (95\%)$$

Corrosion Rate with Uncertainty

Sensor Type	Temp. (°C)	Uncertainty (%)	Corrosion Rate R' (nm/hr) (95%)
Type 1	200	4.1%	1.98 ± 0.08
	300	5.4%	56 ± 3
	350	3.4%	1515 ± 52
	400	5.8%	1973 ± 114
Type 2	600	4.7%	49 ± 2.3
	650	3.5%	121 ± 4.2

Future Pilot Furnace and Plant Testing and Development



Conclusions

- Laboratory experiments showed the feasibility of the sensor concept.
- DC magnetron sputtering deposition and plasma spray are methods that can be used to make wedge-shape coatings on ceramic substrate.
- Uncertainty analysis indicated that the overall measurement uncertainty was within 4%.

Acknowledgment

This project is supported by the US DOE UCR program and the University of Alabama at Birmingham.

A Novel Sensor for Fireside Corrosion Monitoring

Zuoping Li, Heng Ban, Bochuan Lin
Department of Mechanical Engineering
University of Alabama at Birmingham
BEC 356D, 1150 10th Ave. South,
Birmingham, AL 35294-4461
Tel: (205) 934-0011 Fax: (205) 975-7217 E-mail: hban@uab.edu

Abstract

Fireside corrosion in coal-fired power plants is an obstacle to increase the overall efficiency of the plant. Corrosion-induced equipment failure could lead to catastrophic damage and inflict significant loss of production and cost for repair. Monitoring fireside corrosion in a reliable and timely manner can provide significant benefits to the plant operators. There have been many attempts to develop real time continuous corrosion monitoring technologies. However, there is no short-term, on-line corrosion monitoring system commercially available for fireside corrosion to date due to the extremely harsh combustion environment.

This paper reports the results of a laboratory development effort on fireside corrosion monitoring. A novel sensor and the corrosion measurement system were developed for online short-term determination of corrosion rate based on electrical capacitance and thin-film technologies. Laboratory experimental results indicated that an accurate measure of corrosion rate could be made with high sensitivity. An uncertainty analysis of the measurement system was also performed to provide a basis for further improvement of the system for future pilot scale testing and full scale testing in power plants.

1 Introduction

Corrosion of metals exposed to high temperature combustion environments, often in the presence of deposits, has long been a problem in industrial process plants and furnaces. The existence of reducing conditions in low emission operations aggravated furnace wall corrosion [1-6]. Key equipment such as boiler tubes and heat exchangers can be damaged by corrosion, which reduces equipment performance and reliability and, in extreme cases, lead to unexpected failures and shutdowns [7]. For safe, reliable and efficient operation, it is important to detect and quantify the amount of corrosion that exists and the corrosion rate. The main advantage of on-line corrosion monitoring system is to promptly provide the process operator with the information such as warning messages, types of corrosion, predicted time frame for corrosion failure and the specific reason for the corrosion problem on a continuous basis [3,8].

Corrosion monitoring is an essential element of plant reliability programs. Traditionally, inspections of the corrosion are conducted during planned shutdowns and preventive maintenance [5-8]. These post-mortem inspections provide little help in preventing the damage [1]. There have been attempts to develop on-line continuous

corrosion monitoring techniques for corrosion rates. However, these measurement methods still need further research and development efforts before they are mature enough for widespread industrial use. Currently, there is no commercial product available for short-term on-line fireside corrosion monitoring, despite the obvious need.

This research was based on a new method for corrosion measurement and developed a novel sensor for short-term, on-line fireside corrosion monitoring in combustion environments. The main objective of the research was to perform laboratory experiments to prove the feasibility of the concept and the sensor design.

2 Sensor Principle and Methods

2.1 Sensor Principle

The principle of the novel sensor is to convert the thickness measurement, i.e., the loss of a thin layer of metal due to corrosion, to an area measurement. The design of the sensor is similar to an electrical capacitor and the signal is measured by electrical capacitance (EC) technique. A typical EC sensor consists of a ceramic substrate with metal coatings on both sides. The front side coating that is exposed to the combustion has a linear thickness change. A back side coating of non-corroding material is used to form a plate capacitance, as illustrated in Fig. 1.

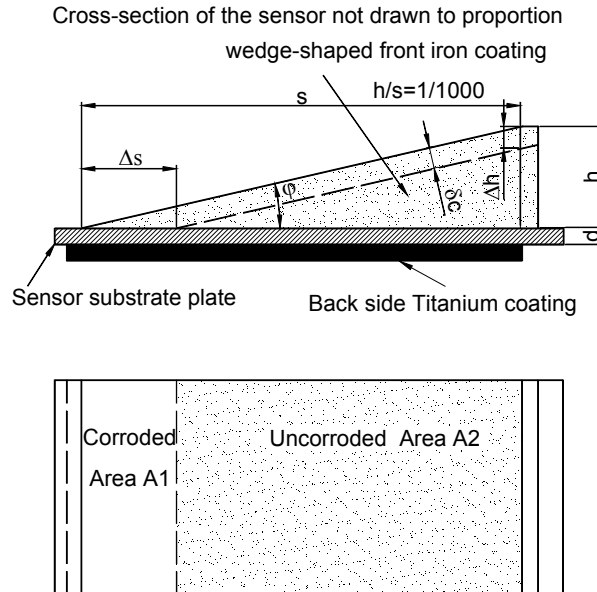


Fig. 1: A schematic diagram for the principle of the sensor.

The sensor capacitance is a function of the overlapping area of the metal coatings, substrate thickness and dielectric properties of the ceramic material. When there is metal loss on the front side coating, the corresponding area of the front side coating will recede. Therefore, there will be a decrease in capacitance produced by the change in overlapping area resulting from coating thickness reduction due to corrosion. The corrosion rate can

be measured as the decrease in electrical capacitance over the time. Because the front side coating exposed to corrosion has a small slope, this arrangement equivalently magnifies a small change in the depth (thickness) to a much larger change in area, which is much easier to measure by electrical capacitance. Corresponding changes in thickness with changes in capacitance can be established experimentally and theoretically based on the sensor coating geometry and the dielectric constant of the ceramic plate. The corrosion rate R (coating thickness decrease per unit time) is given by Eqs. (1)-(2)

$$R = \delta_c / \Delta t = \Delta h \cos \phi / \Delta t \quad (1)$$

$$R = \frac{\Delta C d h}{\varepsilon \Delta t \sqrt{s^2 + h^2}} \cong \frac{\Delta C d h}{\Delta t \varepsilon s} \quad (h \ll s) \quad (2)$$

Where s is the overlapping area per unit width of the sensor, h is the initial maximum thickness of the wedge-shaped coating, Δt is the corrosion exposure time, d is the thickness of sensor substrate, ε is the dielectric constant of substrate, and ΔC is the total capacitance change of the sensor produced by corrosion.

2.2 Substrate Material Selection and Sensor Fabrication

The physical and chemical properties of the sensor substrate material are important factors affecting the sensor design and its performance. Beryllium Oxide (BeO) is a ceramic material that combines excellent electrical insulating properties with high thermal conductivity. It is also corrosion resistant. This unique combination of properties in conjunction with good mechanical strength and thermal shock resistance enable BeO to be the best substrate material.

One of the objectives of this research is to investigate fabrication methods for the wedge-shaped coating on the sensor substrate. DC magnetron sputtering deposition technologies was applied to coat both sides of the sensor substrate. Figure 2(a) shows a fabricated novel sensor based on the design. The sensor has wedge-shaped iron coating on the front side for corrosion and a uniform titanium coating on the other side. The thickness of the front wedge-shaped coating of the sensor varies incrementally from 0 to 15 μm over a length of 15 mm. The backside titanium coating is corrosion-resistant and has uniform coating thickness.



Fig. 2: Pictures of a fabricated sensor, (a) before corrosion (b) after corrosion.

2.3 Temperature Compensation and Corrosion Rate Calculation

During the corrosion experiments, the temperature variations of the sensor elements can produce capacitance fluctuations because the dielectric constant of sensor substrate is temperature dependent. The dielectric constant of the ceramic substrate increases with increasing temperature. As a result, the sensor capacitance increases with increasing temperature. In order to obtain the capacitance change caused by the corrosion, the sensor capacitance has to be evaluated at a constant or nominal temperature. The fireside sensor is usually air-cooled to a temperature close to the boiler tube surface temperature. Small temperature fluctuation is likely to exist, for instance, +/- 1 °C. Therefore, a method for temperature compensation was applied to remove the capacitance fluctuation caused by temperature fluctuations in our laboratory study. The compensated capacitance of the sensor element $C(T, t)$ under temperature T at transient time t is calculated by Eq. (3):

$$C(T, t) = C(T', t) - \frac{dC}{dT}(T' - T) \quad (3)$$

Where $C(T', t)$ is the measured sensor capacitance at temperature T' and time t , and $(T' - T)$ is the temperature difference or fluctuation from the nominal temperature T . The dC/dT value can be measured as the property of the ceramic material. An accurate determination of dC/dT can also be obtained directly from the actual element around exact temperature of interest in the experiment. The recorded data include sensor capacitance and sensor temperature. The small variations in temperature around its set point, together with change in capacitance for a short period can be plotted to acquire the dC/dT value. Within the short period, the actual corrosion is negligible and the capacitance-temperature relationship is assumed to be the material property. Take the corrosion test data at 200°C for example, the typical value of dC/dT used to calculate corrosion rate is shown in Fig. 3. Similarly, the same value can be obtained at other experimental temperature.

After temperature compensation, the total capacitance change ΔC of the sensor element caused by corrosion during exposure time $(t-t_0)$ can be given by Eq. (4)

$$\Delta C = C(T, t) - C(T, t_0) \quad (4)$$

Thus, the corrosion rate R at a test temperature T is given Eq. (5):

$$R = \frac{\Delta C d h}{(t - t_0) \epsilon s} \quad (5)$$

2.4 Experimental Setup

An experimental system with data acquisition, shown in Fig. 4, was set up for the laboratory corrosion experiments to prove the design concept. The furnace was set at a temperature with temperature control. A thermocouple was used to measure real time temperature of the sensor. Data acquisition software was programmed to perform automatic data collection by computer to obtain the test data from the LCR meter and OMEGA Dpi8 thermometer on real time basis, respectively. The 4-wire measurement technique was utilized to measure capacitance of the sensor. The 4-wire technique eliminates the impedance of measurement leads as a source of error.

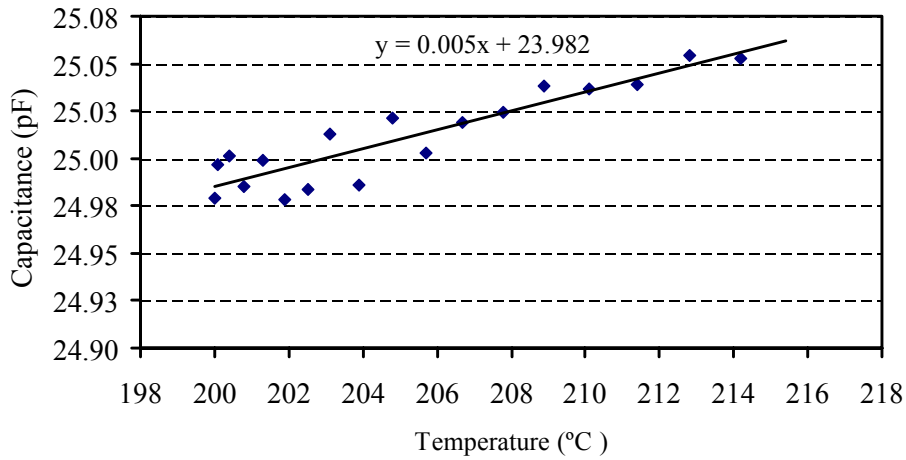


Fig. 3: A typical plot of dC/dT measured from small temperature fluctuations around 200 °C.

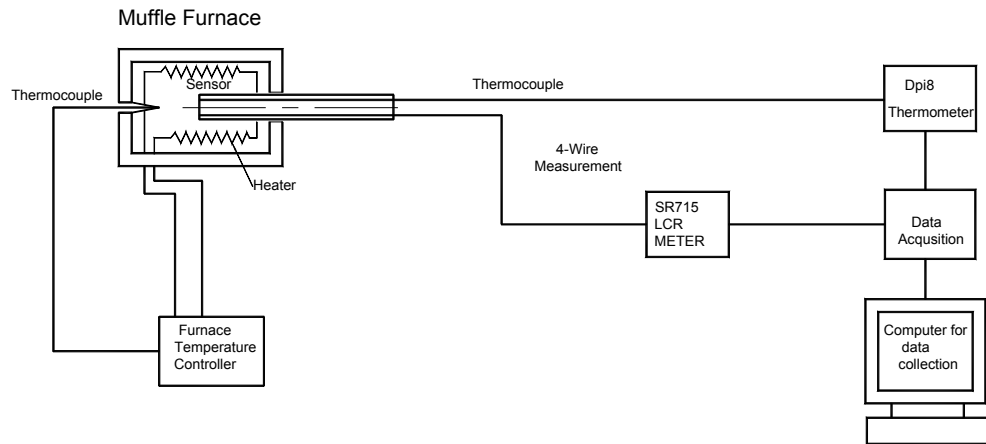


Fig. 4: A schematic diagram of measurement system.

3 Results and Discussions

3.1 Dielectric Constant Measurement Results

The purpose of this measurement was to obtain the influence of temperature on the dielectric constant of BeO, because the correlation between the dielectric constant of the BeO and elevated temperatures is currently not available. In addition, there no dielectric constant data available for BeO at the frequency range of our measurement. The experiment was conducted using a BeO capacitor with no corrosion and varying the furnace temperature from room temperature to over 400 °C. Results in Fig. 5 demonstrate that the dielectric constant of BeO is highly temperature dependent and increased from

6.7 at 150 °C to 7.9 at 450°C. This information was used in the sensor design, in the selection of the measurement instrument, and in the process of evaluating possible uncertainties introduced by the temperature fluctuation.

3.2 Corrosion Measurement Results

Laboratory corrosion experiments were performed using the muffle furnace and fabricated sensors at the temperature of 200°C, 300°C, 350°C and 400°C, respectively. One corroded sensor is shown in Fig. 2(b) and the corrosion of the wedge-shaped coating is apparent. Figures 6-9 show the capacitance of the sensors decrease steadily during exposure period of corrosion for each test temperature. The temperature compensation was applied to process experimental data and Figure 6-9 shows the processed data with 10 point running average. The experimental results clearly proved the feasibility of the sensors concept. It also shows that the fabricated sensors can survive in high temperature environments. The sensitivity of the sensor is high enough to provide on-line continuous corrosion information quickly. In our experiment, an accurate corrosion measurement was obtained in periods as short as in few hours under laboratory conditions. The relationship between corrosion rate and reduction in coating thickness follows the theoretical equation established early in conceptual design. The experimental results were stable and reliable. The high corrosion rates may be possibly attributed to low coating thickness and no oxidation protection scale was formed before the coating was completely corroded away [9].

3.3 Post-Exposure Analysis

Scanning Electronic Microscope (SEM) was used to examine the coating microstructure of the sensors before and after the corrosion test. SEM graphs can provide information about coating microstructure and surface roughness. Microscopic examination revealed that shallow pitting and surface roughness for the corroded sensors. The surface profilometer and digital micrometer were utilized to measure the coating thickness of the sensor elements and provided quantitative physical information for validation of the electrical capacitance measurement. Meanwhile, the optical microscopy also indicated that the coatings successfully survived high temperature tests and there was no peeling or detachment from the substrate.

3.4 Uncertainty Analysis

Uncertainty analysis of the corrosion measurement was performed to quantify the uncertainty of the measurement system. Since the corrosion rate measurement in this research is a multi-variable measurement, uncertainty from each variable will propagate to the final result or overall uncertainty [10-11]. The corrosion rates with uncertainty for the above experimental results under different temperature were calculated and presented in table 1 below. The sensitivity of the measurement system, which depends on the sensor design and the measurement instrument, is a function of the slope of wedge-shaped coating, the dielectric constant and the thickness of the substrate, sensor and coating geometry and the overall precision error of the system. Our experimental results indicate that the sensor is capable of measuring sub-micrometer thickness changes confidently. Such capability can be used for short-term, on-line corrosion monitoring.

Table 1: Average corrosion rates with uncertainty at different test temperature

Sensors	Corrosion Exposure Time (hours)	Temperature (°C)	Corrosion rate with uncertainty (nm/hr)
1	48	200	1.98 ± 0.07
2	6	300	56 ± 2.0
3	0.75	350	1515 ± 38
4	0.5	400	1973 ± 62

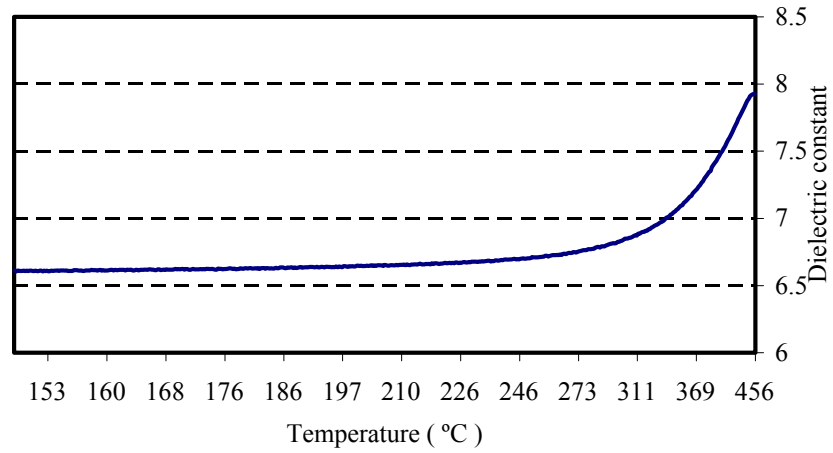


Fig. 5: Dielectric constant change of BeO with temperature at 10kHz.

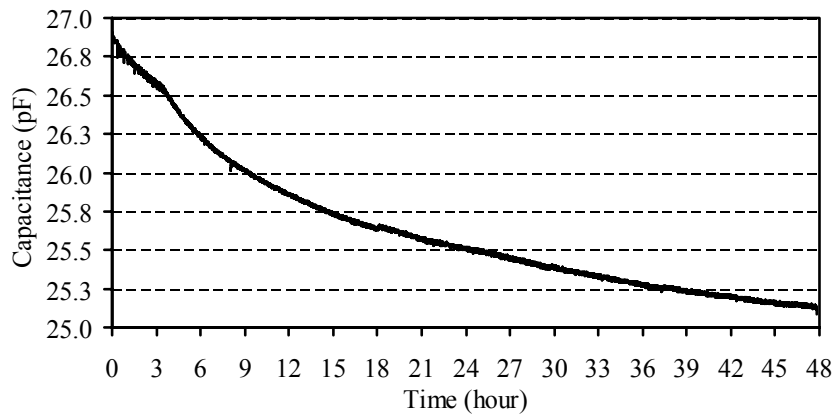


Fig. 6: Capacitance change during corrosion test at 200°C

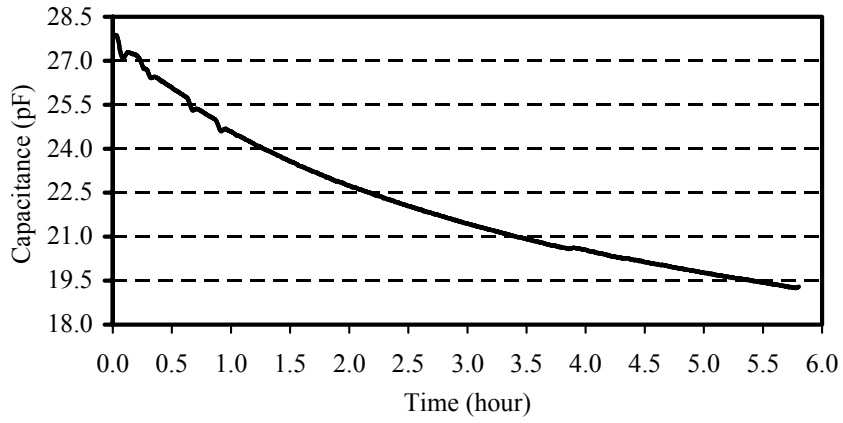


Fig. 7: Capacitance change during corrosion test at 300°C

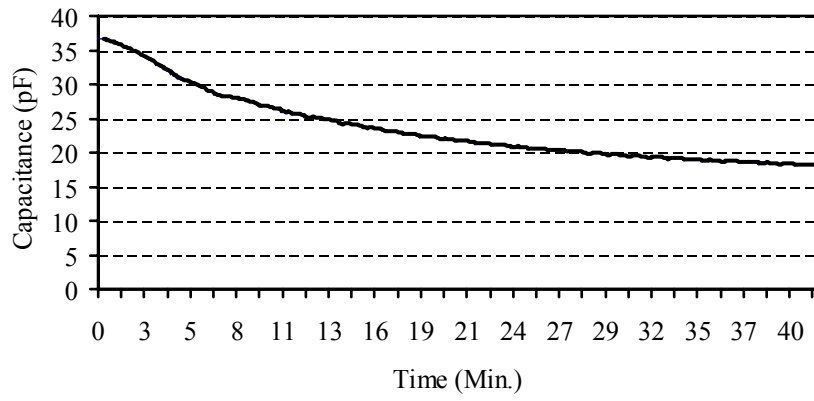


Fig. 8: Capacitance change during corrosion test at 350°C

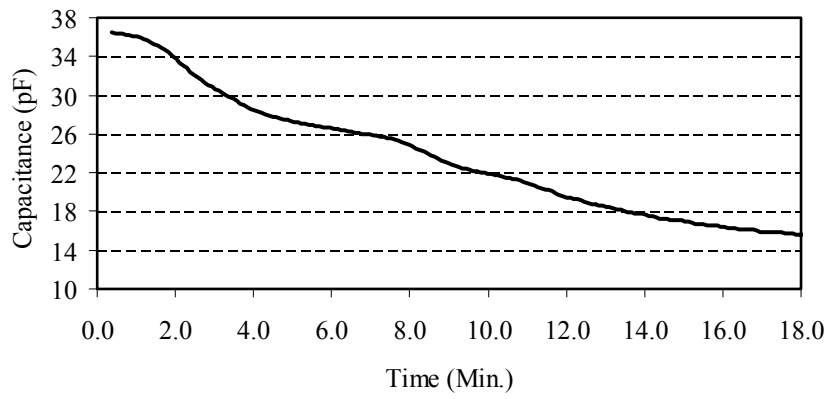


Fig. 9: Capacitance change during corrosion test at 400°C

4 Conclusions

The laboratory corrosion studies have demonstrated that the sensor and measurement system are capable of short-term, on-line corrosion monitoring. In summary, the following conclusions can be drawn from current research:

1. Laboratory proof-of-concept corrosion experiments showed the feasibility of the sensor concept. The sensor showed high signal-to-noise ratio and can detect sub-micrometer thickness changes. The sensor and measurement system obtained corrosion information quickly under different experimental temperatures. The corrosion rates showed strong dependence on temperature ranging from 1.98 nm/hr at 200°C to 1973 nm/hr at 400°C.
2. DC magnetron sputtering deposition is a method that can be used to make wedge-shape coatings on BeO substrate. The coatings survived high temperature environments in our experiment. The fabricated method for the sensors was shown to meet the theoretical design requirements.
3. Uncertainty analysis indicated that the overall measurement uncertainty was within 4% of the measured mean value. Sensitivity analysis of the experimental system showed that the performance of the sensor and corrosion measurement system could lead to short-term on-line corrosion capabilities for fireside corrosion monitoring.

Acknowledgments

This project is partially supported by Department of Energy (DOE) under Contract DE-FG26-01NT41281.

References

- [1] Davis, K. A., Green, G. C., Linjewile, T. and Harding, S., 2001, "Evaluation of an On-line Technique for Corrosion Characterization in Furnaces," *Joint International Combustion Symposium*, AFRC/JFRC/IEA, Kauai, HI.
- [2] Cultler, A. J. B., Flatley, T. and Hay, K. A., 1980, "Fireside Corrosion in Powerstation Boilers," *Combustion*, **12**, pp. 17-25.
- [3] Harb, J. N. and Smith, E. E., 1990, "Fireside Corrosion in PC-fired Boilers," *Progress in Energy and Combustion Science*, **16**, No. 3, pp.169-190.
- [4] Dooley, B. and Chang, P., 2000, "The Current State of Boiler Tube Failures in Fossil Plants," *Power Plant Chemistry 2000*, **2**, No. 4.
- [5] Farrell, D. M. and Robins, B. J., 1998, "Online Monitoring of Furnace Wall and Superheater Corrosion in Power Generation Boilers," VTER Technical Paper, CSS 98, 39th Corrosion Science Symposium, 8th Sept. 98, University of Northumbria at Newcastle, U.K.
- [6] Farrell, D. M. and Robins, B. J., 2002, "On-line Corrosion Mapping Using Advanced Electrical Resistance Techniques," UK NDT 2002 Conference.
- [7] Jaske, Carl E., Beavers, John A. and Thompson, Neil G., 1995, "Improving Plant Reliability Through Corrosion Monitoring," *Fourth International Conference on Process Plant Reliability*, Houston, Texas, USA.

- [8] Kane, R. D., 2002, "Corrosion Monitoring for Industrial and Process Applications," Corrosioneering, Newsletter, InterCorr International, Inc., Houston, Texas USA.
- [9] Fehlner, F. P. and Mott, N. F., 1970, "Oxidation in Thin-Film Range, Oxidation of Metals and Alloys," Papers presented at a Seminar of the American Society of Metals, pp. 37-62.
- [10] Bechwich, T. G., Marangoni, R. D. and Lienhard, J. H., 1995, *Mechanical Measurements, Fifth Edition*, Addison–Wesley Publishing Company, pp. 54-92.
- [11] Figliola, R. S. and Beasley, D. E., 2000, *Theory and Design for Mechanical Measurements, Third Edition*, John Wiley & Sons, Inc. pp. 149-183.



Plant Test of an On-Line Fireside Corrosion Monitor

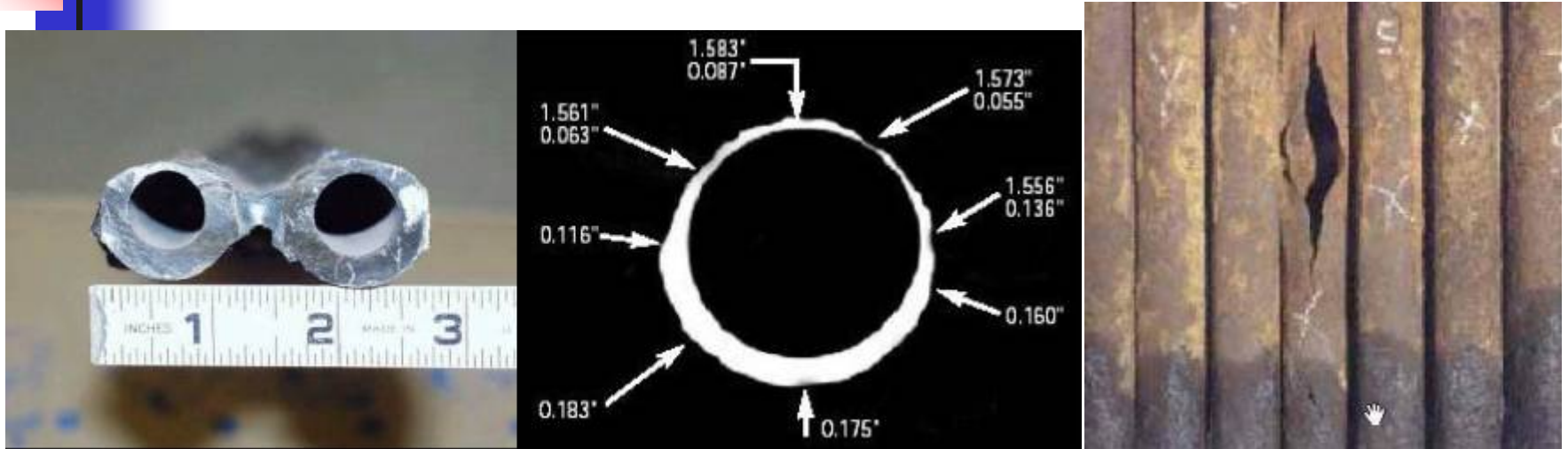
Bochuan Lin, Heng Ban

University of Alabama at Birmingham

Arun Mehta

Electric Power Research Institute

Boiler Tube Fireside Corrosion



Tube failure is the leading cause of boiler shutdowns
Fireside corrosion is a continuing concern, especially in low emission combustion mode and using opportunity fuels. Corrosion cost electric utilities \$6.9 billion/yr in USA (NACE).



Why Corrosion Monitoring

- Diagnoses of corrosion problems
- Advanced warning of system upsets leading to corrosion damage
- Determination of inspections and /or maintenances
- Estimation of the equipment lifetime



Corrosion Monitoring Methods

- **Off-line, non-continuous measurement**
 - Visual Inspection
 - Radiography (X-Ray)
 - Ultrasonic Testing
 - Weight-loss Coupon
- **On-line, continuous measurement**
 - Electric Resistance (ER) Technique
 - Electrochemical Noise (ECN) Technique
 - New technologies in Development

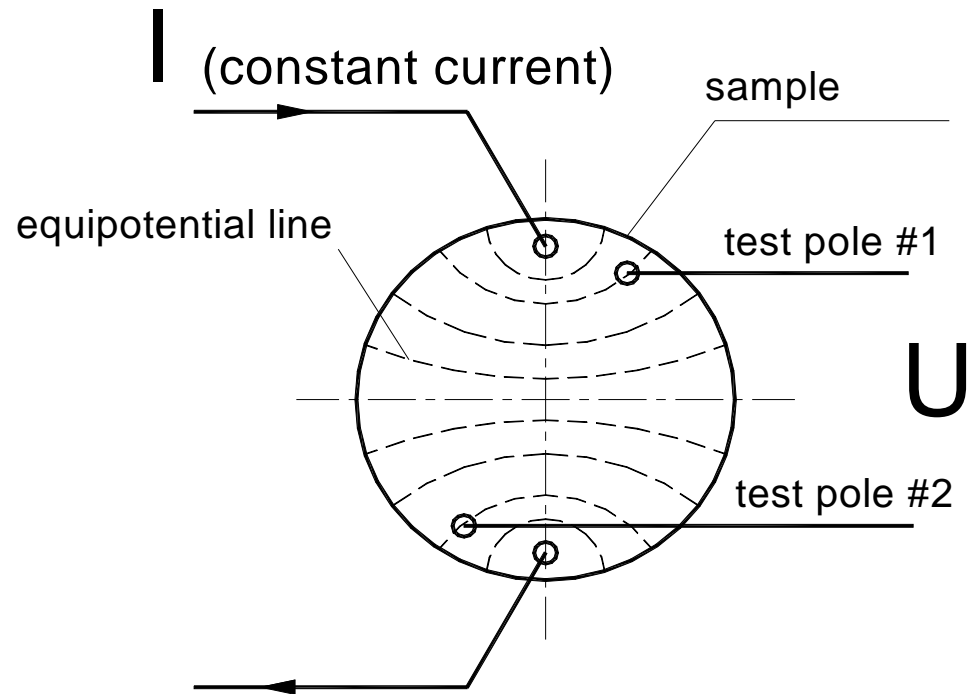


What We Did:

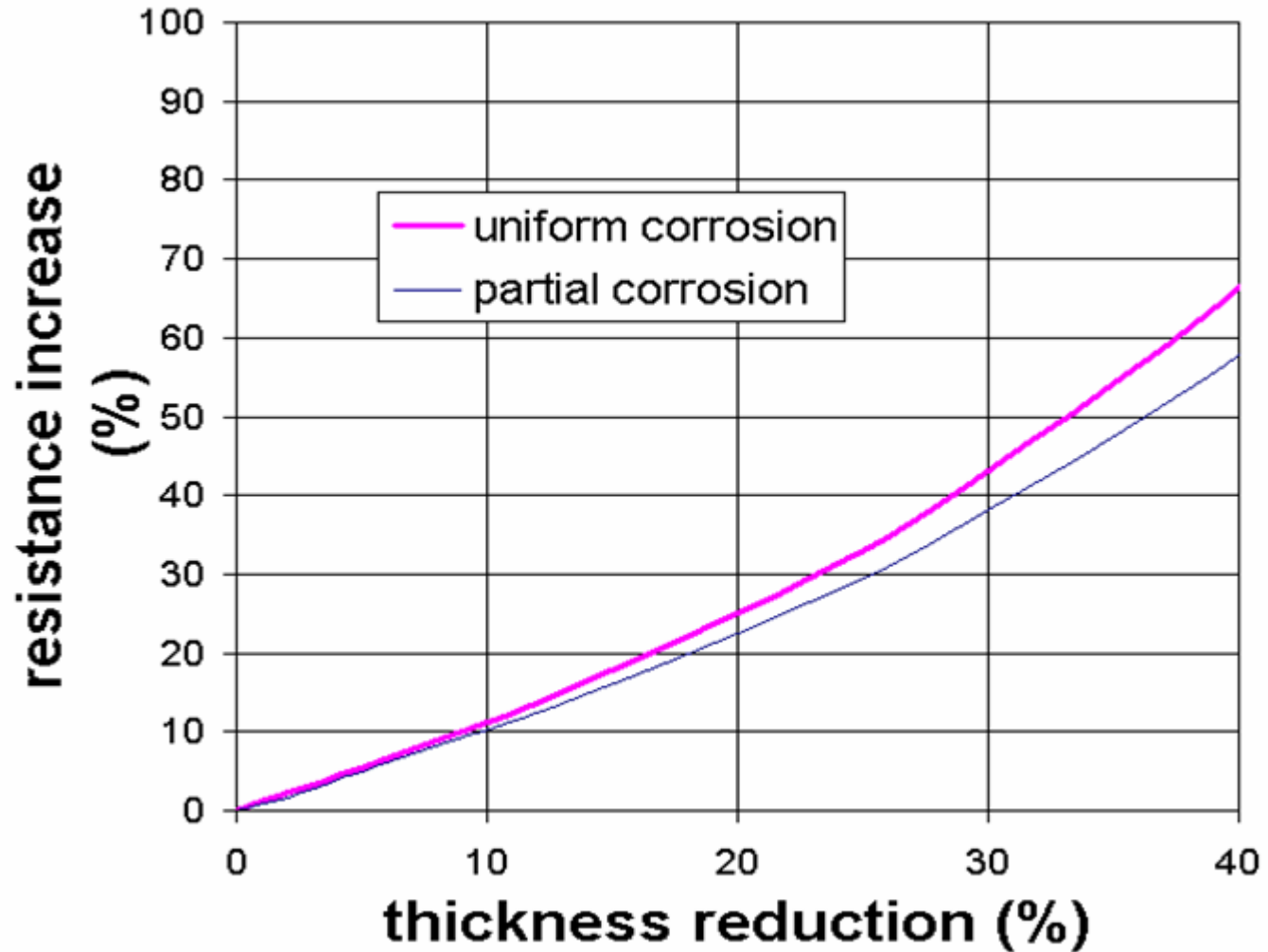
- An on-line fireside corrosion monitoring system based on electric resistance measurement.
- Tested at a tangentially fired PC boiler burning an Eastern bituminous coal.
- Corrosion rate was determined (coupon thickness change).

Measurement Principle

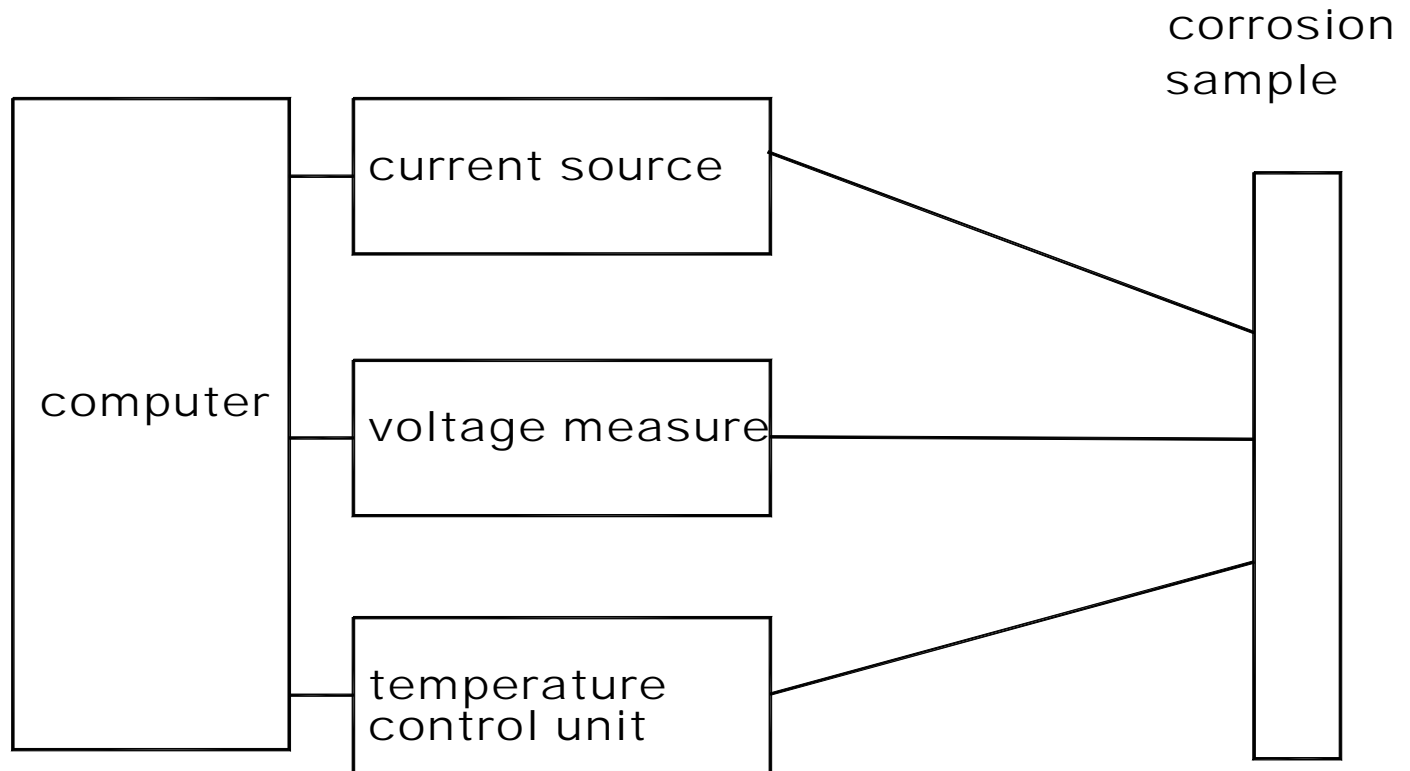
- A sacrificial metal coupon exposed to the corrosive environment.
- The change of the coupon thickness is determined based on the measurement of the coupon electrical resistance change.



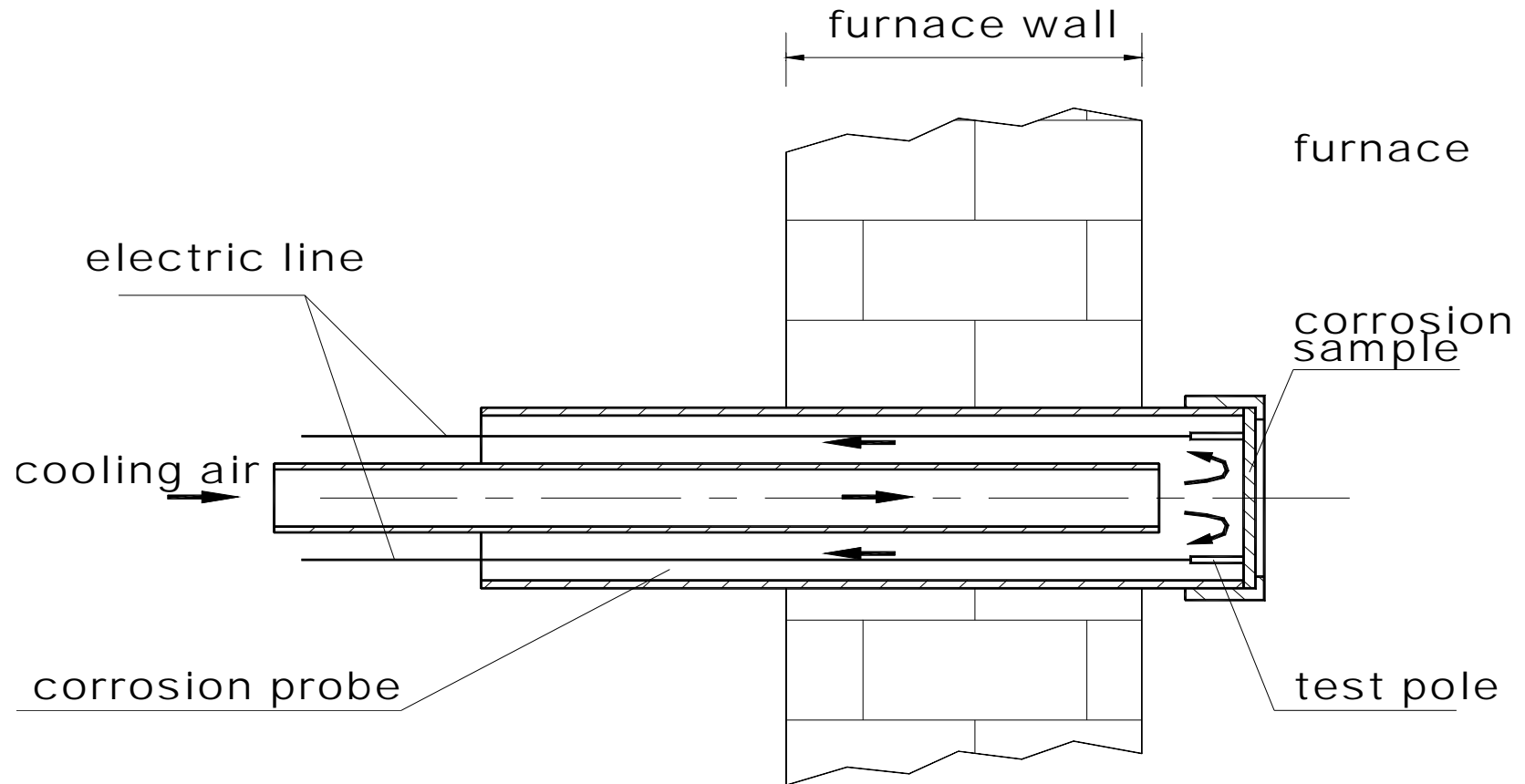
Resistance vs Thickness



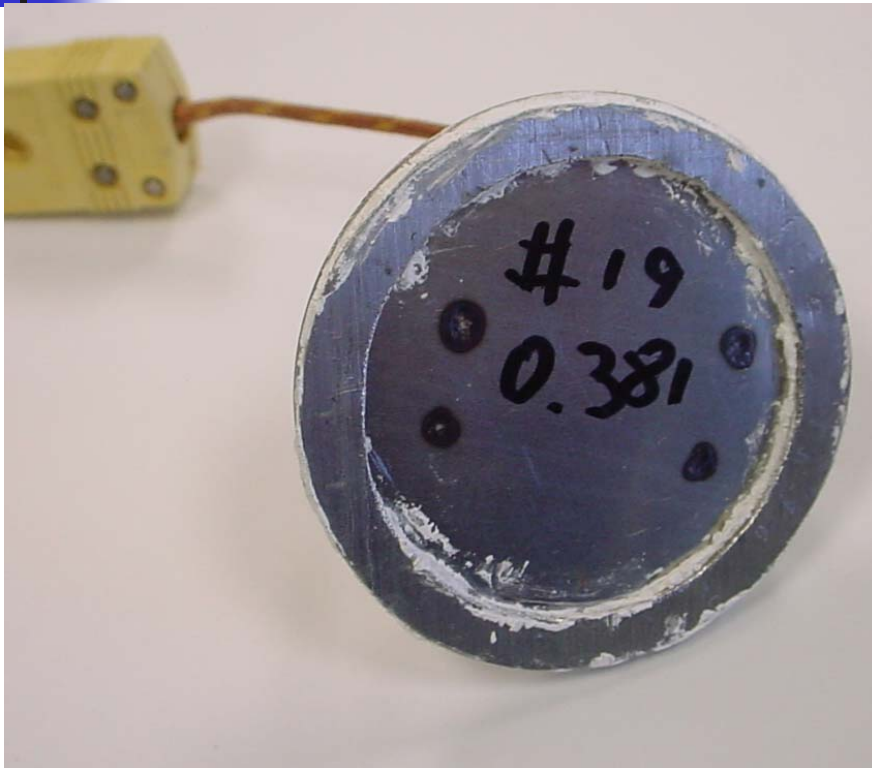
Experimental Setup



Schematic Diagram Of Corrosion Probe



Corrosion Sensor (coupon)



Front view



Back view

Probe Assembly



Probe Installation



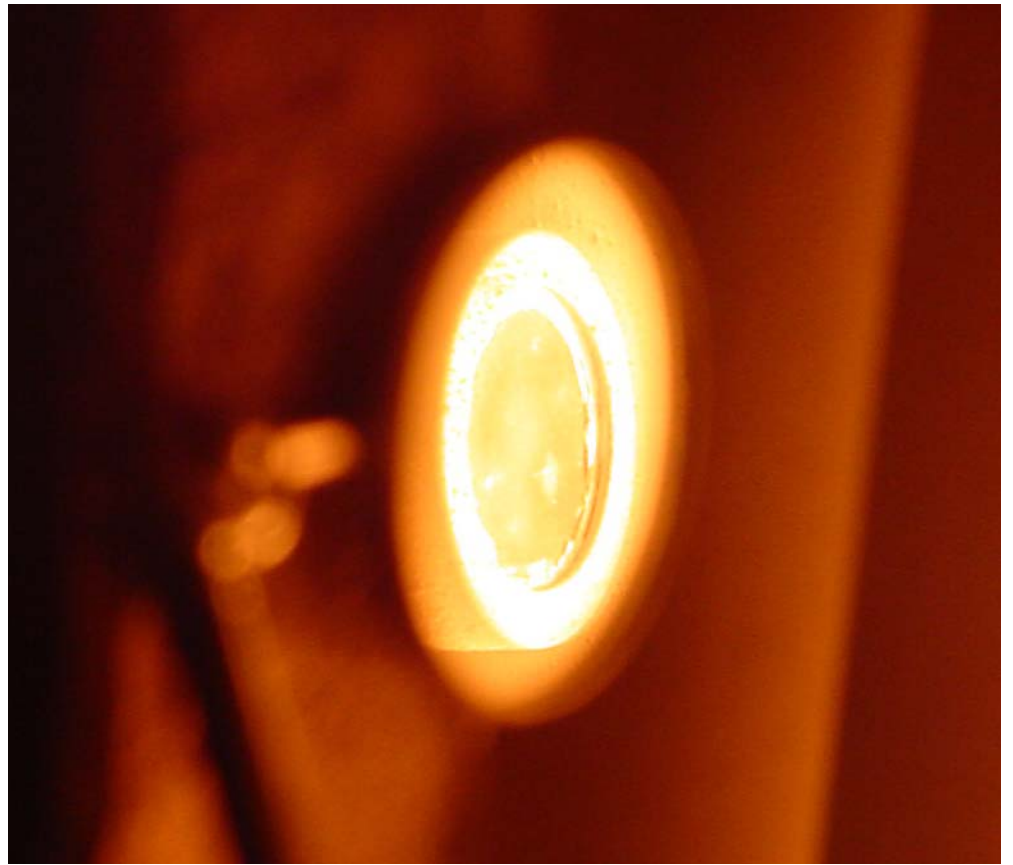
Control and Measurement Unit



Probe Operation



View Port

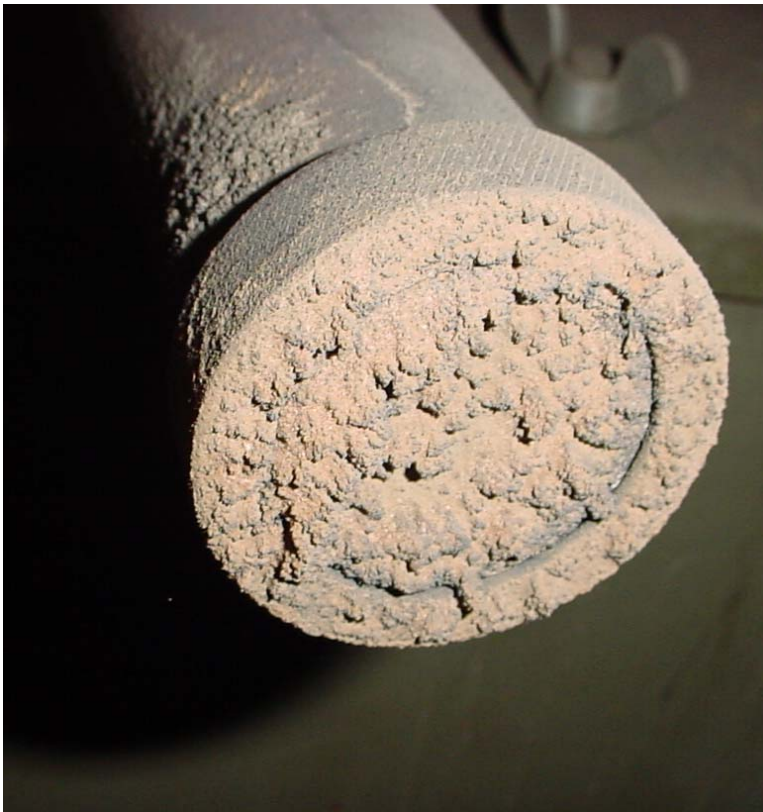


Viewing with a mirror

Resistance Monitoring



Coupon after experiment



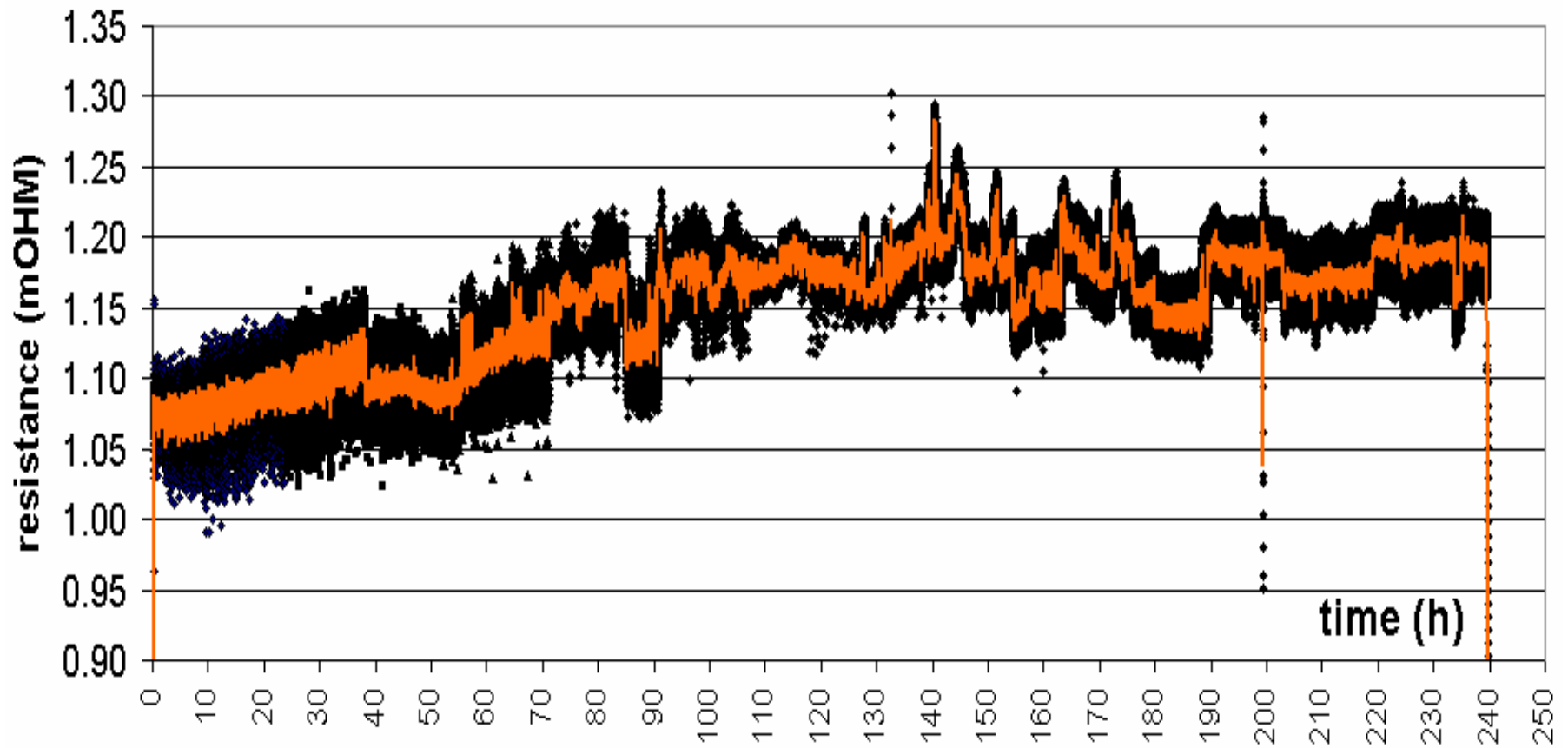


Result and Discussion

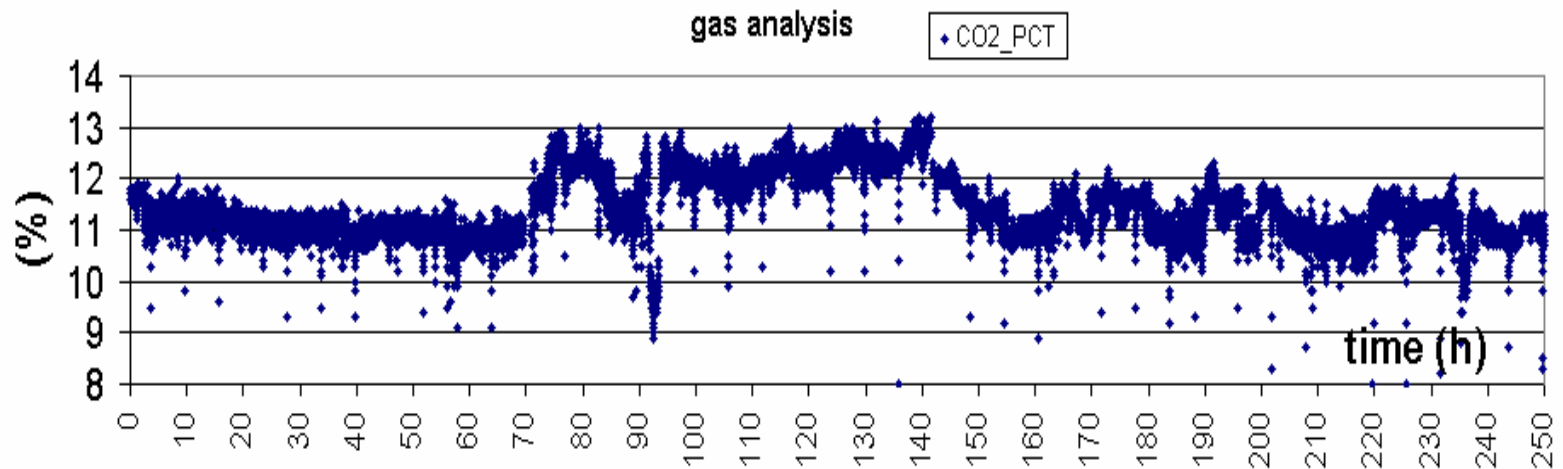
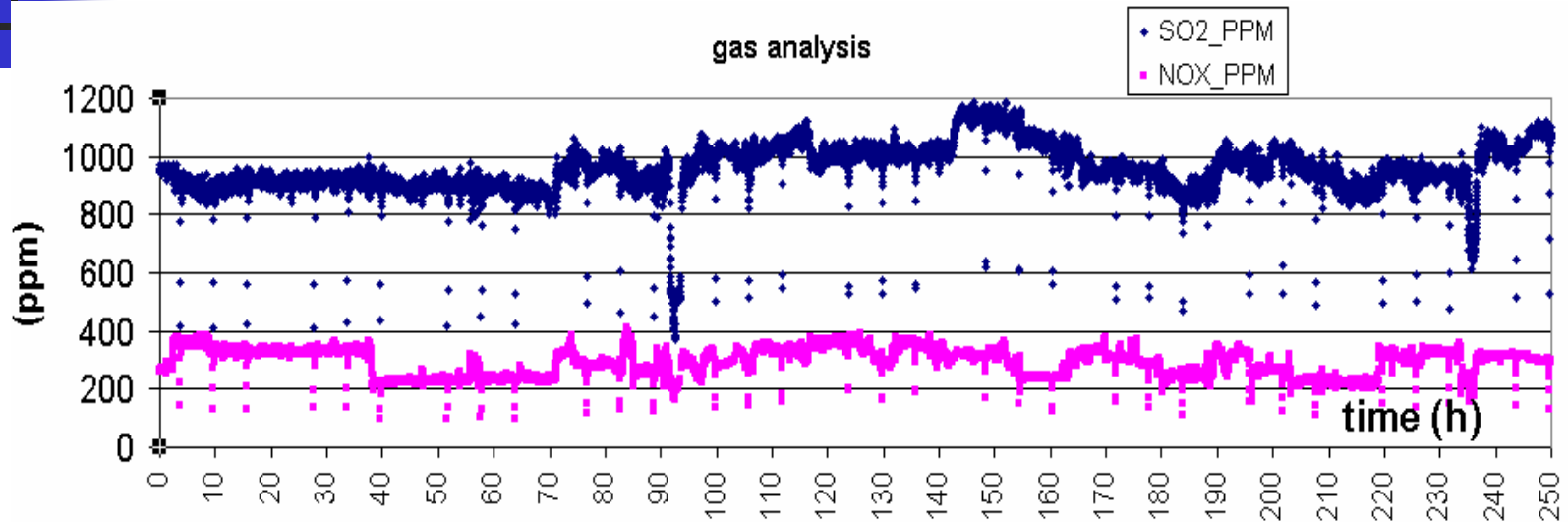
Summary for Run 2

Sample material	Low carbon 1010 steel
Sample thickness	0.381 \pm 0.02mm
Sample temperature	550 °C
Fuel for boiler	Bituminous coal
Position of probe	Boiler front corner wall
Experiment time	240 hours
Quantity of Corrosion	26.7%

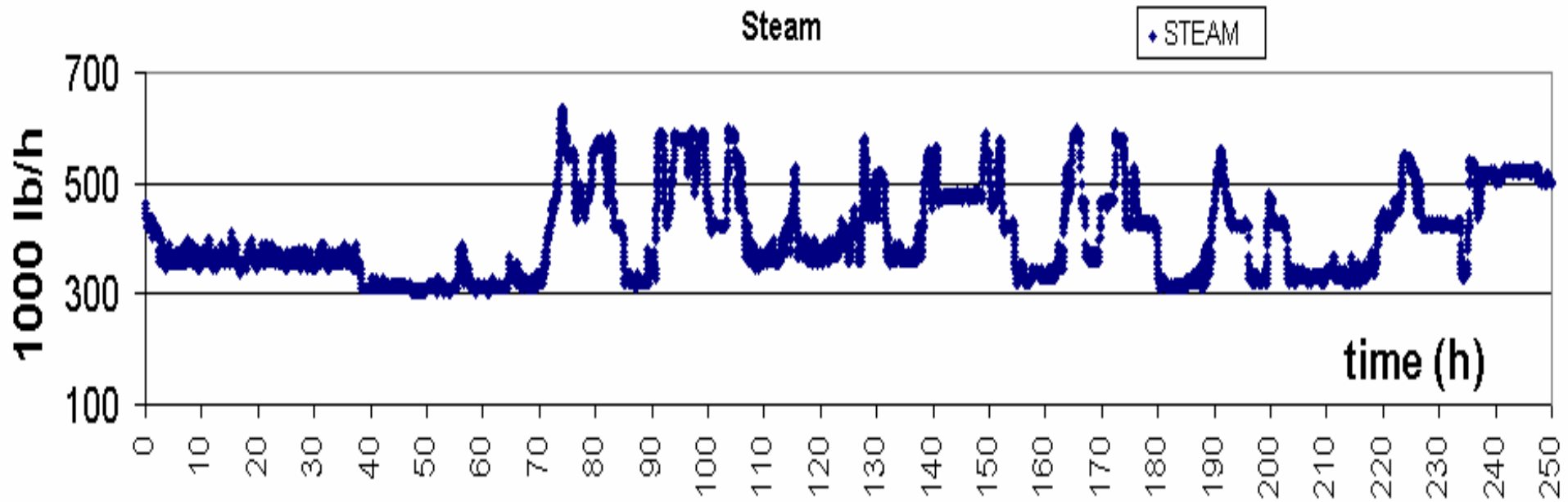
Coupon Resistance vs Time



Flue Gas Analysis



Boiler Steam Loading



Ash Deposition on the Coupon



0 hr



72 hrs



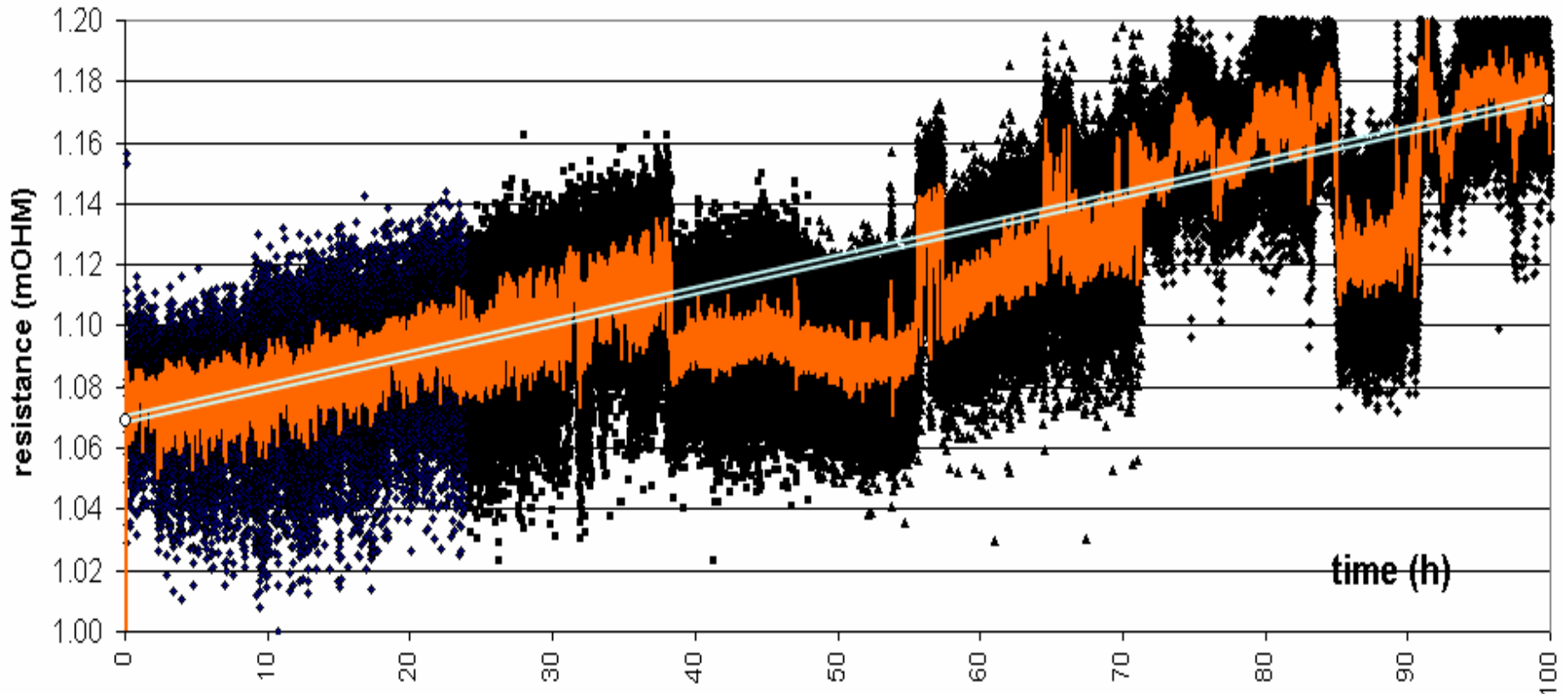
168 hrs



240 hrs



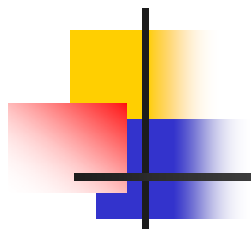
The Resistance Change in First 100 Hours





Conclusion

- The on-line corrosion monitoring system based on electrical resistance can determine the corrosion rate in about 40 hours at a power plant.
- More work is needed to examine the effect of ash deposition on the measurement.

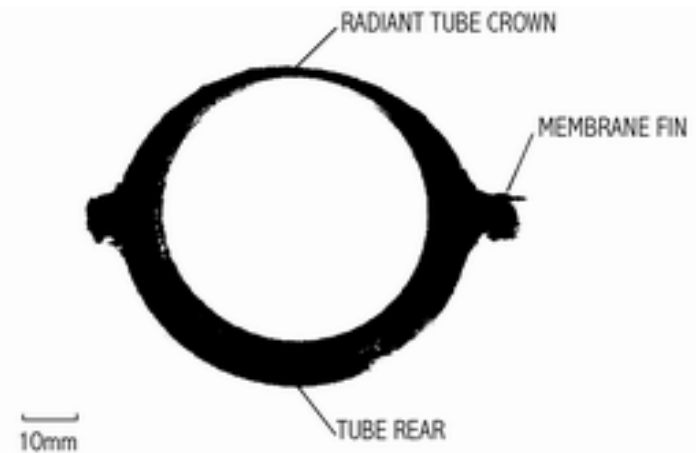
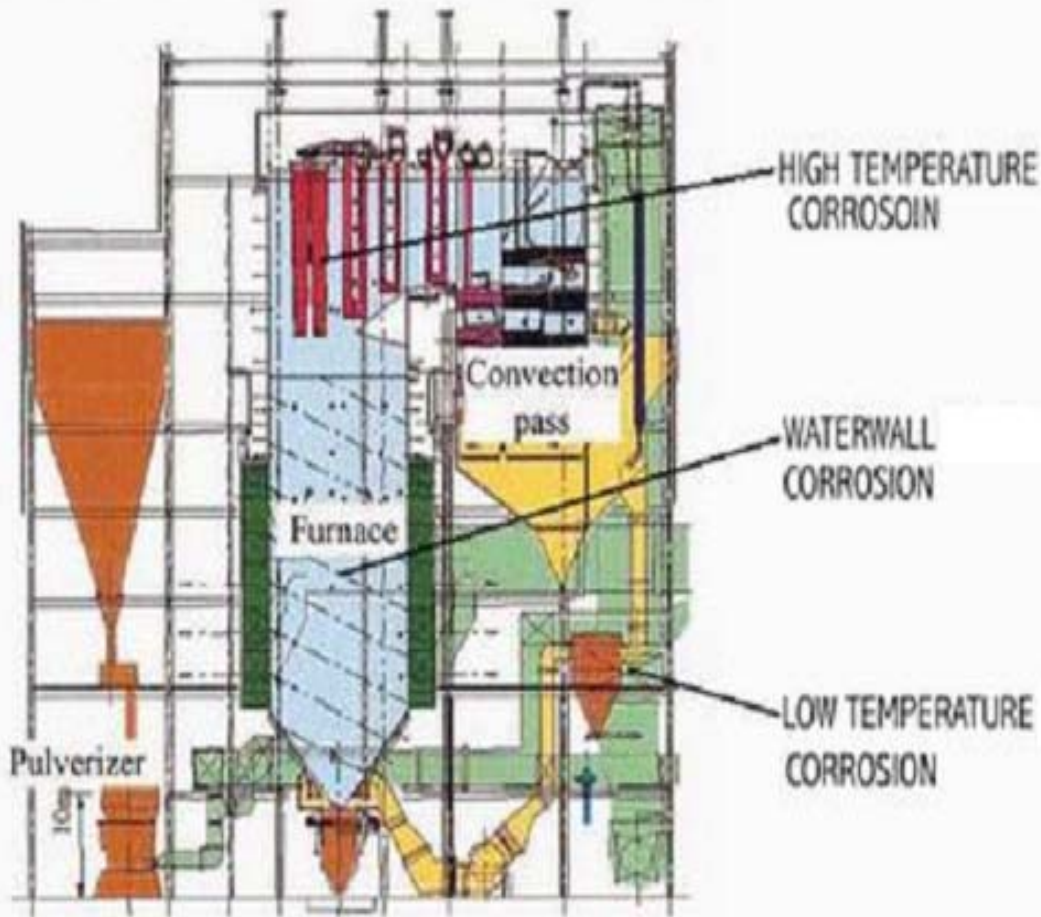


Thanks for
listening!

Question?



Introduction: Fireside Corrosion





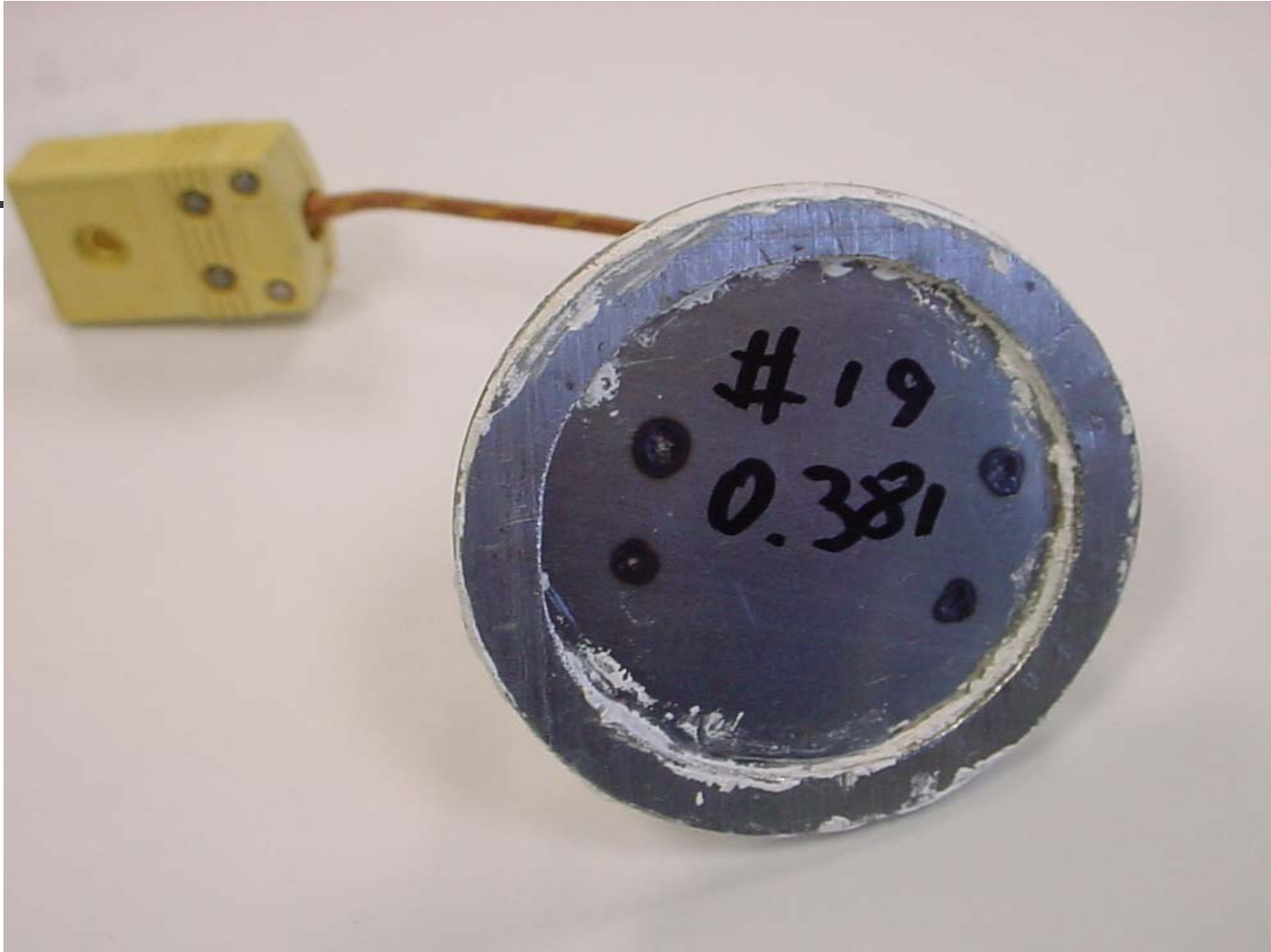
Fireside Corrosion Monitoring

- Many boilers have experienced unacceptable rates of corrosion in furnaces resulting from the introduction of technologies targeting emissions reduction, efficiency improvement, or fuel/oxidant flexibility
- Fireside corrosion causes damage to waterwall tube.
- There is no commercial product available for online fireside corrosion monitoring.



Challenges

- Off-line measurement made during scheduled or forced outages is unable to get instantaneous corrosion information.
- Online-line continuous measurement is still underdevelopment
- Challenge: to measure corrosion rate in one shift (8 hours)



Corrosion sample



Corrosion measuring system

Plant Test of an On-Line Fireside Corrosion Monitor

Bochuan Lin¹, Heng Ban¹ and Arun Mehta²

¹Department of Mechanical Engineering
University of Alabama at Birmingham
BEC 356D, 1150 10th Ave. South, Birmingham, AL 35294-4461
Tel: (205) 934-0011, Fax: (205) 975-7217, email: hban@uab.edu

²Electric Power Research Institute
3412 Hillview Avenue, Palo Alto, CA 94304

ABSTRACT

Many boilers have experienced unacceptable rates of fireside corrosion resulting from the introduction of technologies targeting emissions reduction, efficiency improvement, or fuel/oxidant flexibility. Because fireside corrosion can lead to catastrophic boiler failures, an on-line corrosion monitoring system can be valuable in reducing the overall operating cost. This paper presents the result of an on-line fireside corrosion monitoring system tested at a tangentially fired PC boiler, burning an Eastern bituminous coal. The method was based on the measurement of the coupon electrical resistance to determine the coupon thickness. The probe was mounted on the furnace wall and air-cooled to maintain a constant temperature of the sensing coupon. The corrosion rate was determined from a four-wire resistance measurement with computer data acquisition. It was shown that the measurement system can successfully determine the corrosion rate. The result also indicates that better temperature control or temperature compensation, and measures to remove ash deposition are needed to allow the probe to measure corrosion rate accurately in a prolonged period.

INTRODUCTION

The corrosion of waterwall tubes due to chemical attack occurring on the furnace side of the heat exchanging surfaces in industrial furnaces is known as external or fireside corrosion [1,2]. Fireside corrosion is characterized by the relatively high temperature and the unique environment encountered in the furnaces. Figure 1 shows the major areas of corrosion in a typical coal-fired steam generator, and Figure 2 shows a cross-section of a corroded waterwall tube. Many power plants that rely on steam from boilers have experienced unacceptable rates of corrosion in furnaces resulting from the introduction of technologies targeting emissions reduction, efficiency improvement, or fuel/oxidant flexibility [3,4,5].

The waterwall tubes experience the largest heat flux, about 200-500 kW/m², of all boiler tubes due to the large temperature gradient between hot gases in the combustion zone and a relative cool waterwall tube at about 350-450 °C. High temperature corrosion occurs at the superheater or reheater where the nominal temperature is above 500 °C. The symptoms of waterwall tube fireside corrosion are the thinning of the tube, as shown in Figure 2, and increased tube strain.

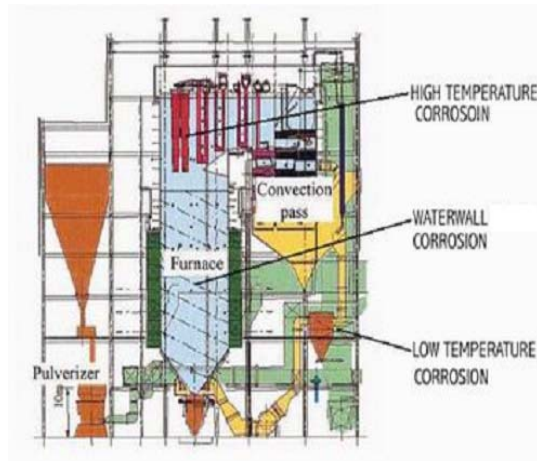


Figure 1. A schematic diagram showing the location of corrosion in a typical steam boiler

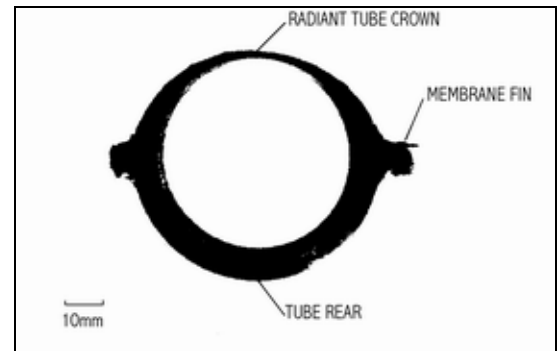


Figure 2. Membrane fireside corrosion

Fireside corrosion is a continuing problem in Kraft recovery boilers in the pulp and paper industry. It is also an increasing concern for coal fired power plants due to operations such as low NO_x firing and fuel changes from the use of biomass, spot-market coal, or other opportunity fuels. Water tube damage from accelerated corrosion can cause catastrophic equipment failure, explosions, and forced plant outages. The resulting economic impact from repair and loss of production can be debilitating.

Currently, there is no commercial product available for online fireside corrosion monitoring despite the industrial demand. At present, downtime visual inspection and ultrasonic tube thickness measurement are standard techniques for identifying corrosion after-the-fact during scheduled or forced outages. These techniques provide little help in preventing the damage.

This paper presents the result of an on-line fireside corrosion monitoring system tested at a tangentially fired PC boiler burning an Eastern bituminous coal. The probe was mounted furnace on the furnace wall and air-cooled. The corrosion rate was determined from a four-wire electrical resistance measurement with computer data acquisition. The corrosion rate was determined based the coupon electrical resistance change, which reflects the coupon thickness change. The tests show that the measurement system can successfully determine the corrosion rate.

MEASUREMENT PRINCIPLE

The measurement method uses a sacrificial metal coupon exposed to the corrosive environment and determines the rate of the average coupon thickness recession. The relative change of the coupon thickness is determined based on the measurement of the coupon electrical resistance change. Because the electrical resistance of a current path increases when the cross sectional area of the conductor is reduced, the metal loss due to corrosion can be detected by an electrical resistance-measuring instrument. The sensing coupon is made of a circular disk of the alloy of concern with four electrical connections. A DC constant current is applied through the two opposite electric connections and the voltage between the other two electric connections is measured, as shown in Figure 3.

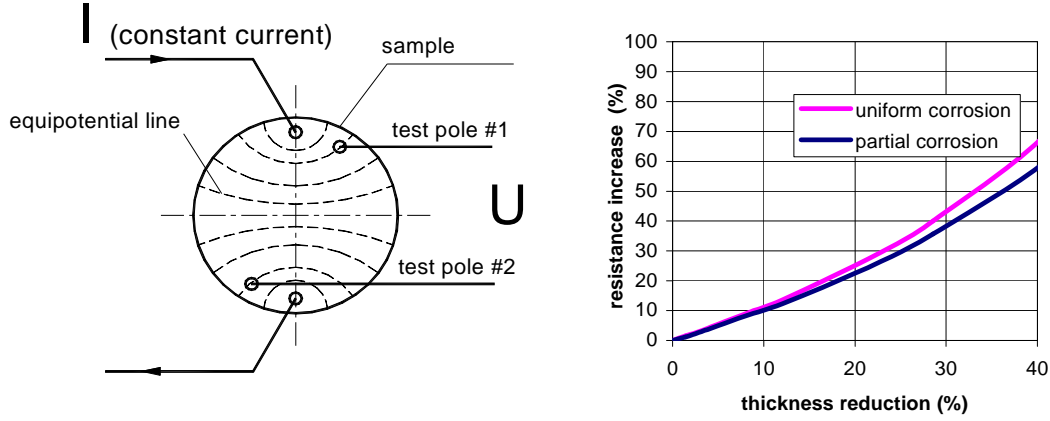


Figure 4. Resistance change with thickness

The corrosion of coupon material will reduce the thickness of the coupon, and lead to an increase of measured resistance. Since the electric current is maintained at constant, the voltage between the test poles 1 & 2 will increase as the thickness decreases. Figure 3 shows the theoretical relationship between the measured voltage and the coupon thickness in relative percentages. Figure 3 was calculated using a commercial finite element package to model the geometry effect of a specific coupon size and the location of the four electric connections. The curve for partial corrosion was calculated to account for the fact that there is little corrosion on the rim of the coupon due to sealing o-ring. Figure 3 shows an approximate linear relationship when the change of resistance is not significant.

The method to determine coupon thickness is straight forward if a linear relationship is assumed between the resistance and thickness. The measured voltage U is:

$$U = K \frac{1}{\Delta} I_{const} \quad (1)$$

and the resistance R between the test poles is:

$$R = \frac{U}{I_{const}} = \frac{K}{\Delta} \quad (2)$$

where : K a constant determined by the material and geometry of the coupon,
 Δ the thickness of the coupon,
 I_{const} the constant electric current.

The thickness (Δ) and the resistance (R) of the coupon can be calculated based on the initial values of Δ_o , and R_o :

$$\Delta = \frac{R_o}{R} \Delta_o \quad (3)$$

Therefore, the percentage change of thickness $P_\Delta = \frac{\Delta_o - \Delta}{\Delta_o}$ and the resistance $P_R = \frac{R - R_o}{R_o}$

follows the equation below:

$$P_R = \frac{P_\Delta}{1 - P_\Delta} \quad (4)$$

EXPERIMENTAL SETUP

The measurement system for the on-line corrosion testing consists of (1) temperature control unit, (2) constant current power source, (3) precise voltage measurement unit, and (4) computer control and data processing unit. Figure 5 is a diagram of the system. The corrosion coupon was installed on the tip of a probe to be installed through the observation port of the furnace wall, shown in Figure 6. Because the electric conductivity of sample material is a function of temperature, an air-cooling system with a PID temperature controller was used to maintain a stable temperature of the coupon.

Figures 6 & 7 are pictures of the corrosion coupon and the instrument cabinet respectively. The measurement system is programmed to operate autonomously and allows periodic downloading of data.

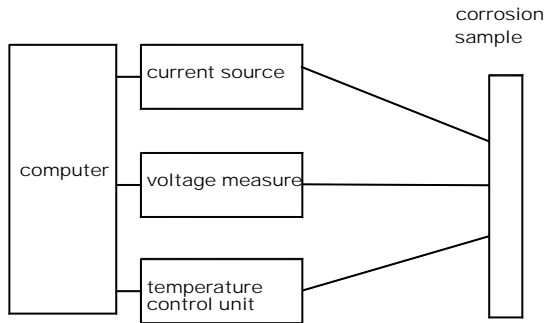


Figure 5. Corrosion testing system.

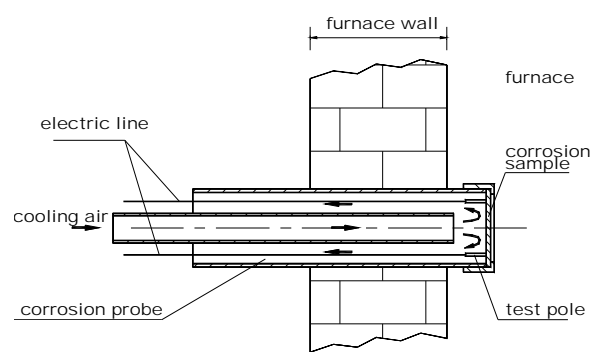


Figure 6. Schematic diagram of corrosion probe.

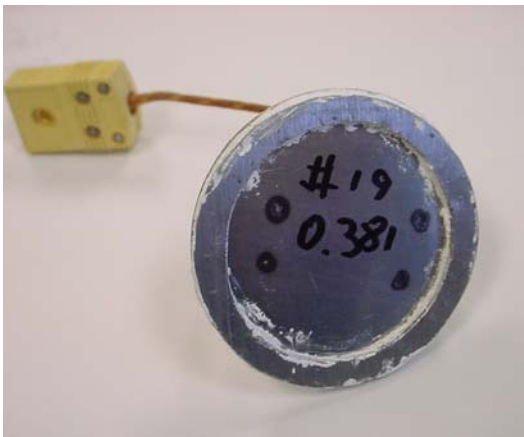


Figure7. Corrosion coupon



Figure 8. Measurement system

RESULT AND DISCUSSION

The experiment was carried out in a power plant boiler (Steam flow rate: 600,000 lb/hr). The unit is tangentially fired burning an Eastern bituminous coal. The corrosion probe was inserted into the boiler through the inspection port on the corner one floor above the nozzle, as shown in Figure 8. One of the corrosion experimental results is summarized in Table 1 and the detailed resistance data and overall furnace operation parameters are presented in Figure 9-10.

Figure 9 shows the coupon resistance change for a testing period of 240 hours. The

temperature of the coupon was set to 550 °C during the period. The resistance of the coupon increased steadily during the first 140 hours, and stayed approximately flat for the remaining 100 hours. The resistance also has significant fluctuations as spikes and sometimes a slight decrease in the periods of a few hours. Figure 10 showed the flue gas analysis result and the steam load change for the experimental period. It is apparent that the changes in the SO₂, NO_x, and CO₂ concentrations are somewhat correlated to the steam loading of the unit. The fluctuations in coupon resistance also have corresponding changes when the furnace loading condition is changed. Figure 11, in situ pictures of the coupon in the furnace, shows the development of ash deposit on the coupon surface. The ash deposition was slight in first 72 hrs, and there was a heavy ash layer on the sample surface after 168 hrs till the end of experiment. The coupon corrosion and ash deposition, after the coupon is removed, is also shown in Figure 11, with dark layers of metal corrosion and yellowish ash on the surface.

Table 1. Result summary for one corrosion experiment

Coupon material	Low carbon 1010 steel
Initial thickness	0.381 ±0.02mm
Temperature	550 °C
Fuel for boiler	Bituminous coal
Position of probe	Boiler corner port 1
Experiment time	240 hours
Actual Corrosion	26.7%

Overall, the resistance of the coupon increases with time. The resistance of coupon increases from about 1.07 mOhm to 1.18 mOhm, about 10.2% in Figure 9. According to Fig. 4, the resistance increase should be almost proportional to thickness decrease. Therefore, the thickness change determined by the electrical resistance measurement is about 10.5%. But the coupon thickness measurement after the coupon is removed from the furnace showed an actual thickness decrease of 26.7%. Such difference between resistance measurement and actual thickness reduction is likely originated from the spatial and temporal non-uniformity of the coupon temperature. To convert the resistance to the thickness, it is required that the resistance values are compared at a fixed reference temperature. Because the resistance is a function of temperature, a temperature drift can lead to erroneous result for the coupon thickness calculated from resistance data. For example, if the coupon temperature is decreased, the measured resistance will also be lower even if the thickness of the coupon is decreased. The reason for the temperature variation in the experiment may be due to the ash deposition on the coupon surface. The ash deposit can cause spatial temperature variation of the coupon surface when the ash is not uniformly distributed on the surface. The deposition and falling-off of the ash from the surface can also cause temperature variation temporally. Therefore, the resistance may be masked by the temperature effect, and the direct comparison of the resistance is not appropriate. In Fig. 9, the resistance data show a trend of increasing fluctuations, corresponding to the ash deposition process initially and probably the deposition and detachment of the ash layer afterwards.

Based on the result in the first 100 hours, the average corrosion rate is calculated to be around 1×10^{-6} m/h in Figure 12. The corrosion rate can also be extracted from the data in the first 40 hrs as 1×10^{-6} m/h. During these periods, the ash deposition is not significant and the

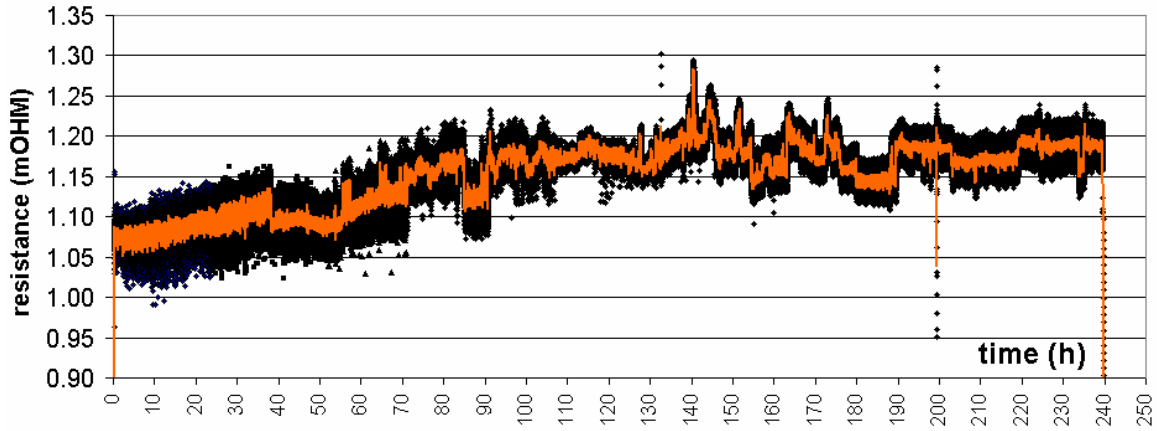


Figure 9. Corrosion measurement result of sample resistance v.s time.

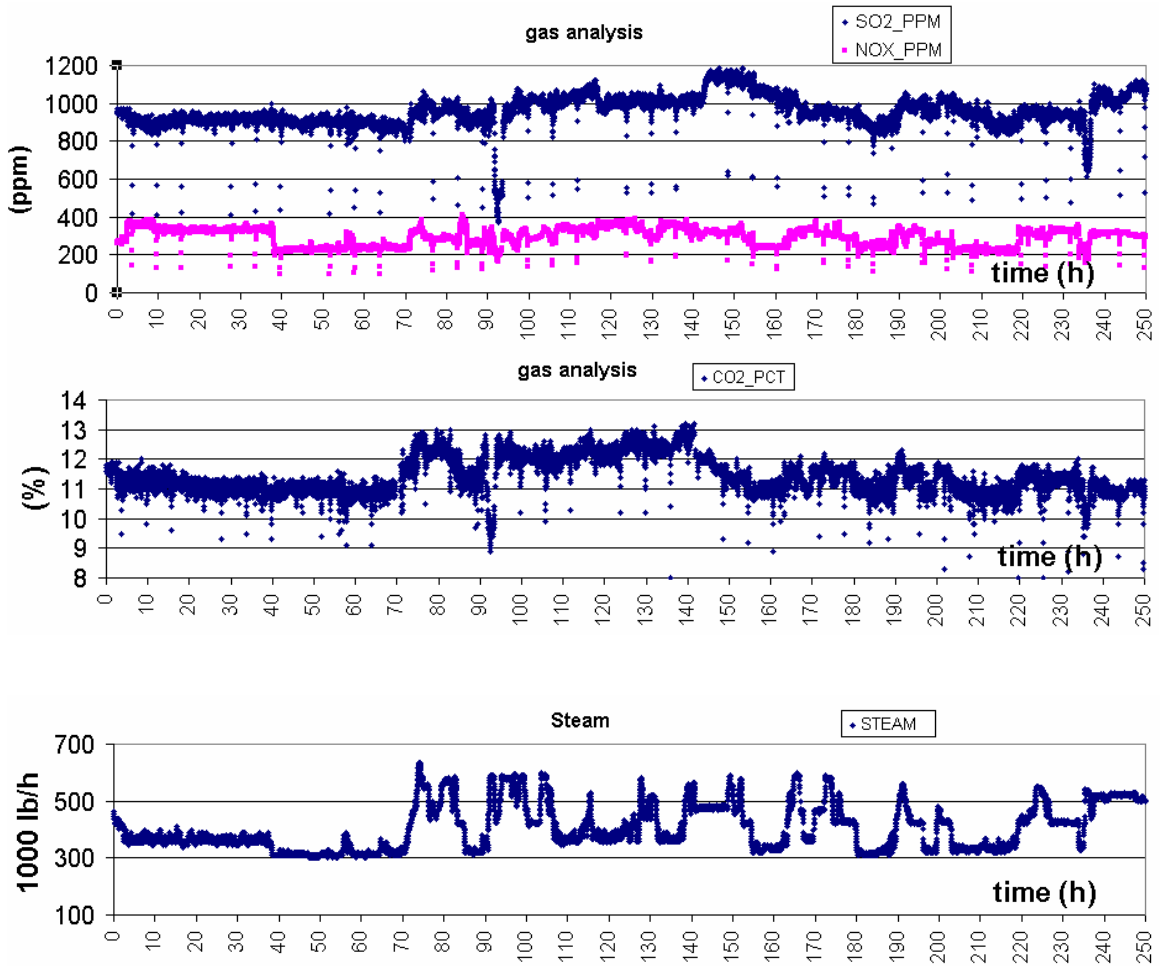


Figure 10. Flue gas analysis and steam loading.

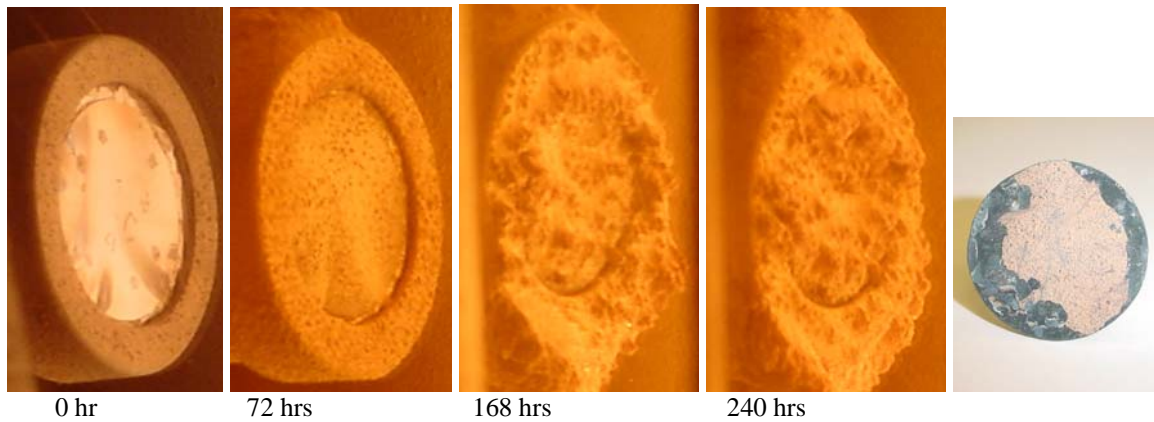


Figure 11. Ash depositing and oxide coating on the coupon surface.

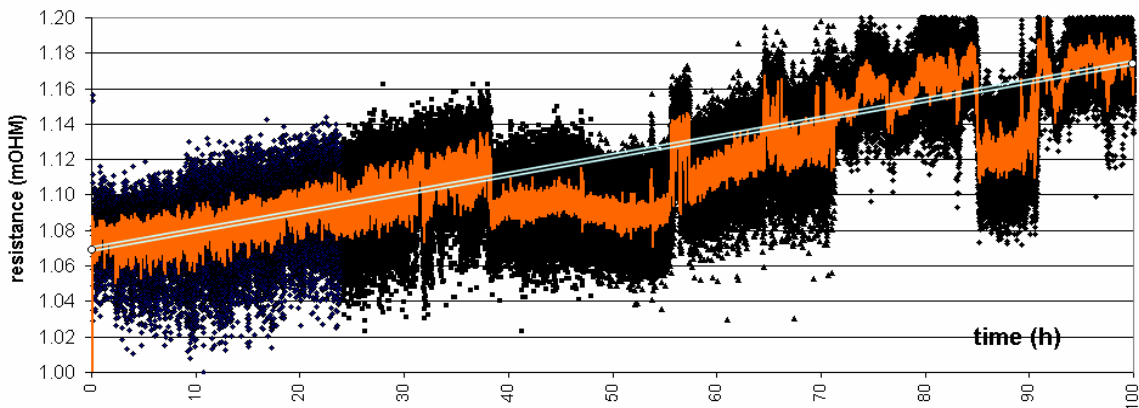


Figure 12. The resistance measurement in the first 100 hours.

effect of ash deposit is much less. This rate value of 1×10^{-6} m/h is about twice as much as the actual average corrosion rate of 0.42×10^{-6} m/h. Because the corrosion tends to be faster initially, the result is believed to be reasonable. The commonly accepted “normal” corrosion rate is about 0.1×10^{-6} m/h at lower temperatures of about 400. Because the temperature in this experiment is higher at 550 °C, the corrosion rate is higher as expected.

CONCLUSION

The on-line corrosion monitoring system based on electrical resistance can determine the corrosion rate in about 40 hours under the experimental conditions at a power plant. The coupon had significant ash depositions during the 240 hour test and the non-uniformity of the coupon temperature caused significant errors in coupon thickness calculation. Better temperature control or temperature compensation, and measures to remove ash deposition are needed to allow the probe to measure corrosion rate accurately in the prolonged period.

ACKNOWLEDGEMENT

This work was partially supported by the Electric Power Research Institute (EPRI), Department of Energy and the University of Alabama at Birmingham. The authors wish to thank Douglas Boylan of the Southern Company Service and Billy Zemo of the Alabama Power Company for their assistance in the plant experiment. Conclusions and statements made in this paper are those of the authors and in no way reflect the endorsement of the funding agency.

REFERENCE

1. Harb, J.N.; Smith, E.E., Fireside Corrosion In PC-Fired Boilers, *Progress in Energy and Combustion Science*, v 16, n 3, 1990, p 169-190.
2. Tran, H.; Barham, D., Fireside Corrosion In Kraft Recovery Boilers. *An overview of chemistry, Notes - Tappi Press*, 1991, 1991 Kraft Recovery Operations: Short Course, Jan 6-11 1991, Orlando, FL, USA, p 279.
3. La Fond, John F.; Verloop, Arie; Walsh, Allan R., Engineering Analysis Of Recovery Boiler Superheater Corrosion, American Society Of Mechanical Engineers, Fuels and Combustion Technologies Division (Publication) FACT, v18, 1994, Combustion Modeling, Scaling and Air Toxins, *Proceedings of the 1994 International Joint Power Generation Conference*, Oct 2-6 1994, Phoenix, AZ, USA, p 201-209.
4. Sethi, V.K.; Wright, I.G.; Nagarajan, V.; Krause, H.H., Solving Fireside Corrosion Problems In Incinerators, *Materials Performance*, v 31, n 11, Nov, 1992, p 43-46.
5. Krause, H.H., Fireside Corrosion Problems In Refuse-Fired Boilers, *Materials Performance*, v 33, n 3, Mar, 1994, p 63-69.
6. Clark, F. and Morris, C.W., Combustion Aspects Of Furnace Wall Corrosion, *Corrosion Resistant Materials in Coal Conversion System*. D. B. Meadowcroft and M. I. Manning (Eds), pp. 47-61, Applied Science Publishers, London (1983).

Measurement of Waterwall and Superheater Corrosion with Biomass Co-firing

Heng Ban, PhD, PE, Associate Professor

Department of Mechanical Engineering

University of Alabama at Birmingham

1150 10th Ave. S., Birmingham, AL 35294

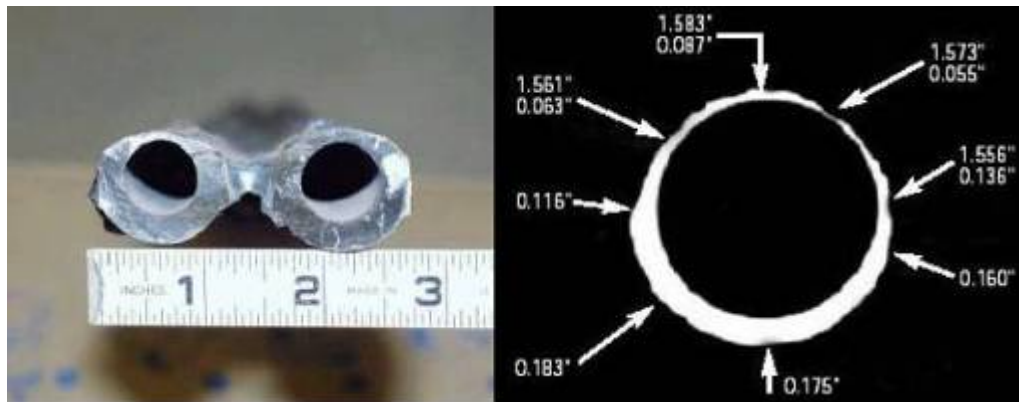
Tel: (205) 934-0011, Fax: (205) 975-7217, hban@uab.edu

Project Participants

- **Billy Zemo**, Plant Gadsden, Alabama Power Company
- **Charles Boohaker**, Southern Company Service
- **Bochuan Lin**, Mechanical Engineering, University of Alabama at Birmingham

Why Corrosion Monitoring

- Diagnoses of corrosion problems
- Advanced warning of system upsets leading to corrosion damage
- Determination of inspections and/or maintenances
- Estimation of equipment lifetime



Recent EPRI & DOE Efforts

- Reaction Engineering Inc. used ECN.
- DOE NETL Albany Research Center is testing ECN.
- Alstom tested panel resistance method.
- Southern Research Institute and UAB tested and developed ER.
- UAB developed Capacitance method.

Corrosion Work at UAB

- Resistance Sensor
 - Lab sensor development
 - Pilot coal combustor testing
 - **Power plant measurement**
- Capacitance Sensor
 - Lab development
 - Pilot coal combustor testing

Objectives

- Power plant testing of ER probe and measurement system.
- Measurement of waterwall and superheater fireside corrosion rate.
- Compare the corrosion rates for coal and switchgrass-coal co-firing

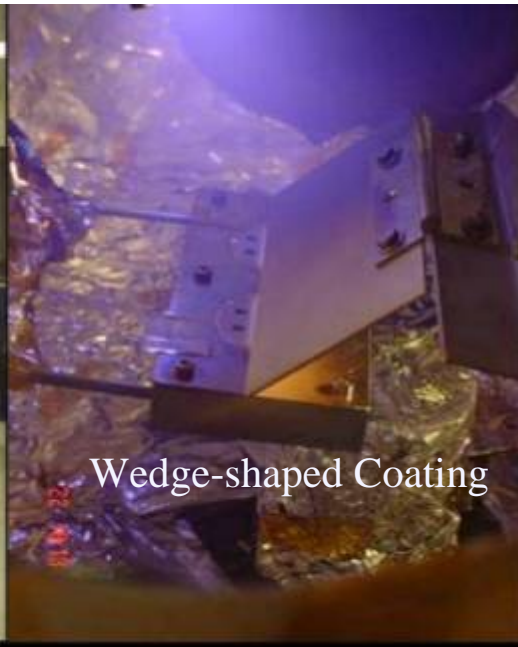
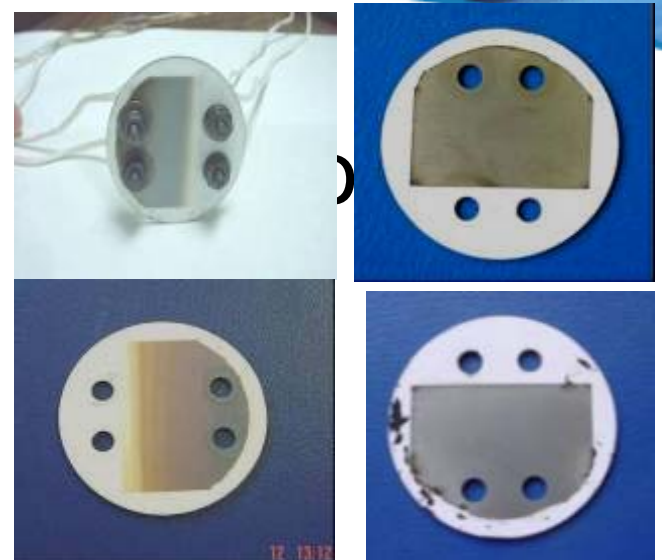
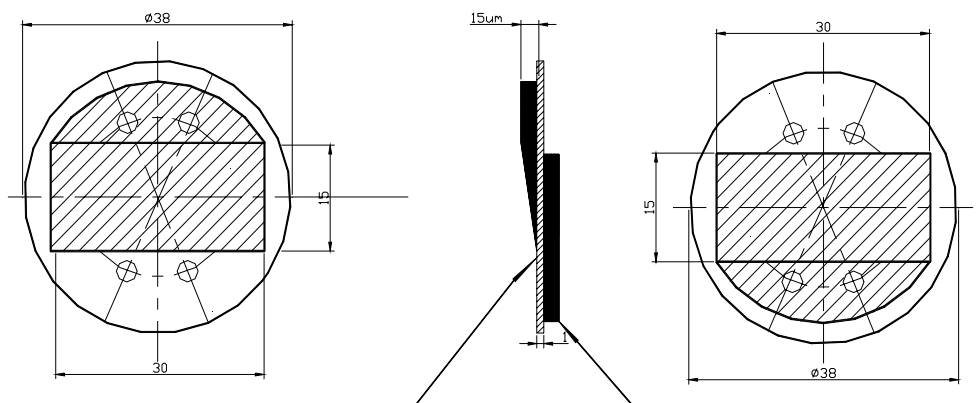
PURE ENERGY

Commercial ER Corrosion Probes



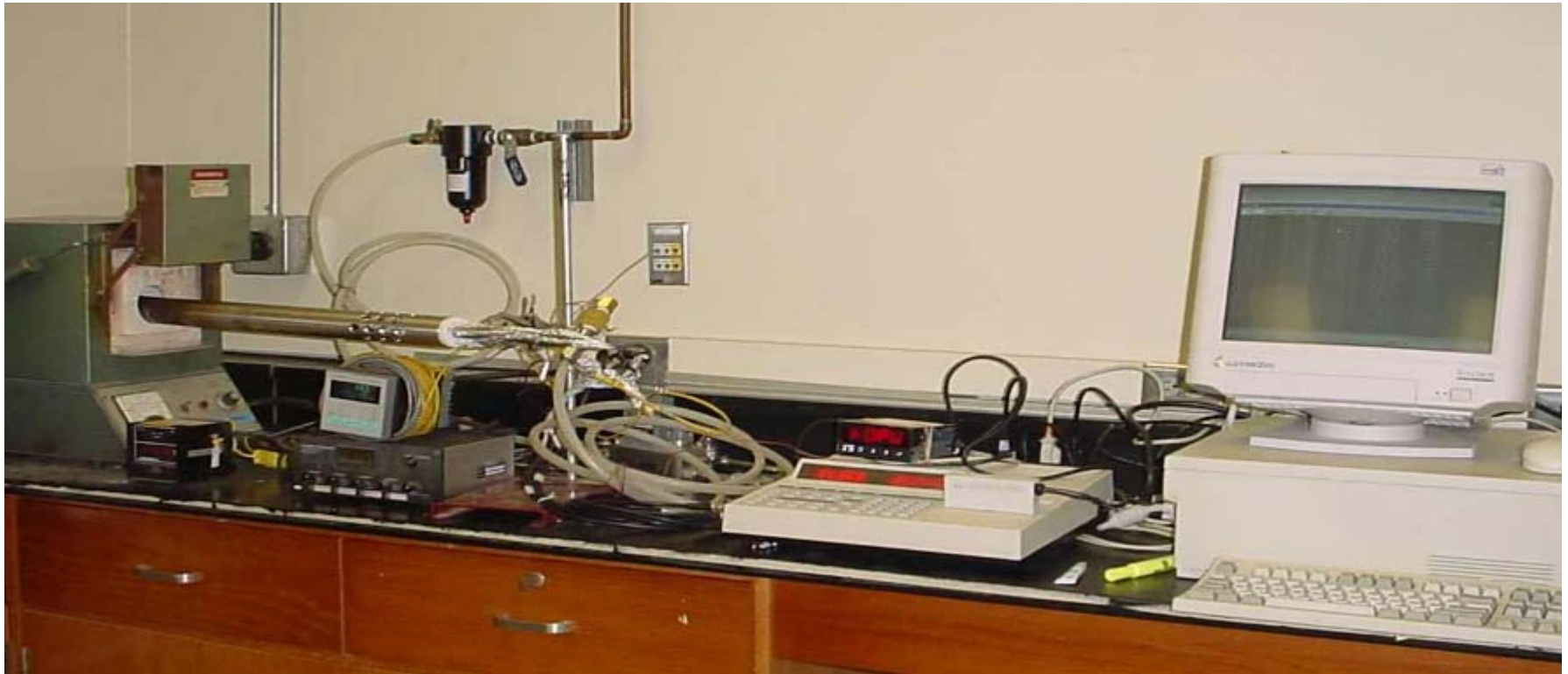
PURE ENERGY

Coating not drawn to scale



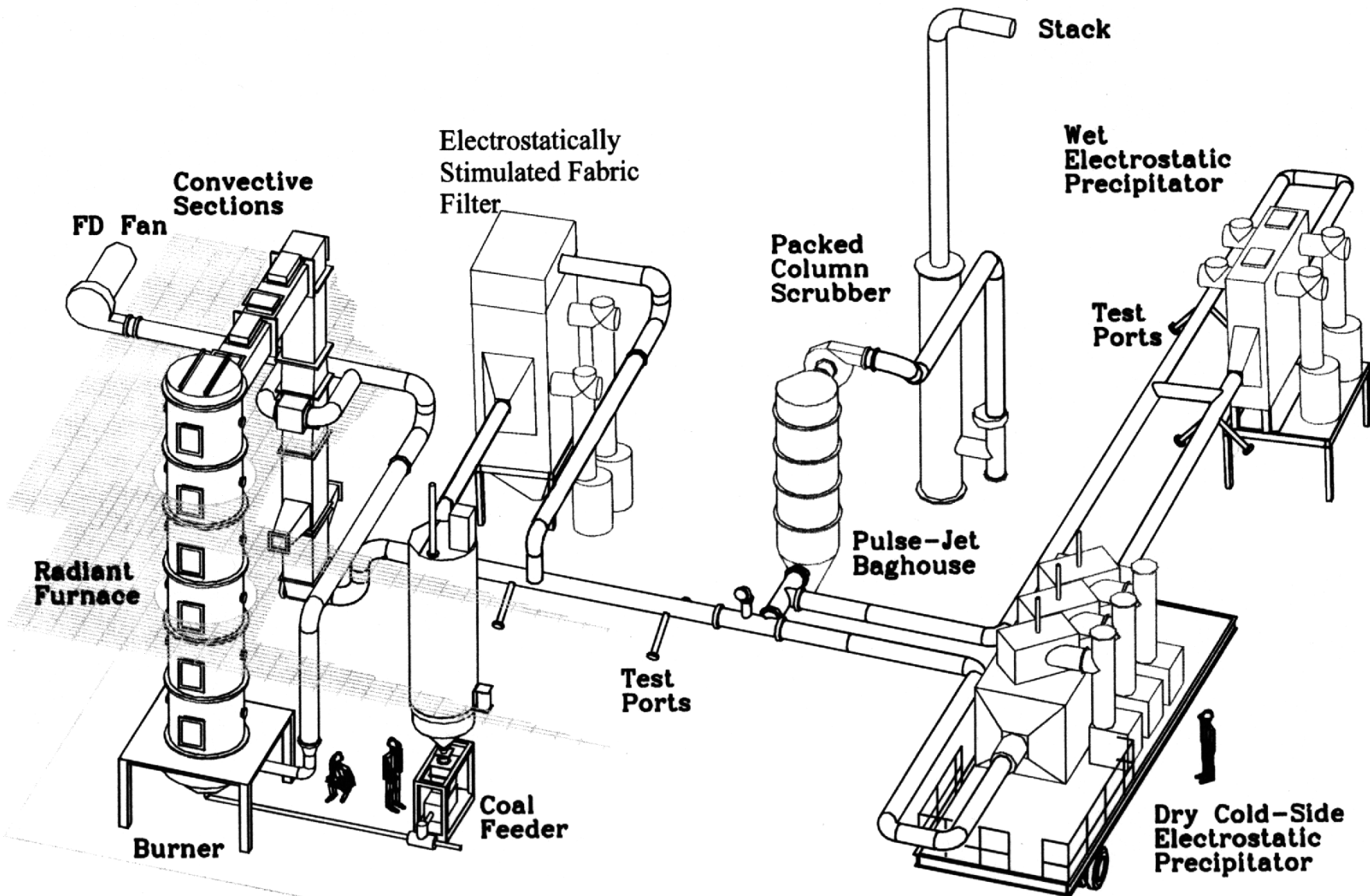
PURE ENERGY

Laboratory Setup



SOUTHERN RESEARCH COMBUSTION RESEARCH FACILITY

Birmingham, AL



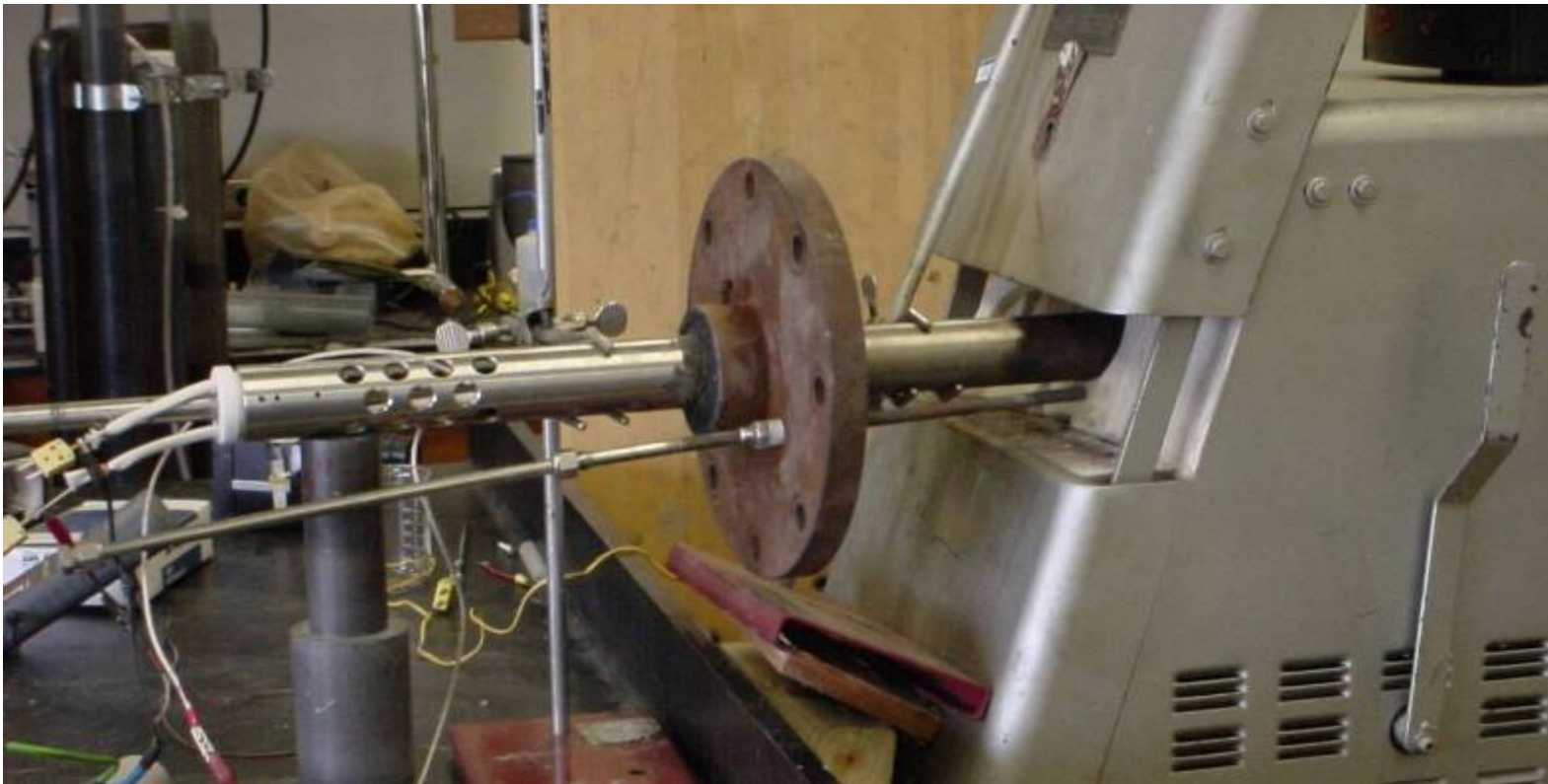
PURE ENERGY



Corrosion Probe at SRI Combustor



Probe Picture



PURE ENERGY

Plant Gadsden, Switchgrass Co-Firing



Corrosion probe & Sensor Assembly



PURE ENERGY

Plant Measurement



0 hr



72 hrs



168 hrs



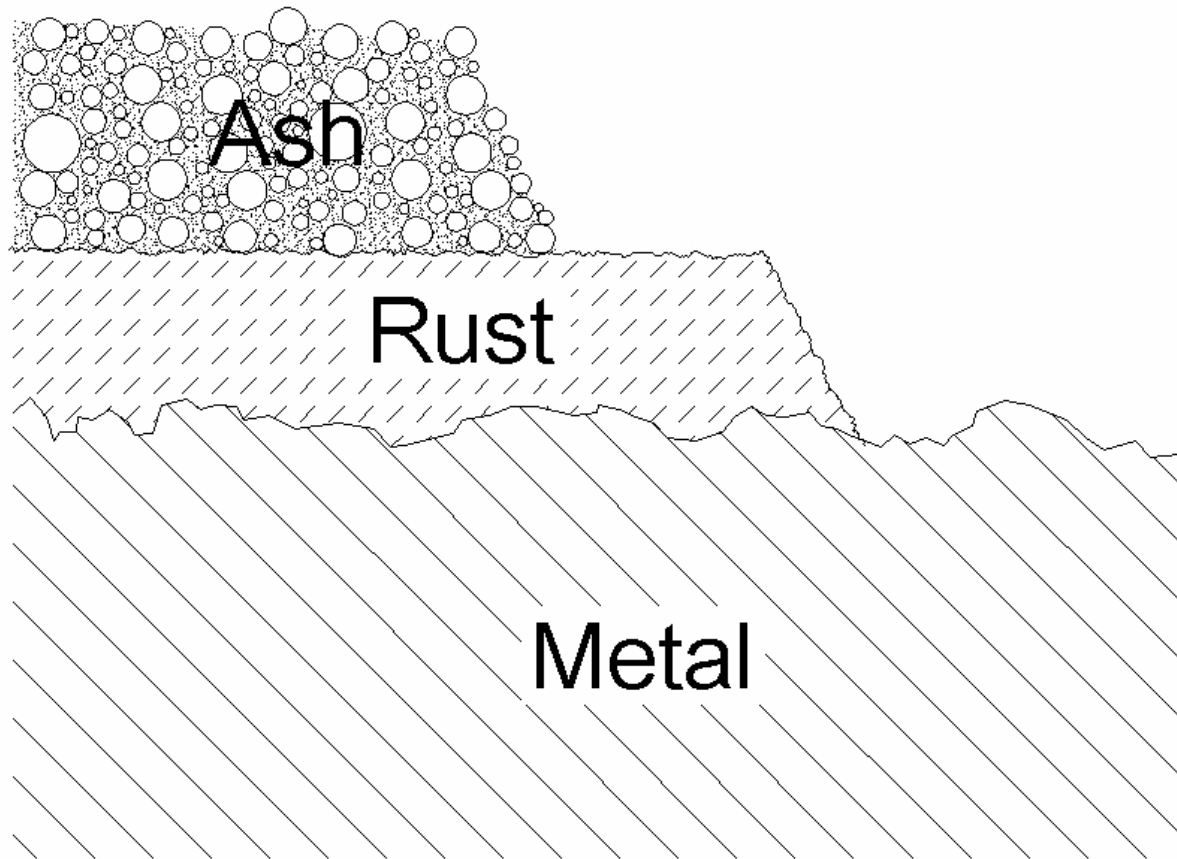
240 hrs

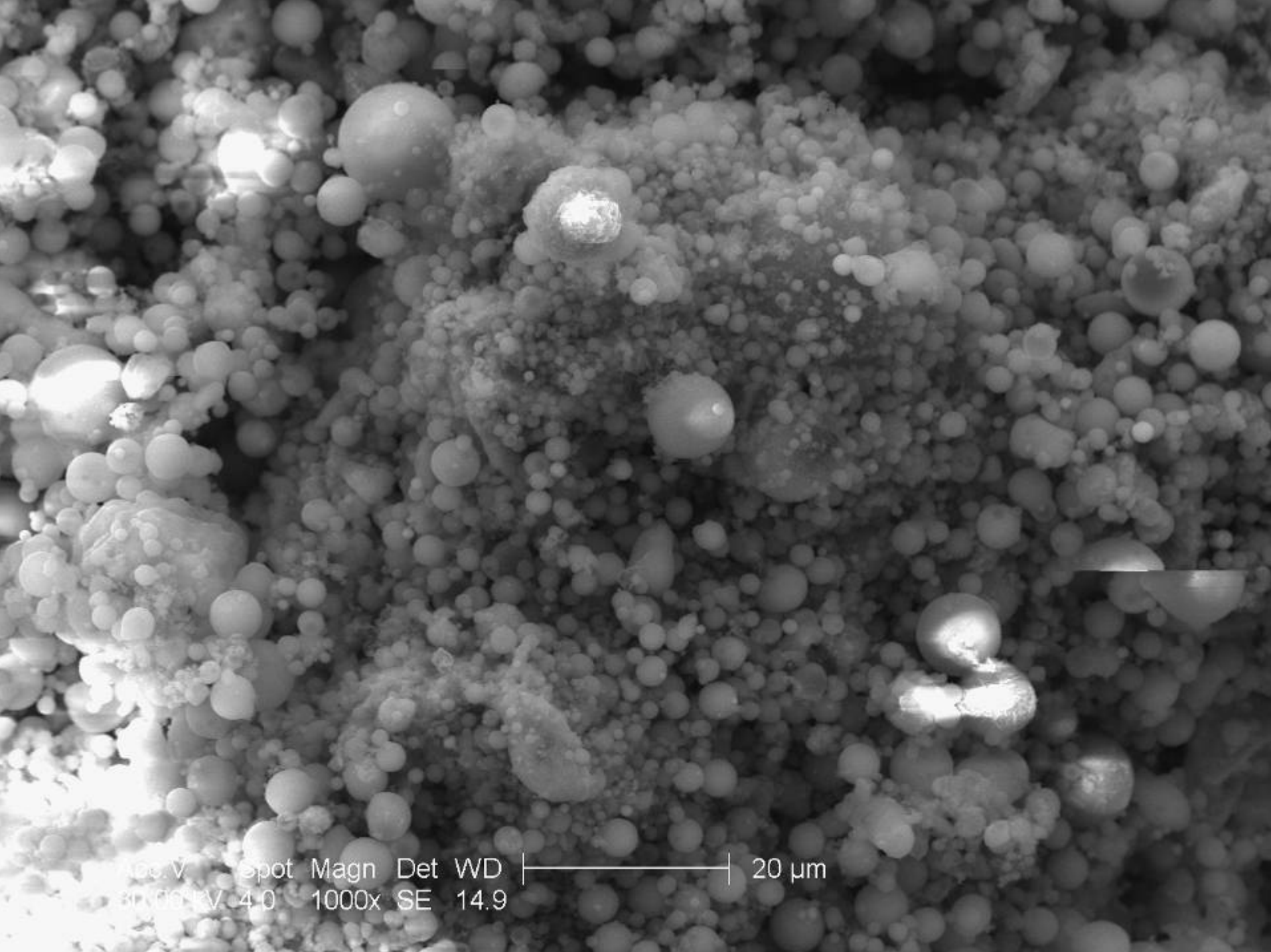
PURE ENERGY

Probe after experiment



Layers on Metal Surface

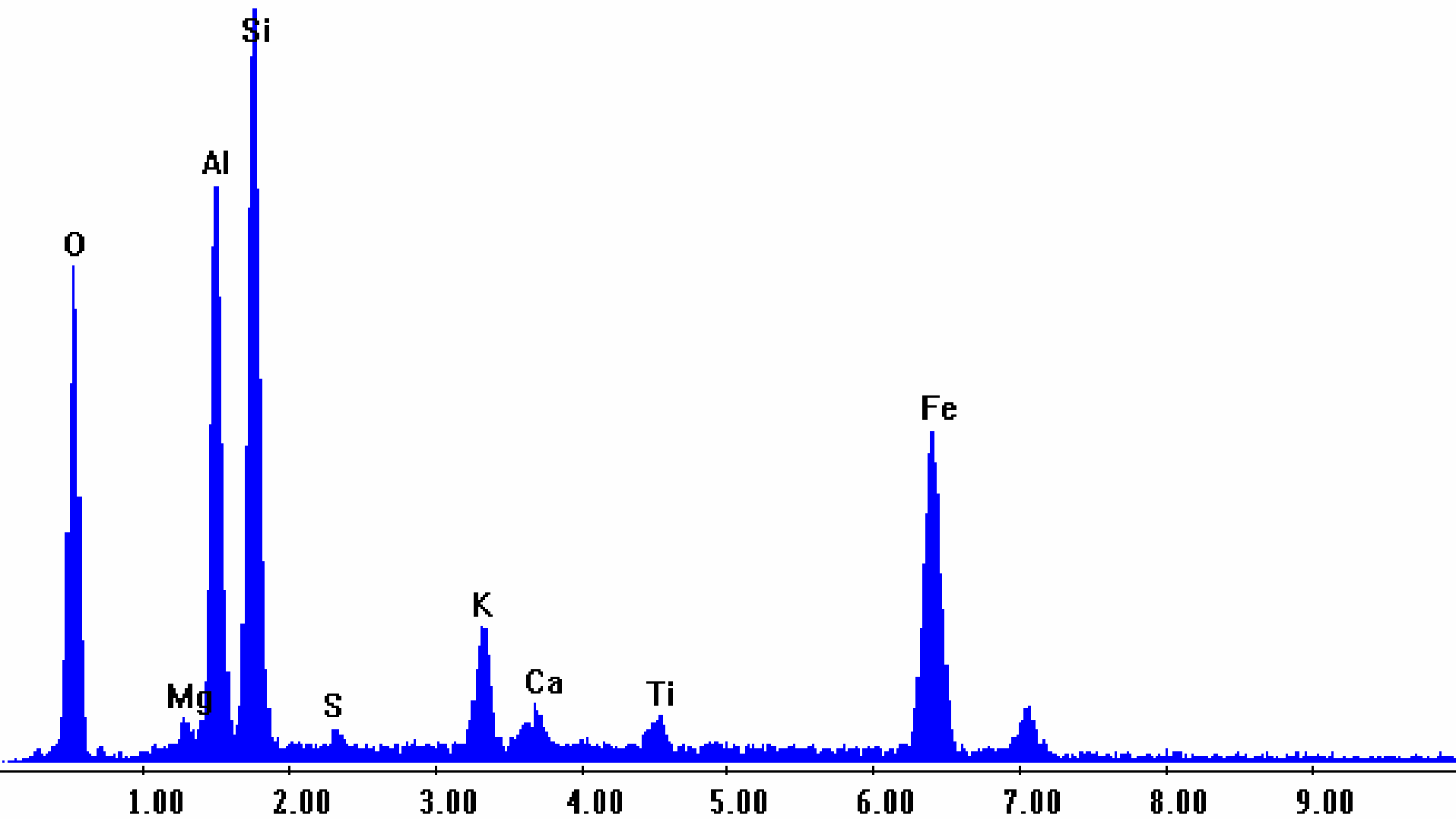




Acc.V Spot Magn Det WD
30.00kV 4.0 1000x SE 14.9

20 μ m

Label A:



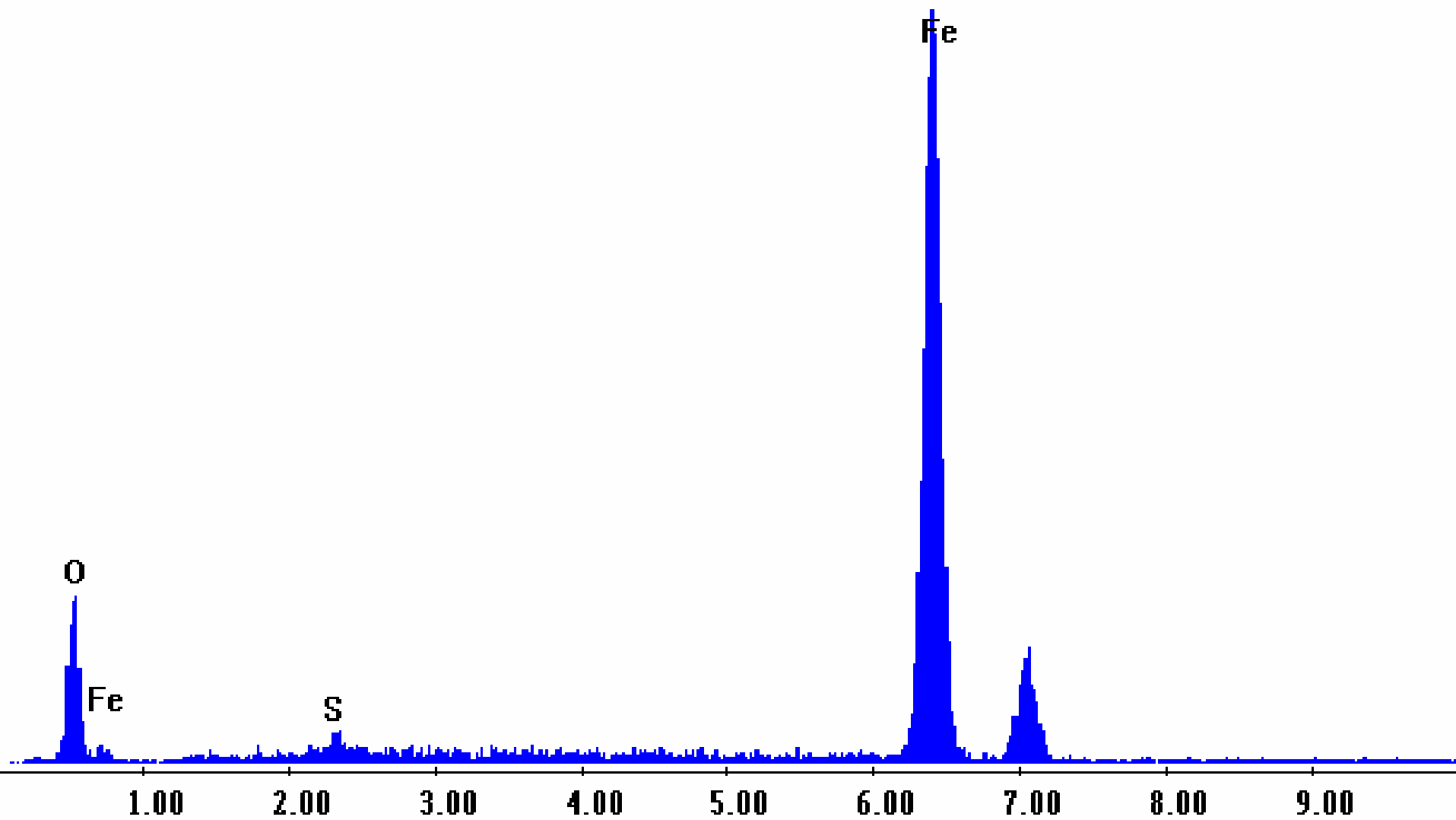
Lower
Substrate

Upper
Substrate

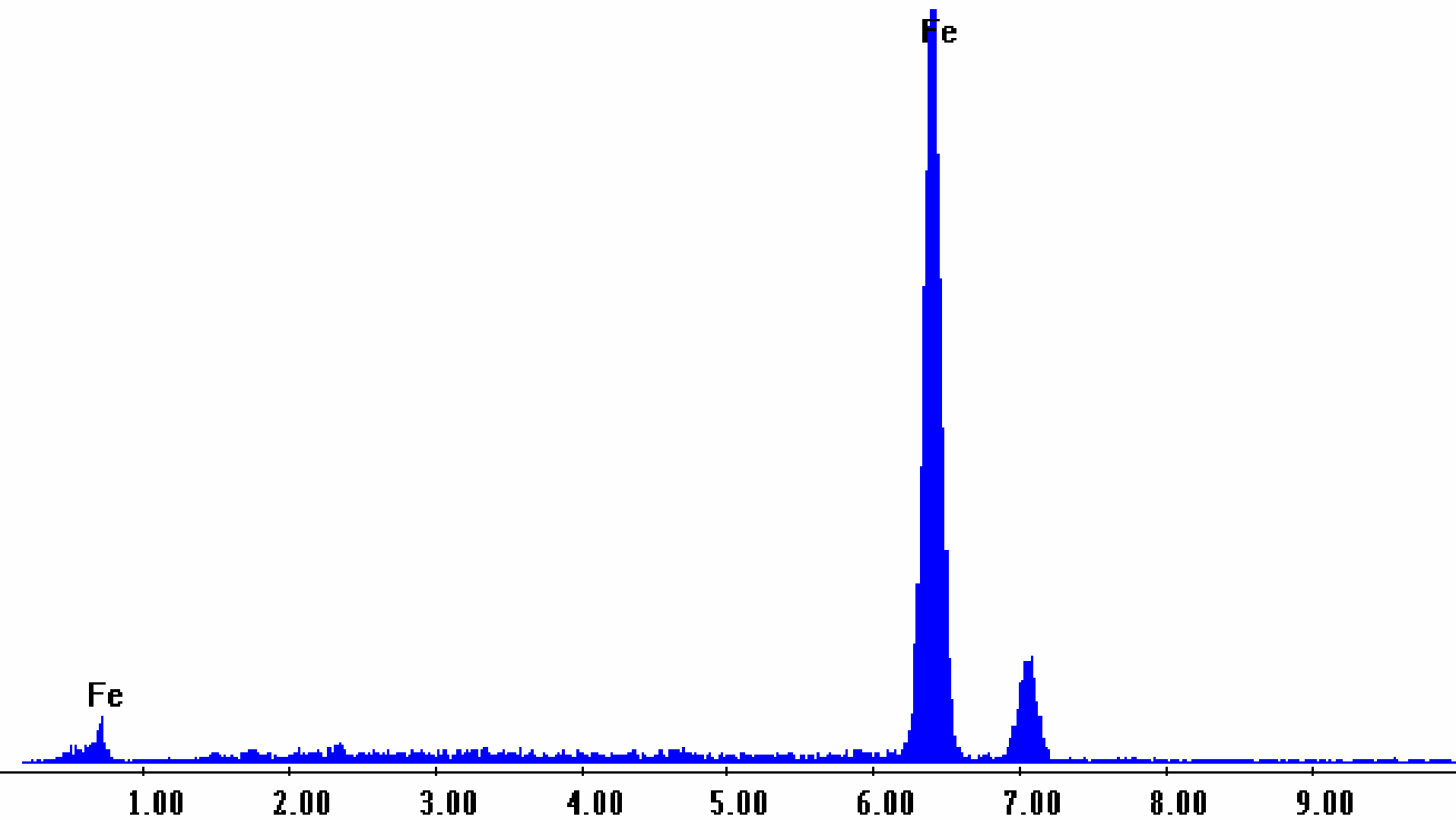
Acc.V Spot Magn Det WD |-----| 50 μ m
30.00 kV 4.0 500x SE 8.3

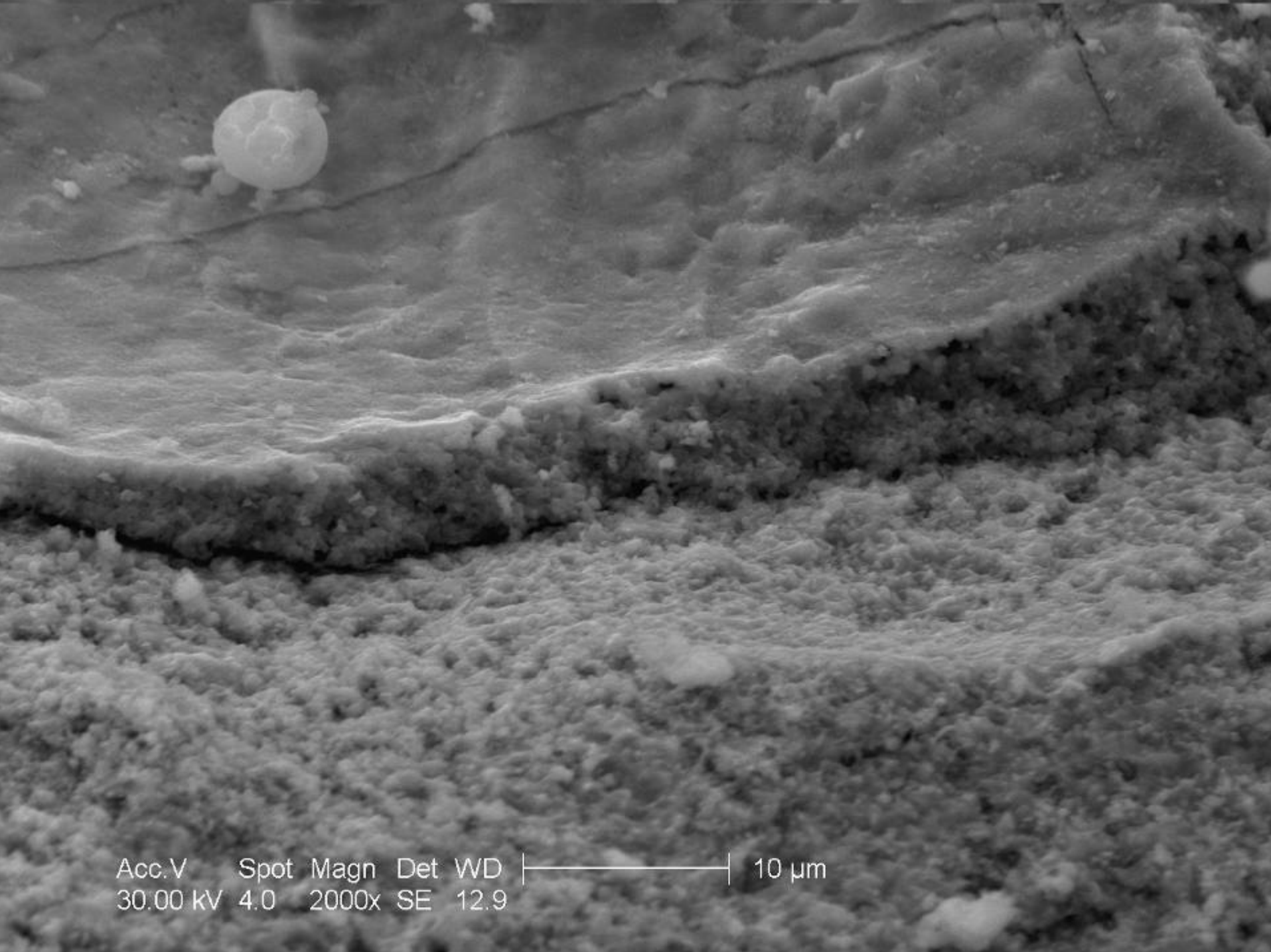
SEM Image of Waterwall Coal #2 Area 2

Label A:

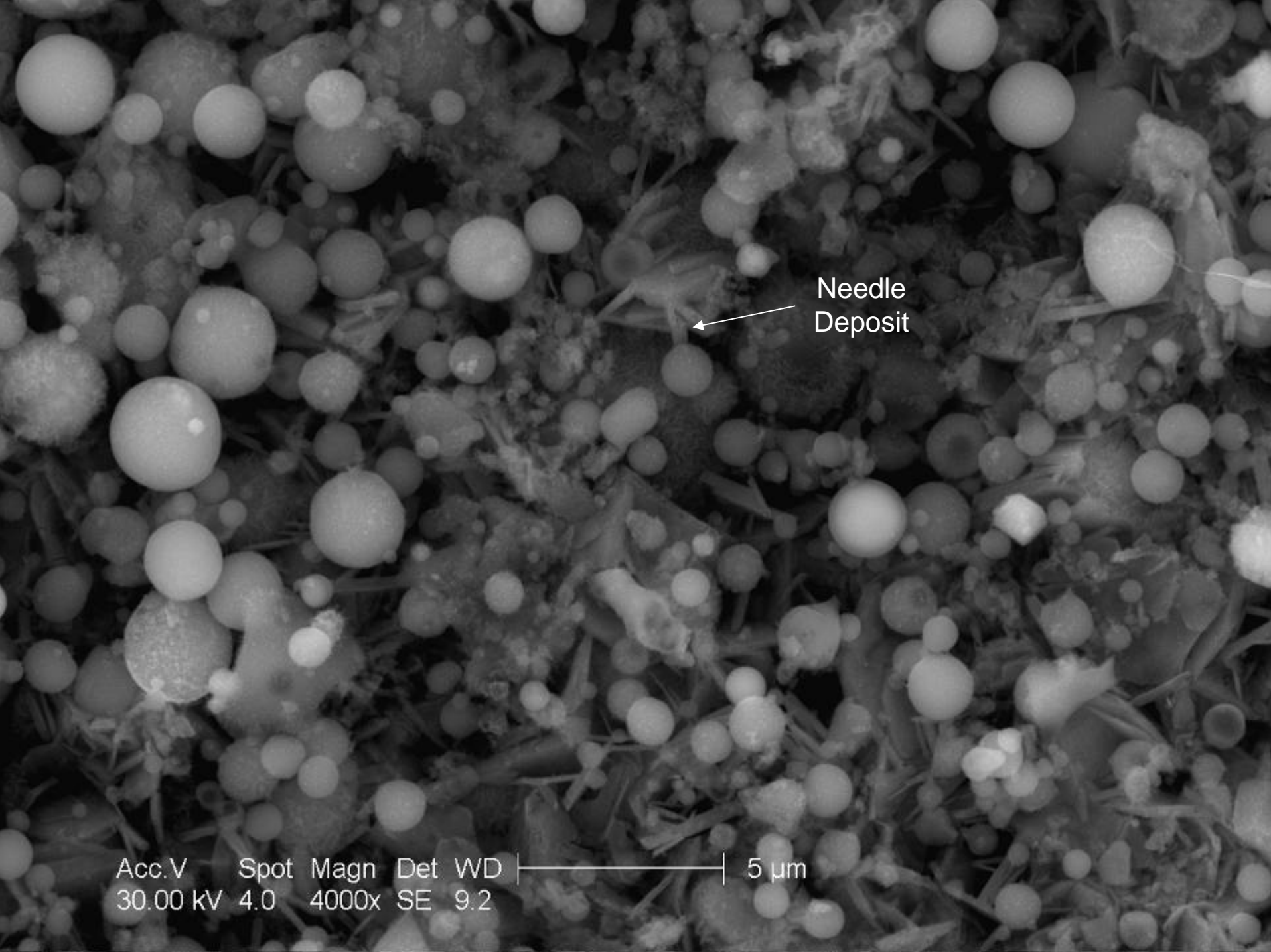


Label A:





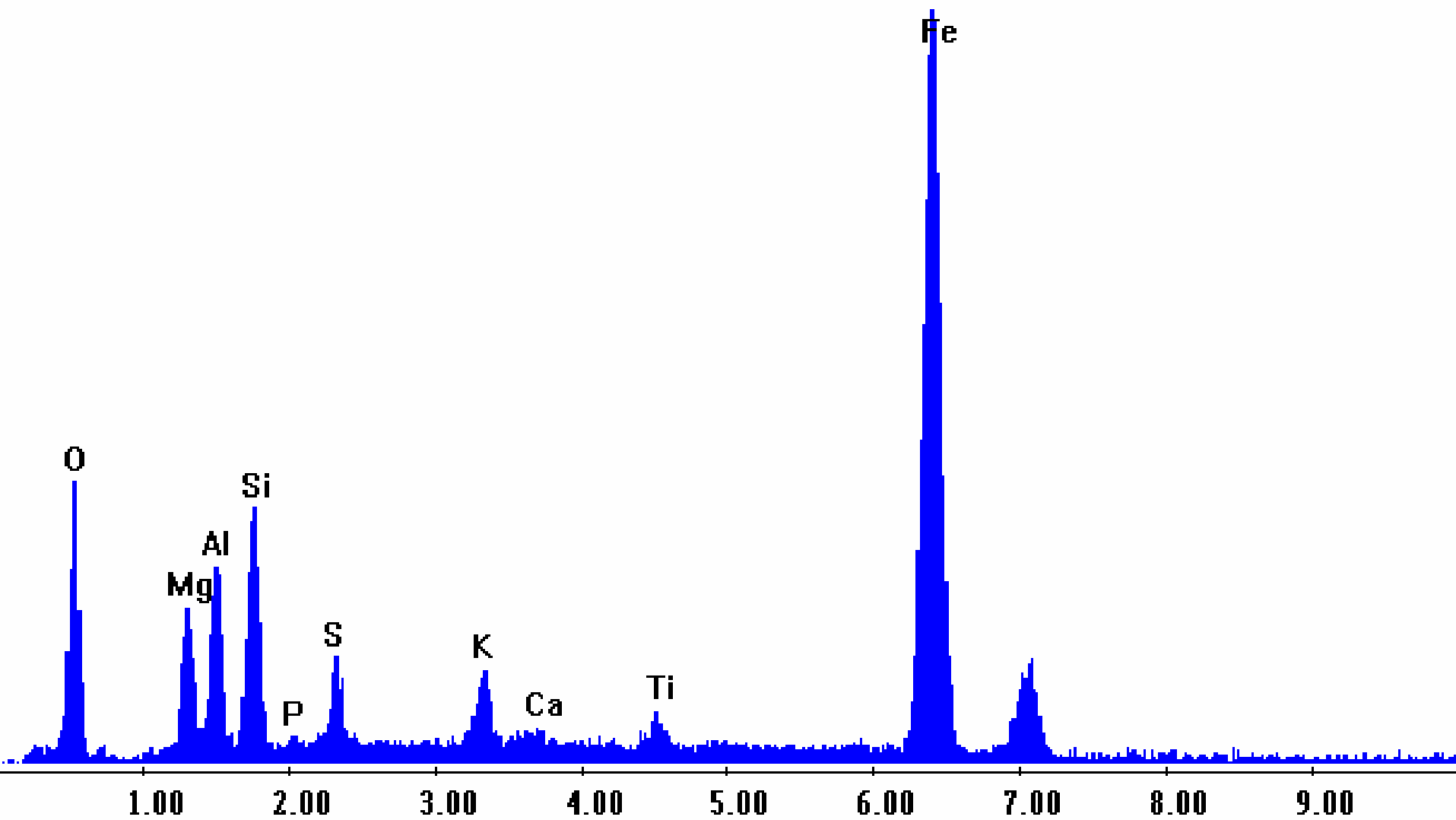
Acc.V Spot Magn Det WD |-----| 10 μ m
30.00 kV 4.0 2000x SE 12.9

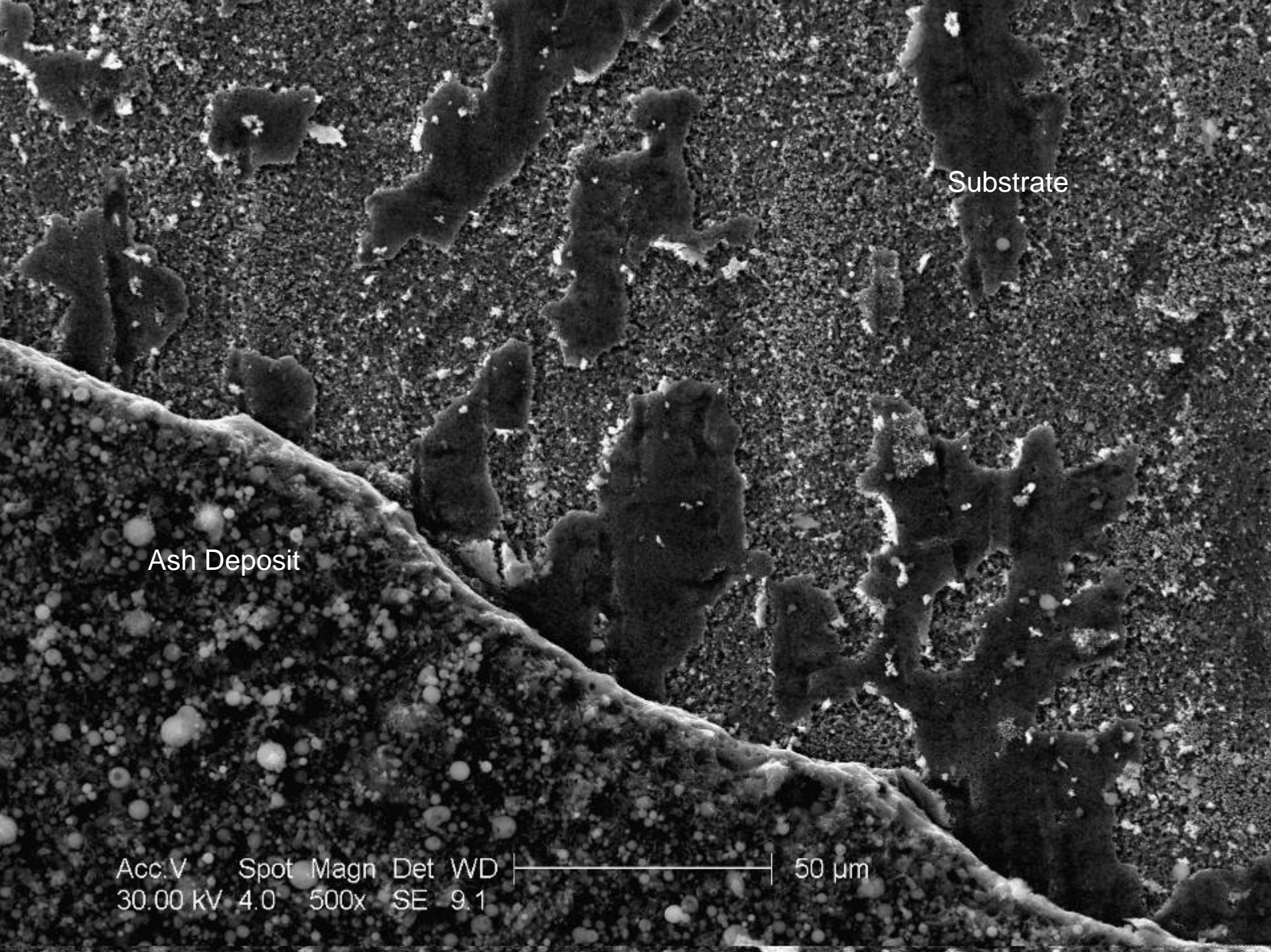


Needle
Deposit

Acc.V Spot Magn Det WD |-----| 5 μ m
30.00 KV 4.0 4000x SE 9.2

Label A:



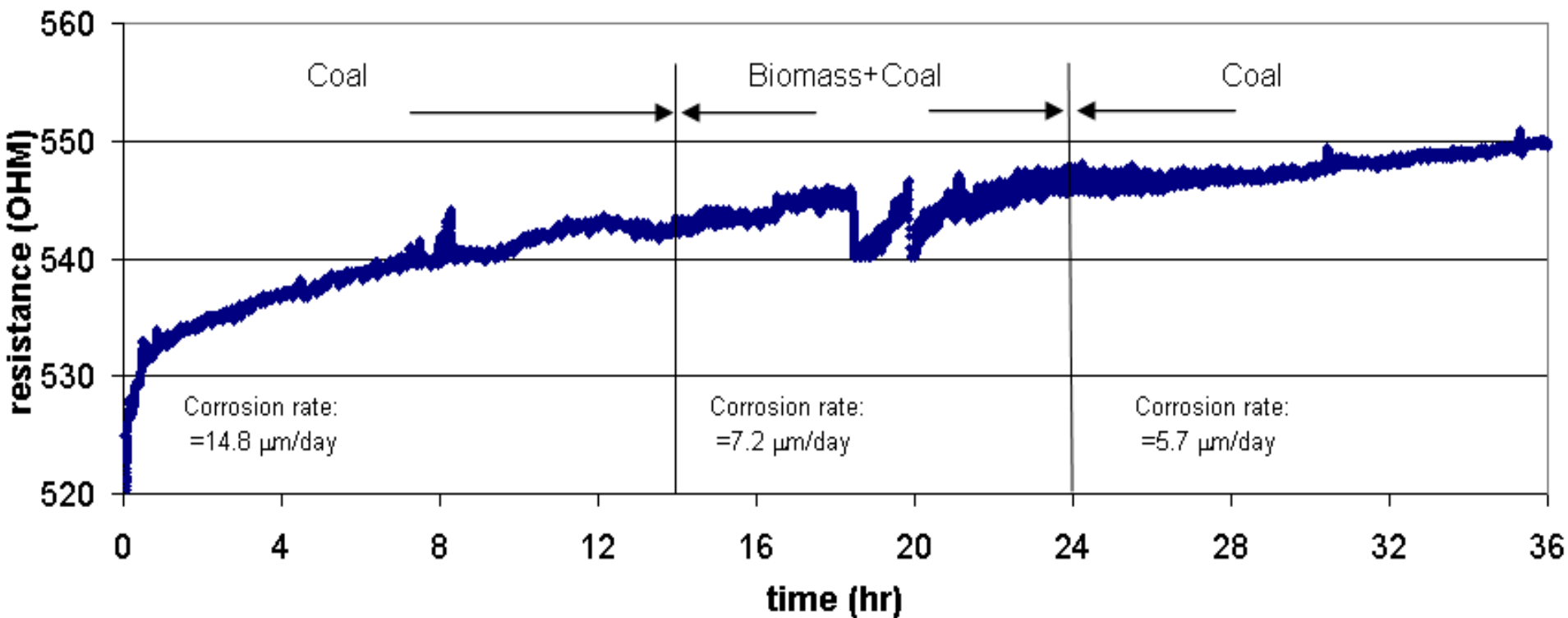


Substrate

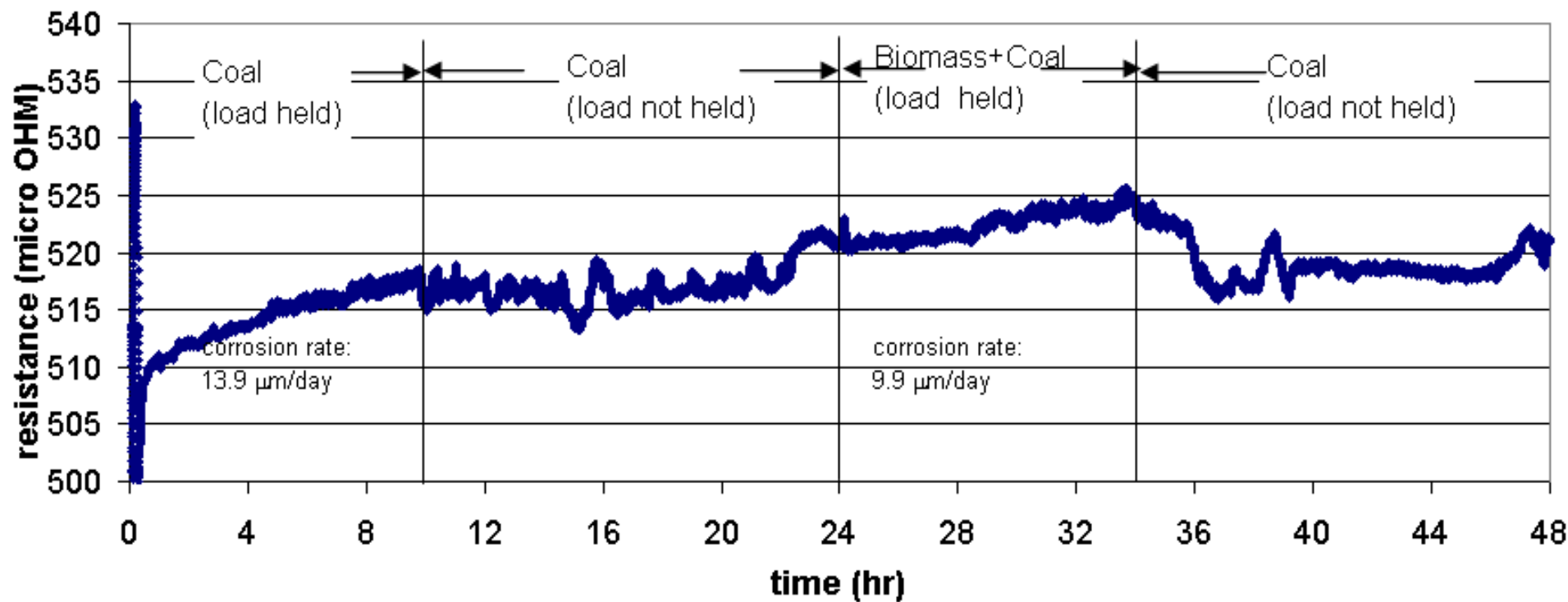
Ash Deposit

Acc.V Spot Magn Det WD |-----| 50 μ m
30.00 kV 4.0 500x SE 9.1

Sensor Resistance Data



Repeat Run



PURE ENERGY

Location	Fuel sequence	Steam (lb/h)	Corrosion rate (µm/day)	
			100% Coal	Biomass
Superheater	100% coal Biomass+coal 100% coal	530,000	13.9 (0-10 hr)	9.9 (24-34 hr)
Superheater	100% coal Biomass+coal 100% coal	530,000	14.8 (0-14 hr) 5.7 (24-40 hr)	7.2 (14-24 hr)
Superheater	Biomass+coal	530,000		27.2 (1-6.5 hr)
Superheater	Biomass+coal	530,000		28.2 (1-7hr)
Waterwall	100% coal	320,000	7.24 (0-20hr)	
Waterwall	Biomass+coal 100% coal	530,000	9.11 (10-24 hr)	
Waterwall	100% coal Biomass+coal 100% coal	530,000	17.3* (0-14 hr) 10.9(32-72 hr)	

Conclusions

- The ER probe can be used to determine corrosion in short measurement period.
- The corrosion rates for biomass co-firing and coal were measured.
- The differences between biomass and coal corrosion are still to be understood.
- More testing is needed to validate data.

Questions?

E. C. Gaston Steam Plant



Fireside Corrosion Monitoring

- Effort at UAB -

Heng Ban, Associate Professor

University of Alabama at Birmingham

Department of Mechanical Engineering

1150 10th Avenue South, Birmingham, AL 35294-4461

Tel: (205) 934-0011, Fax: (205) 975-7217, hban@uab.edu

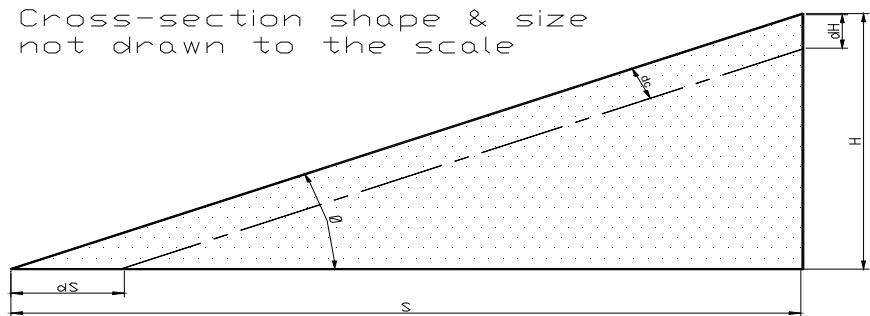
Outline of Work

- Resistance Sensors
 - Lab sensor development
 - Pilot coal combustor testing
 - Power plant measurement
- Capacitance Sensors
 - Lab development
 - Pilot coal combustor testing

Capacitance Principle

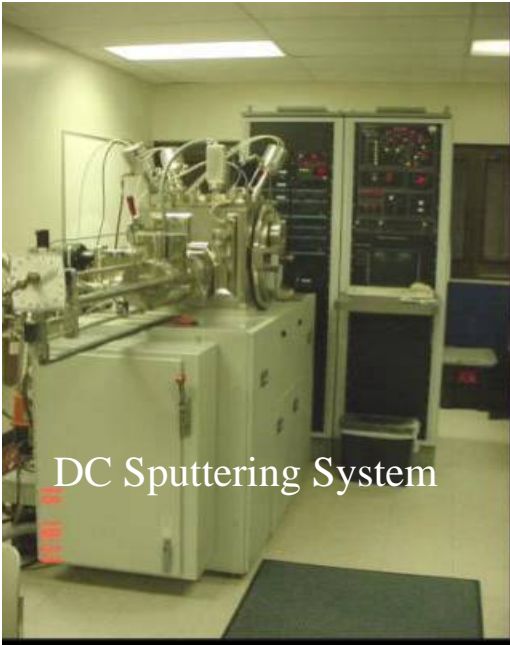
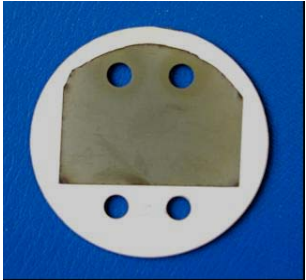
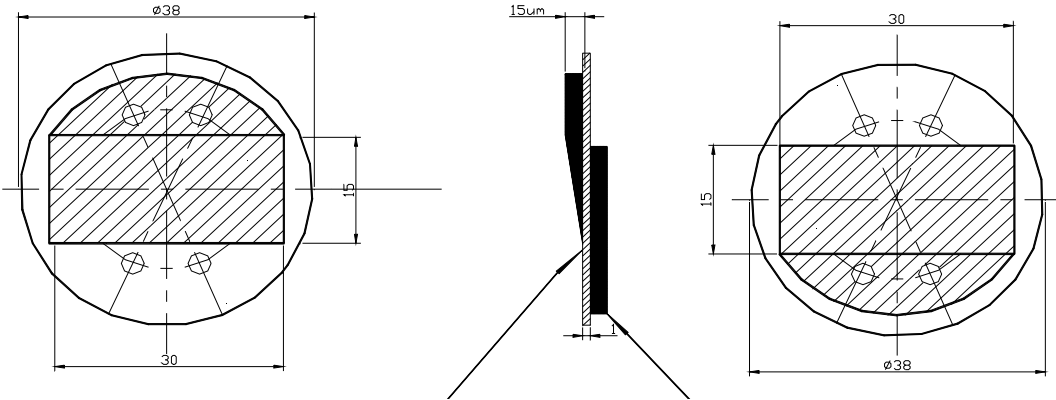
Thickness => Area/Length

- Convert thickness measurement to length/area measurement. For example, $2\ \mu\text{m}$ in thickness change can be turned into a 2 mm length change (or area).
- Measure electrical capacitance change to determine the area change.

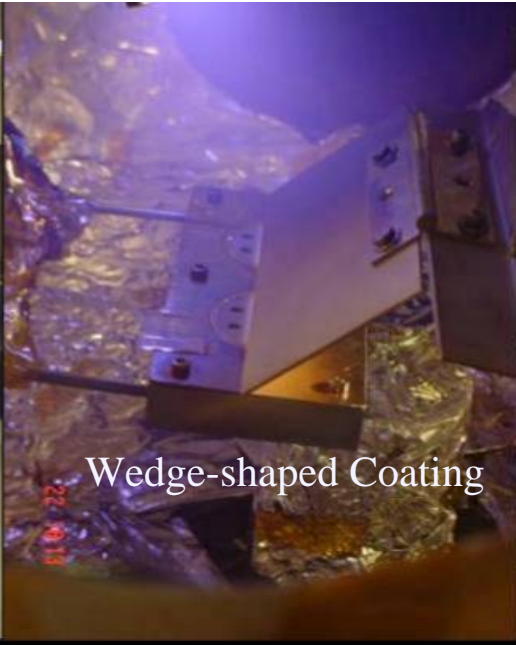


Sensor Fabrication

Coating not drawn to scale



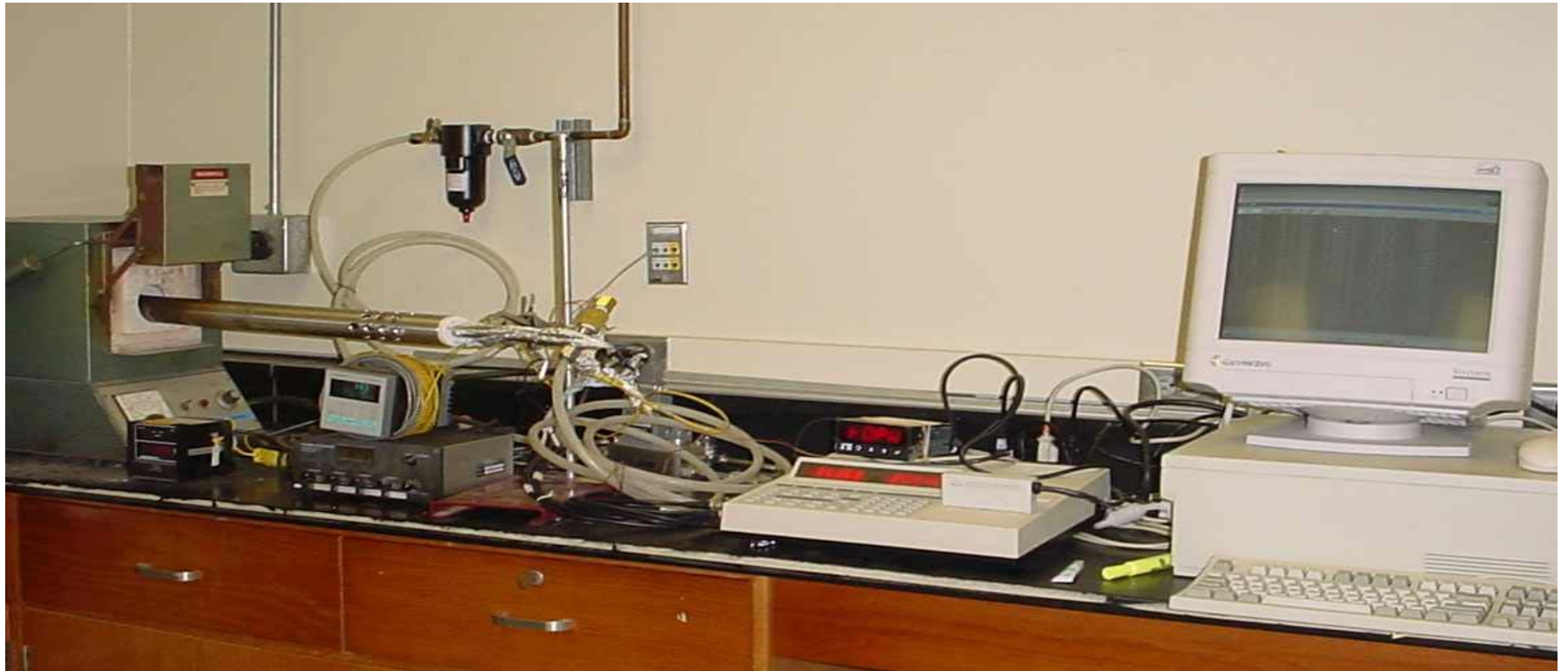
DC Sputtering System



Wedge-shaped Coating

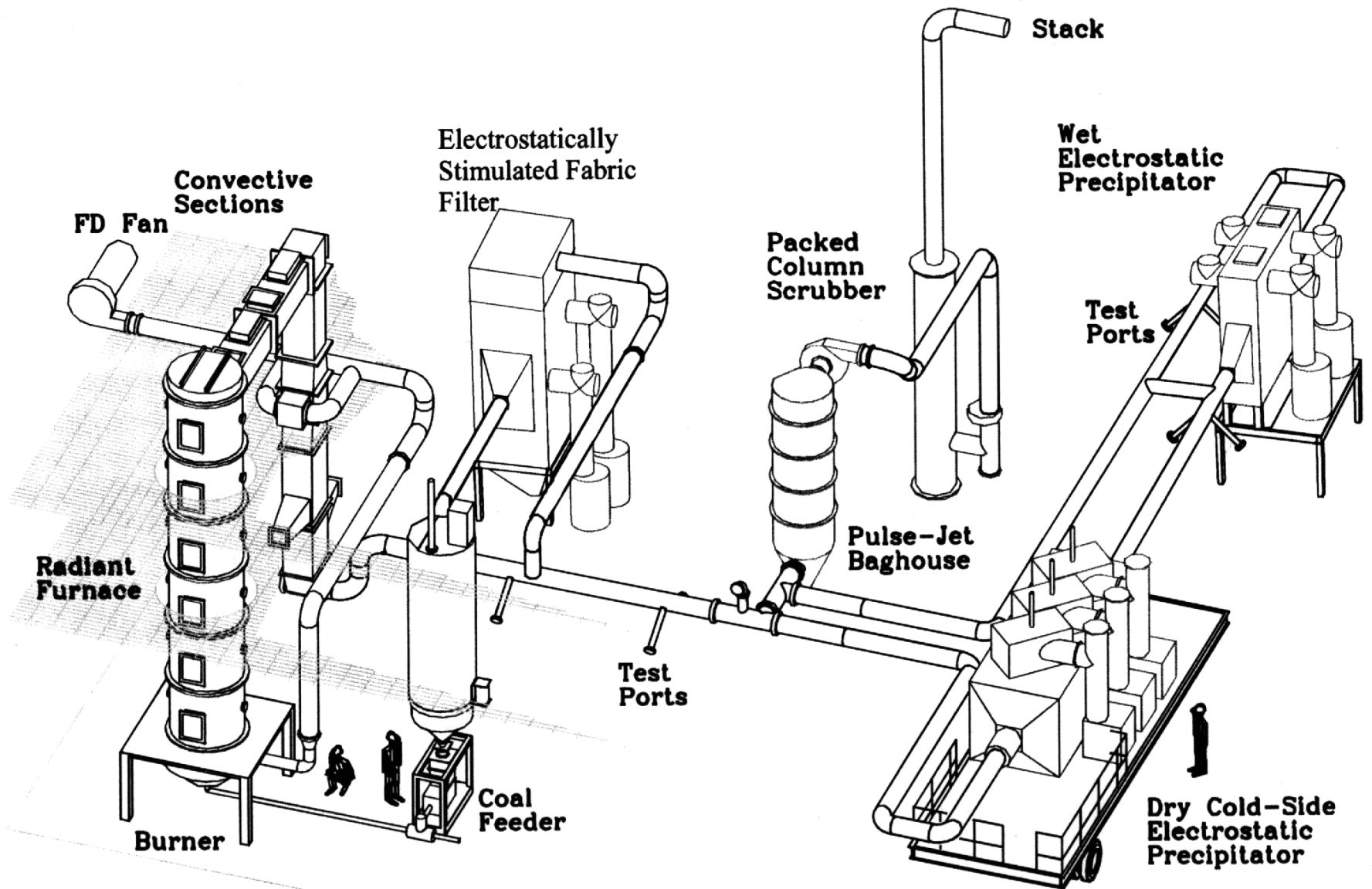


Laboratory Setup



SOUTHERN RESEARCH COMBUSTION RESEARCH FACILITY

Birmingham, AL



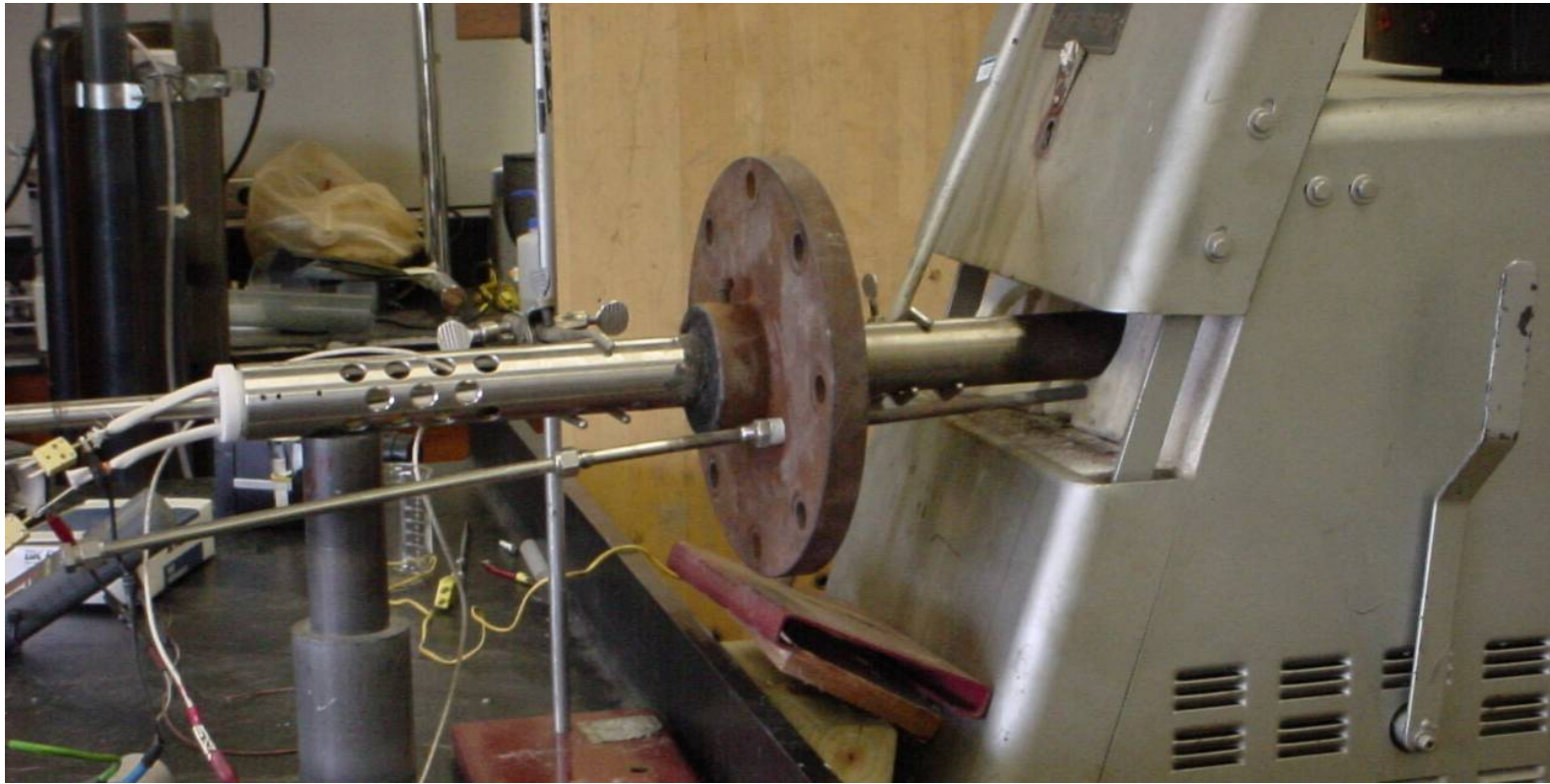
Corrosion Probe at SRI Combustor



Commercial Corrosion Probes for Low Temperature Applications



Probe Picture



Power Plant with Biomass Co-Firing



Plant Measurement



0 hr



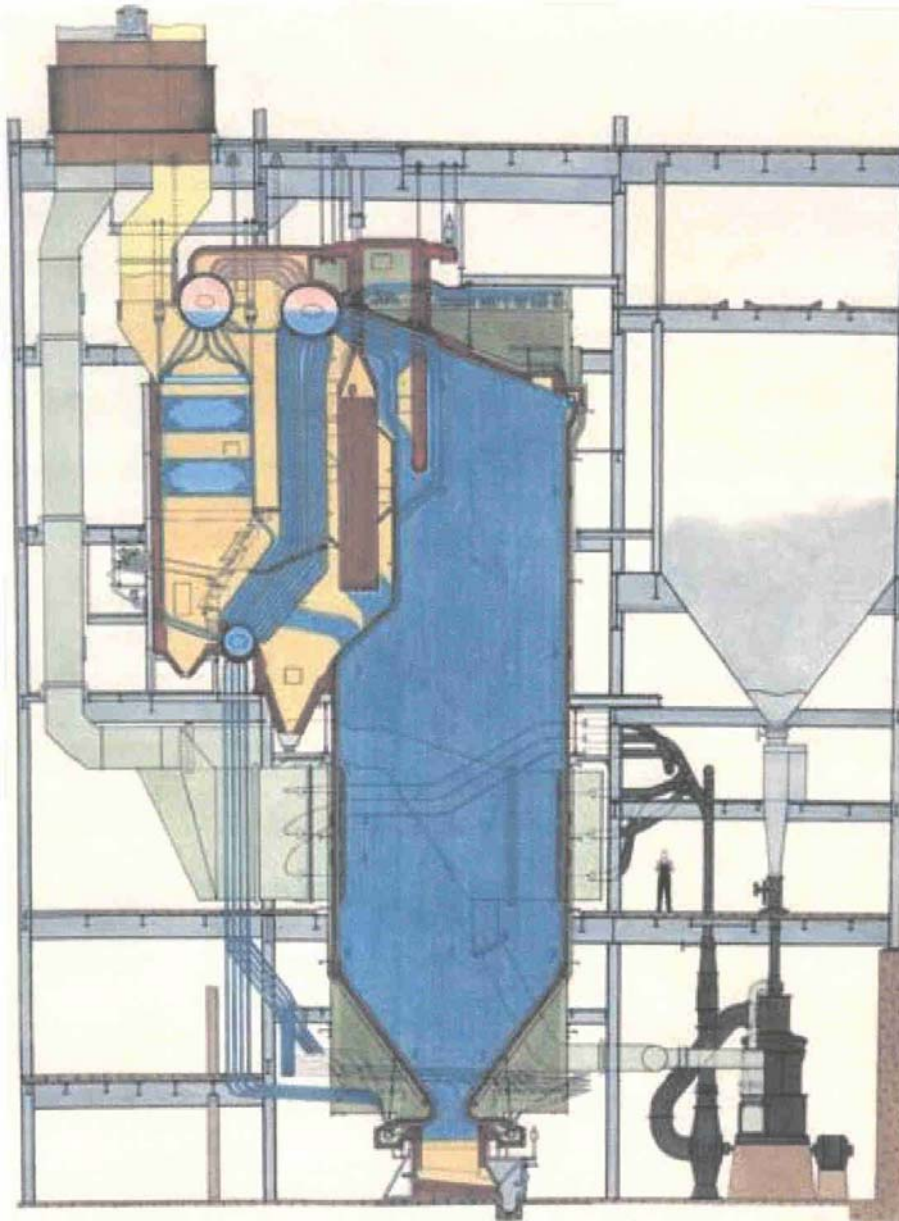
72 hrs



168 hrs



240 hrs



C-E STEAM GENERATORS 1 & 2

MAX. CONT. CAP.—400,000 LB PER HR AT 873 PSI AND 840 F TOTAL TEMP.

GADSDEN STEAM STATION

Alabama Power Company, Gadsden, Ala.

Designed and Built by COMBUSTION ENGINEERING-SUPERHEATER, INC.

TO		CONTRACT DATA SHEET		FROM SALES DATA DIVISION November 8, 1950	
TAB 15 and 23		DISTRICT OFFICE N.Y., BIRMINGHAM CREDITED WITH SALE & CHARLOTTE		File alphabetically ALA Destroy sheet dated	
PURCHASER		COMMONWEALTH & SOUTHERN CORPORATION, NEW YORK, N. Y.			
USER		1-2 ALABAMA POWER COMPANY, GADSDEN, ALABAMA			
PLANT NAME	GADSDEN PLANT	CONS. ENGR.	-	INDUSTRY	P. U.
PROPOSED FUEL		E. BITUMINOUS AND NATURAL GAS.		ASH FUS. TEMP. F	2200
F.O. 60.0 % VOL.		35.7 % MOIST. 10 % (AF) ASH 4.3% SUL.		BTU PER LB AS FIRED	13,133
Methane 85.0 % Ethane 5.0 % CO ₂ N ₂ and other inert gases 10.0 %				HARDGROVE GRIND	57
FUEL BURNING EQUIPMENT		CONT. NO.	28746-RB	6 - No. 593 Raymond Bowl Mills	
and Type TV Burners					
FURNACE	CONT. NO.	28746-CFF	SQ.FT.H.S. PER FURN.	9486	TYPE OF BOTTOM
Roof - finned; Front, Sides & Rear - Plain					
FRONT TO REAR	22'-4-1/2"	WIDTH	28'-7-1/2"	VOLUME	35,500 CU.FT. GROSS
BOILER	CONT. NO.	28746-BV	NO.	2	SQ.FT. H.S.EA.
DESIGNATION		28'-7-1/2" 27-3/49-3 VE 4/12 60-54/36 31.5		MFR.	C-E
				STEAM WASHER	BOILER NUMBER
				-	1 and 2
SUPERHEATER	CONT. NO.	28746-SH	TYPE	Wesco 2-Stage	
CONTROL RANGE	300,000 to 600,000 with by-pass damper		SQ.FT. H.S.	13,679	
REHEATER	TYPE	None		SQ.FT. H.S.	-
ECONOMIZER	CONT. NO.	28746-COVS	NO.	2	
TYPE	CF-I 33W x 16H x 28'-7-1/2" 1G.			SQ.FT. H.S.EA.	17,100
AIR HEATER	CONT. NO.	28746-CAHL	NO.	4	
TYPE	20-1/2 V 56			SQ.FT. H.S.EA.	63,000
MISCELLANEOUS DATA		Contract included structural steel, steel-encased settings, ductwork, insulation, soot & ash hoppers, soot blowers.			
EXPECTED PERFORMANCE					
LB STEAM PER HR-ACTUAL	150,000	500,000	*600,000 -	Max. Cont.	*Guaranteed
FEEDWATER TEMP. TO Economizer	270	345	365		
FEEDWATER TEMP. FROM Boiler	376	435	456		
STEAM TEMP. F	775	860	*860		
HEAT RELEASE BTU/CU.FT./HR.	5600	17,800	21,000		
TEMP. GAS FROM AIR HEATER	272	317	335		
TEMP. AIR FROM AIR HEATER	444	529	554		
OVERALL EFFICIENCY %	86.3	87.9	*87.55		

FORM 1-2-50

COMBUSTION ENGINEERING - SUPERHEATER, INC., 200 MADISON AVENUE, NEW YORK, N. Y.

Corrosion probe (left) and sensor assembly (right)



Probe after experiment



Corrosion Sensor after Tests (left: waterwall; right: superheater)



E. C. Gaston Steam Plant

The E. C. Gaston Steam Plant is a 5-unit coal fired plant with a combined output of 1,880 megawatts. The Plant is located near Wilsonville, Alabama in Shelby County.



Waterwall and Superheater Corrosion Measurement at Plant Gadsden

Heng Ban, PhD, PE, Associate Professor

Department of Mechanical Engineering

University of Alabama at Birmingham

1150 10th Ave. S., Birmingham, AL 35294

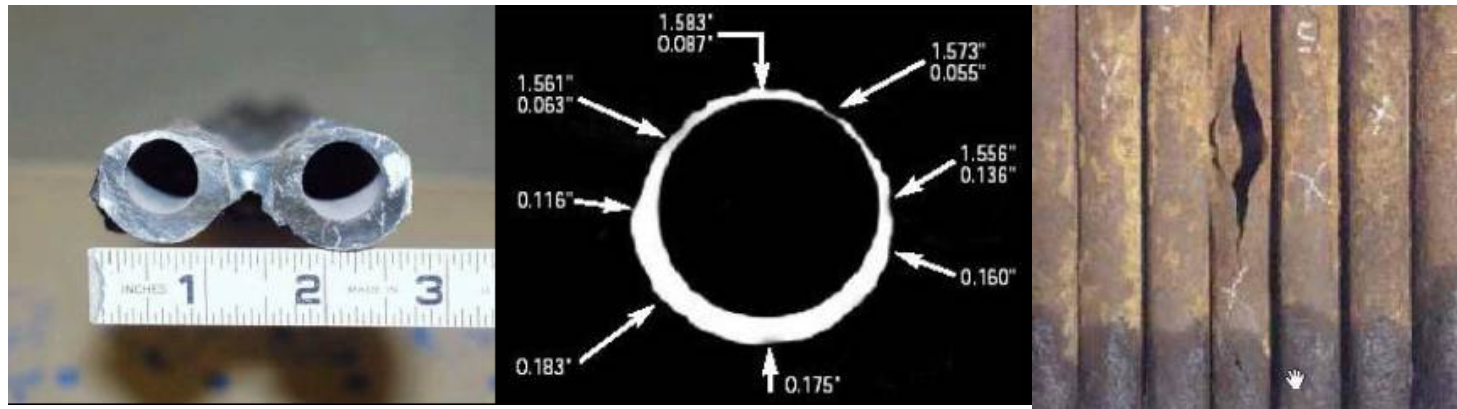
Tel: (205) 934-0011, Fax: (205) 975-7217, hban@uab.edu

Project Participants

- **Billy Zemo**, Plant Gadsden, Alabama Power Company
- **Charles Boohaker**, Southern Company Service
- **Bochuan Lin**, Mechanical Engineering, University of Alabama at Birmingham

Why Corrosion Monitoring

- Diagnoses of corrosion problems
- Advanced warning of system upsets leading to corrosion damage
- Determination of inspections and/or maintenances
- Estimation of equipment lifetime



Recent EPRI & DOE Efforts

- Reaction Engineering Inc. used ECN.
- DOE NETL Albany Research Center is testing ECN.
- Alstom tested panel resistance method.
- Southern Research Institute and UAB tested and developed ER.
- UAB developed Capacitance method.

Corrosion Work at UAB

- Resistance Sensor
 - Lab sensor development
 - Pilot coal combustor testing
 - **Power plant measurement**
- Capacitance Sensor
 - Lab development
 - Pilot coal combustor testing

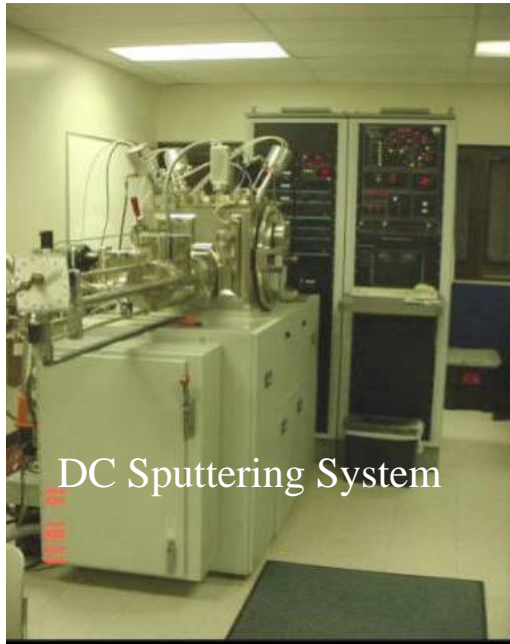
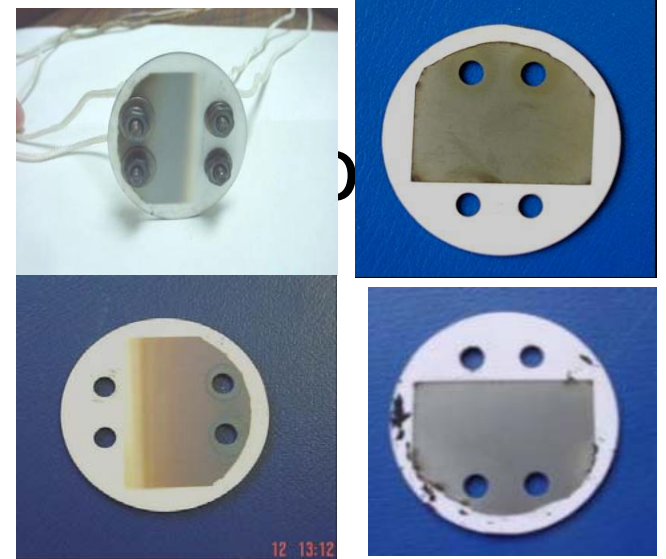
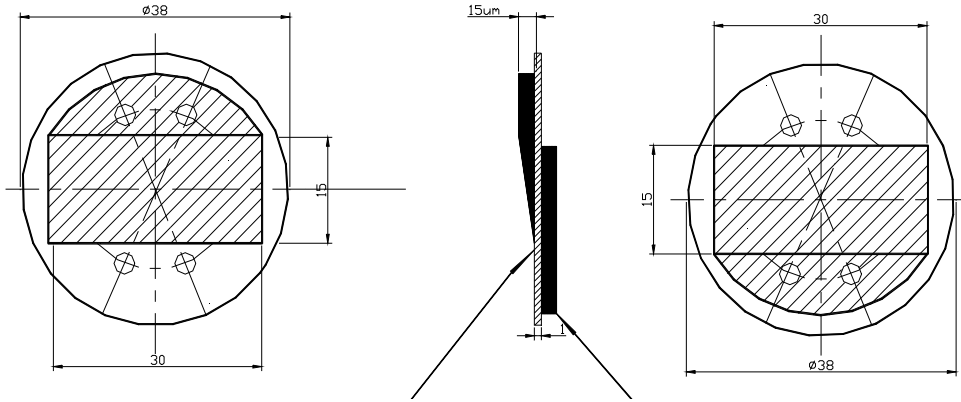
Objectives

- Power plant testing of ER probe and measurement system.
- Measurement of waterwall and superheater fireside corrosion rate.
- Compare the corrosion rates for coal and switchgrass-coal co-firing.

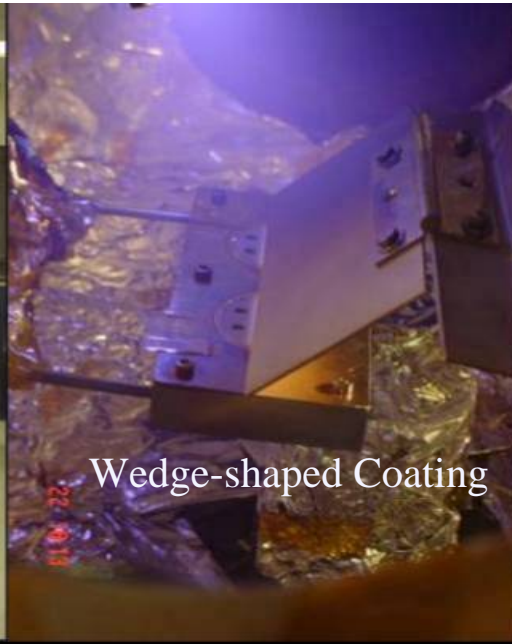
Commercial ER Corrosion Probes



Coating not drawn to scale



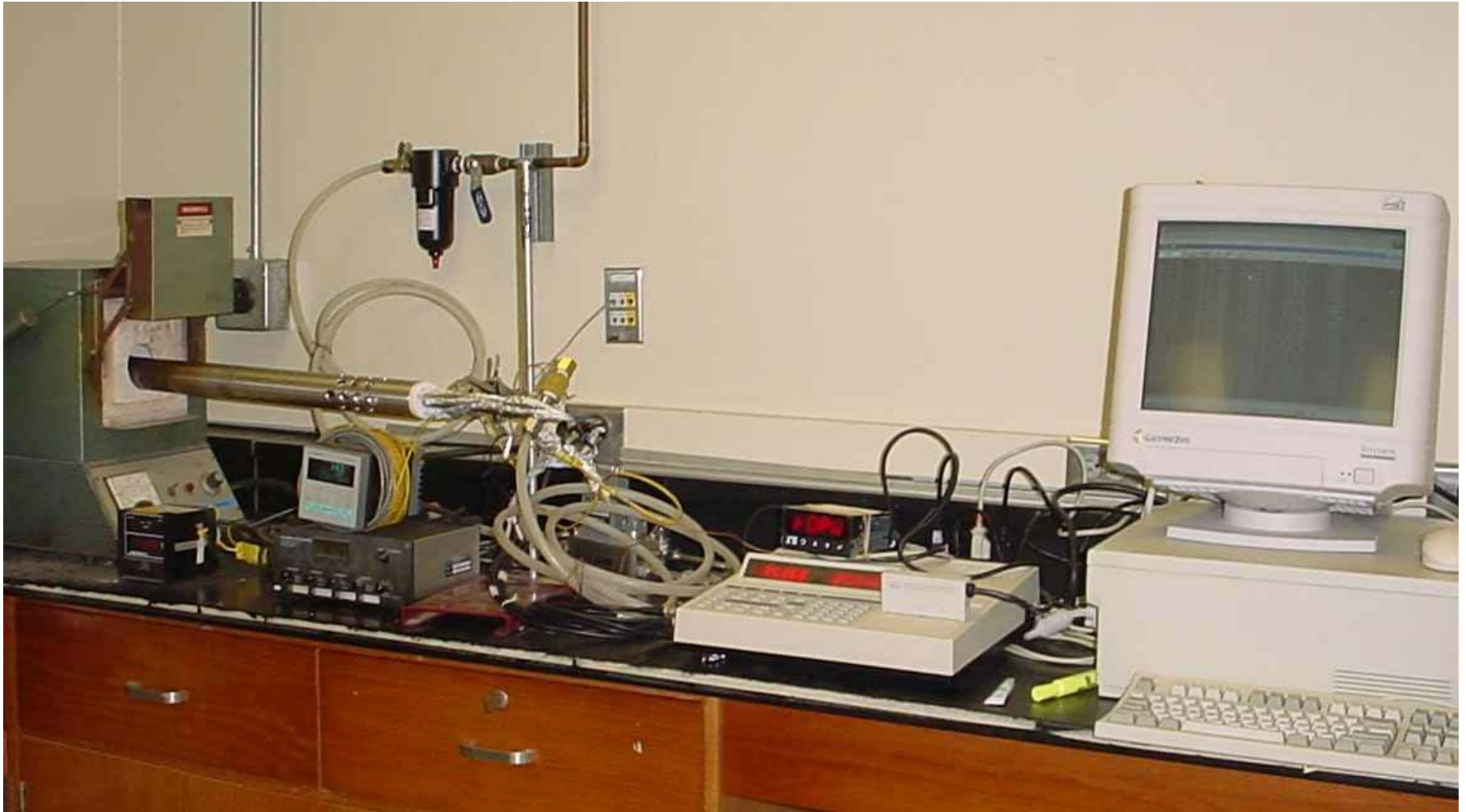
DC Sputtering System



Wedge-shaped Coating

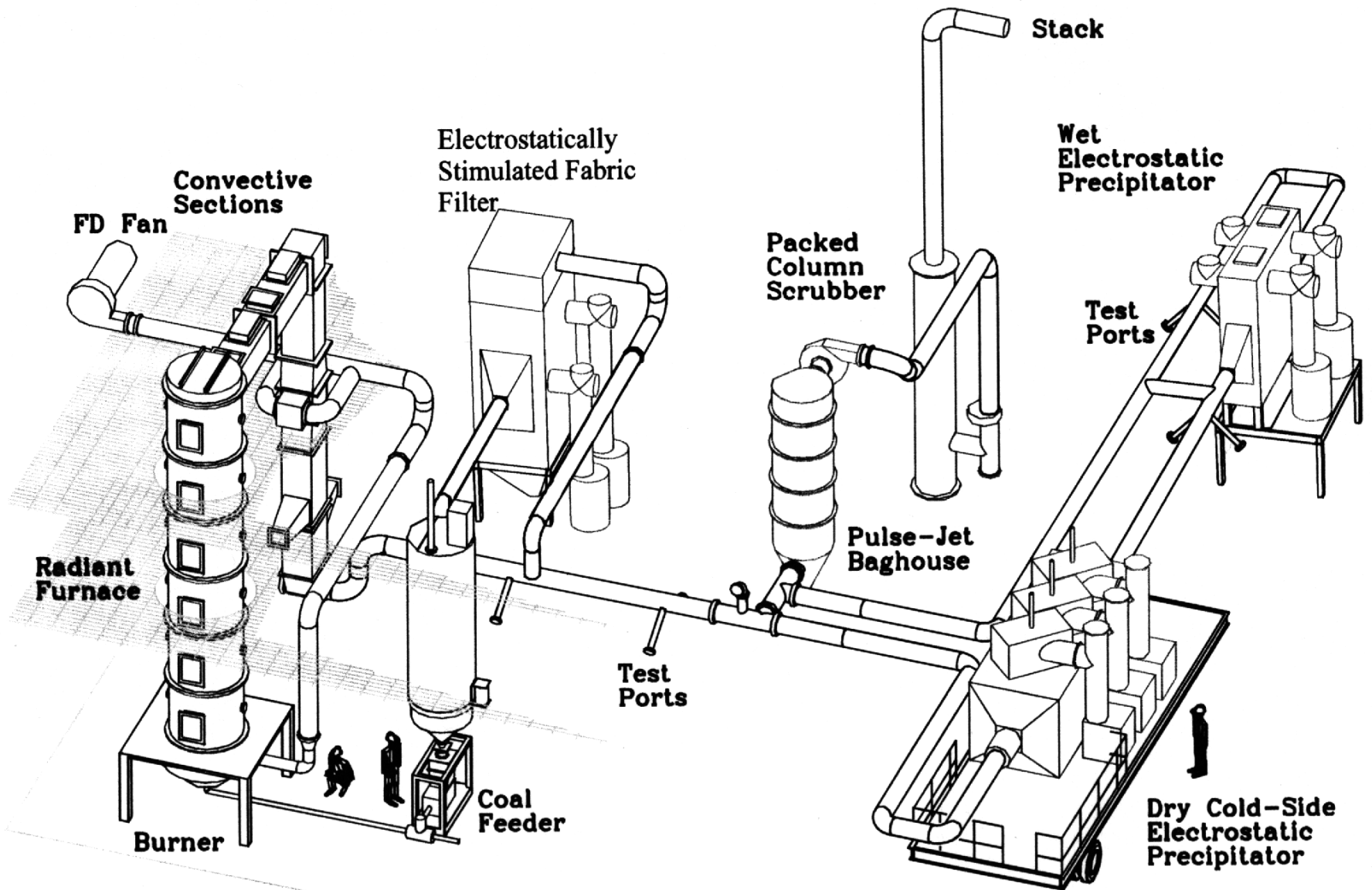


Laboratory Setup



SOUTHERN RESEARCH COMBUSTION RESEARCH FACILITY

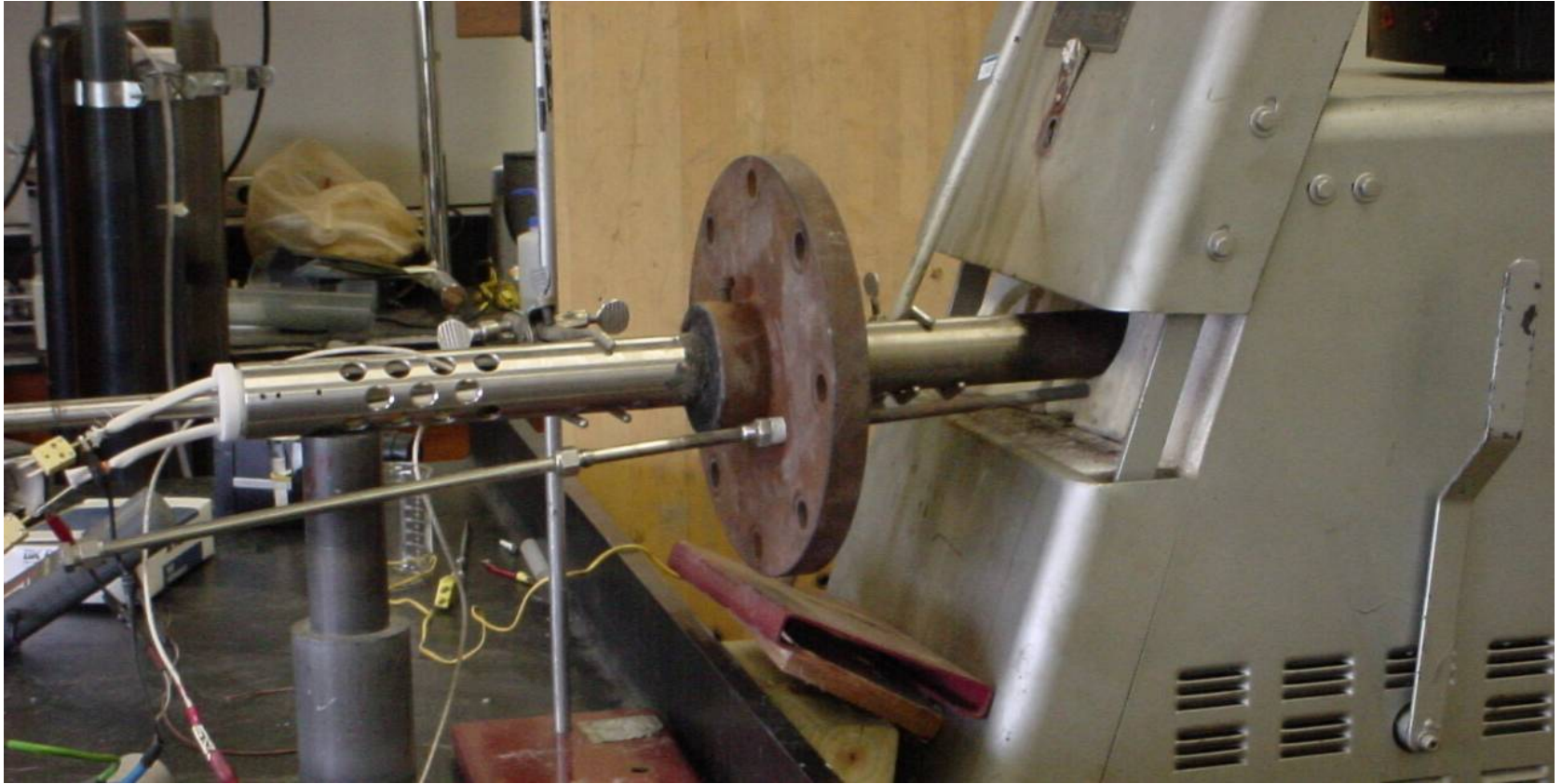
Birmingham, AL



Corrosion Probe at SRI ombustor



Probe Picture



Plant Gadsden, Switchgrass Co-Firing



Corrosion probe & Sensor Assembly



Plant Measurement



0 hr



72 hrs



168 hrs

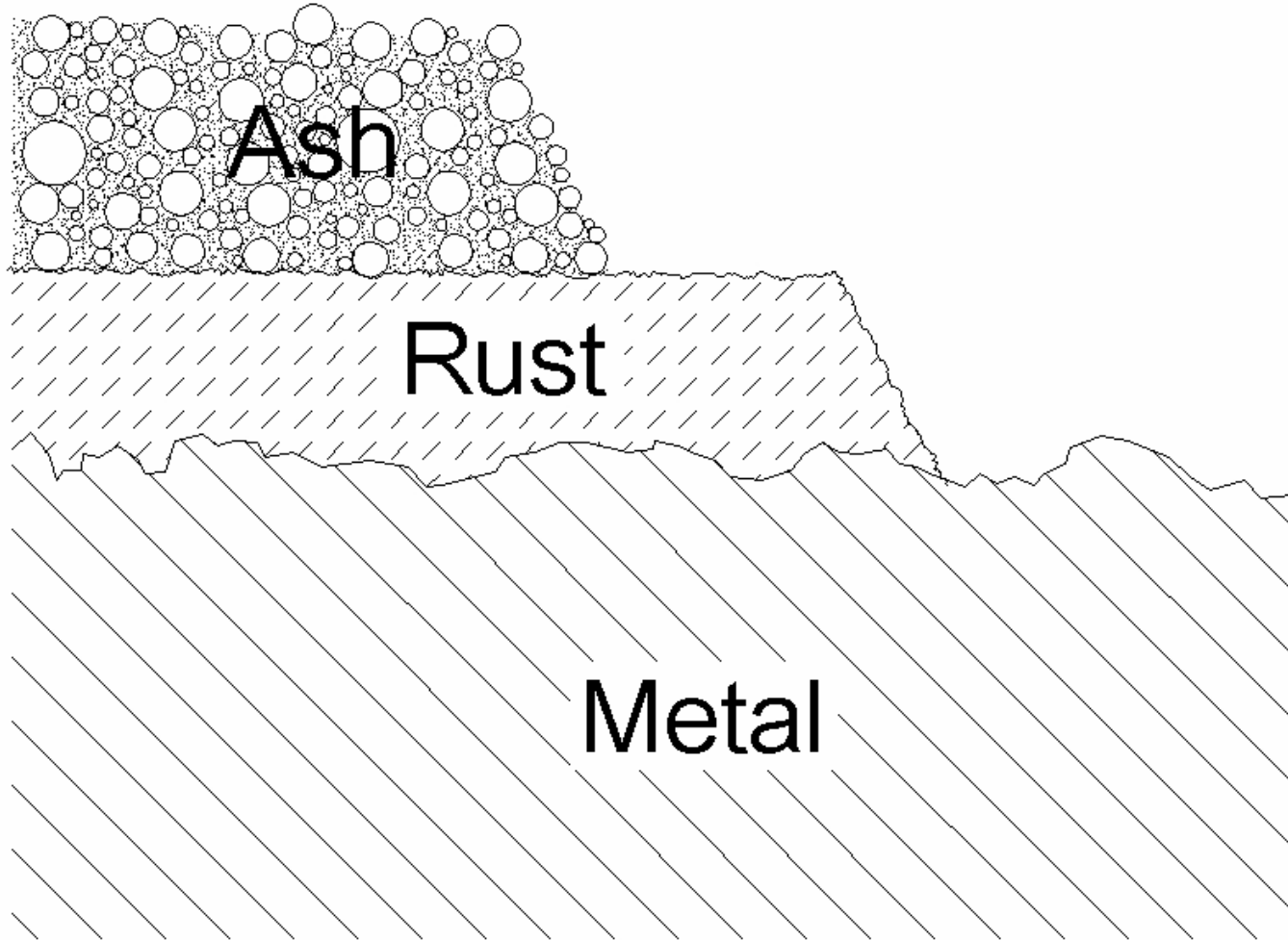


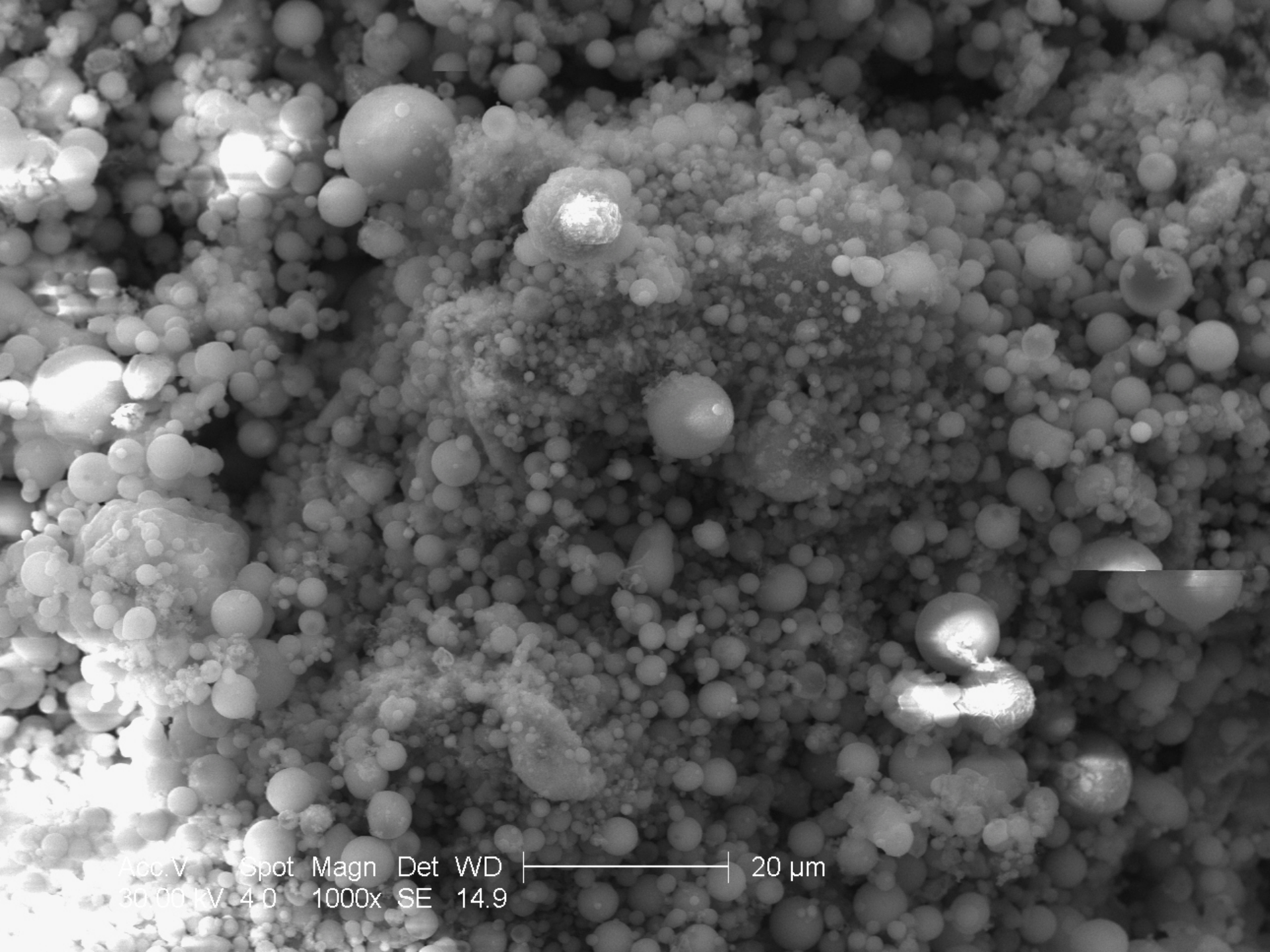
240 hrs

Probe after experiment



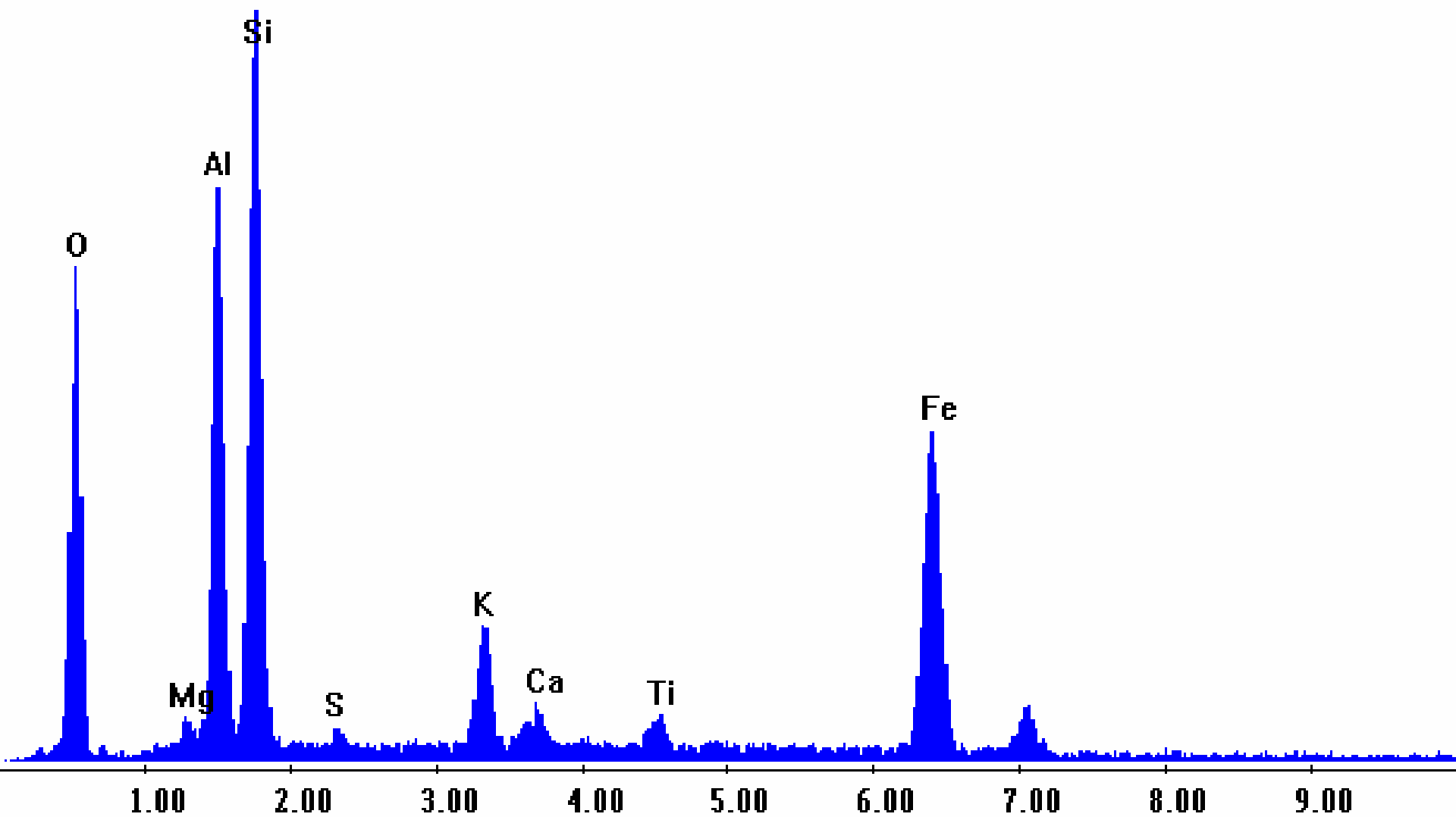
Layers on Metal Surface





Acc.V Spot Magn Det WD |-----| 20 μm
30.00 kV 4.0 1000x SE 14.9

Label A:



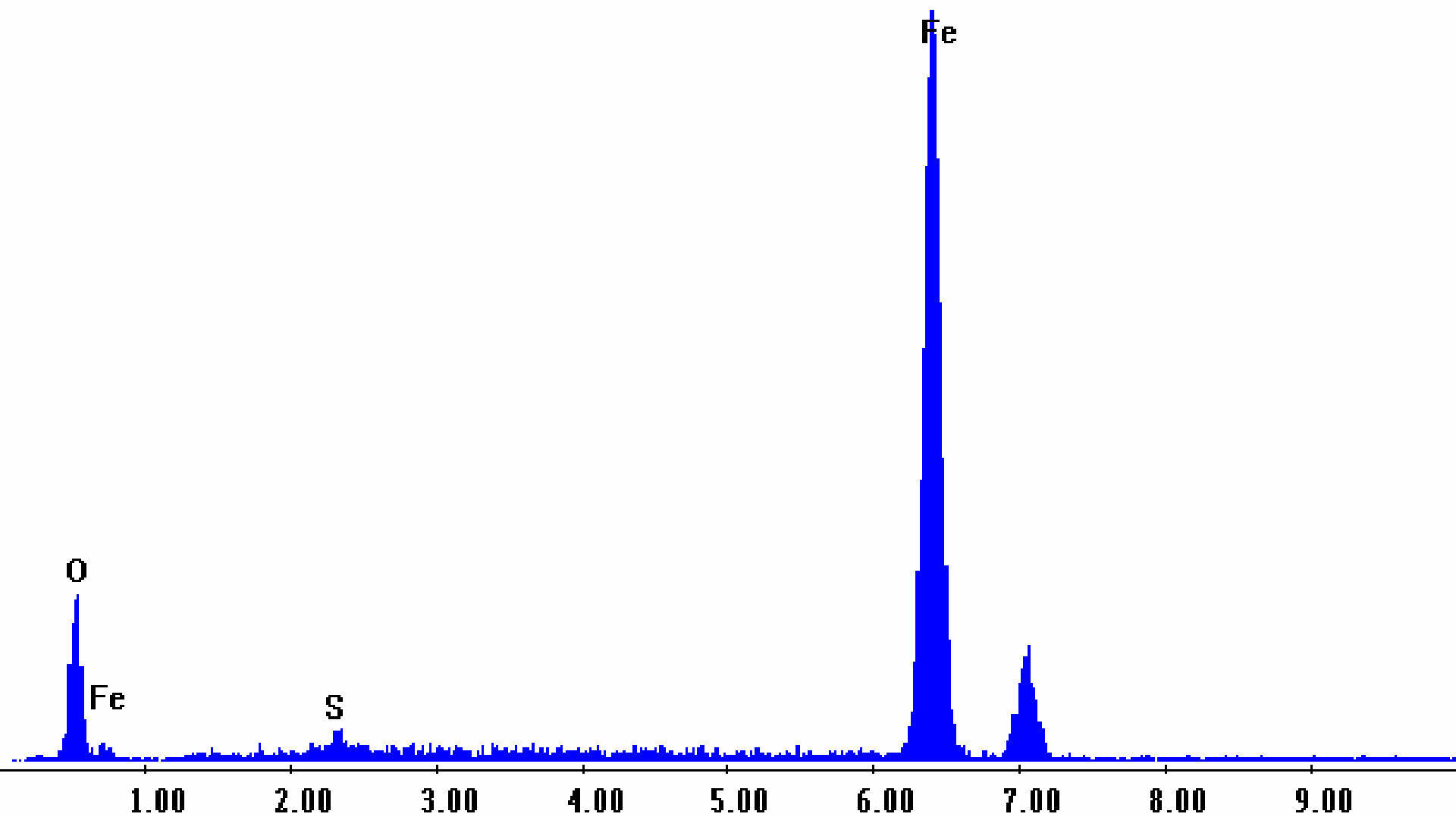
Lower
Substrate

Upper
Substrate

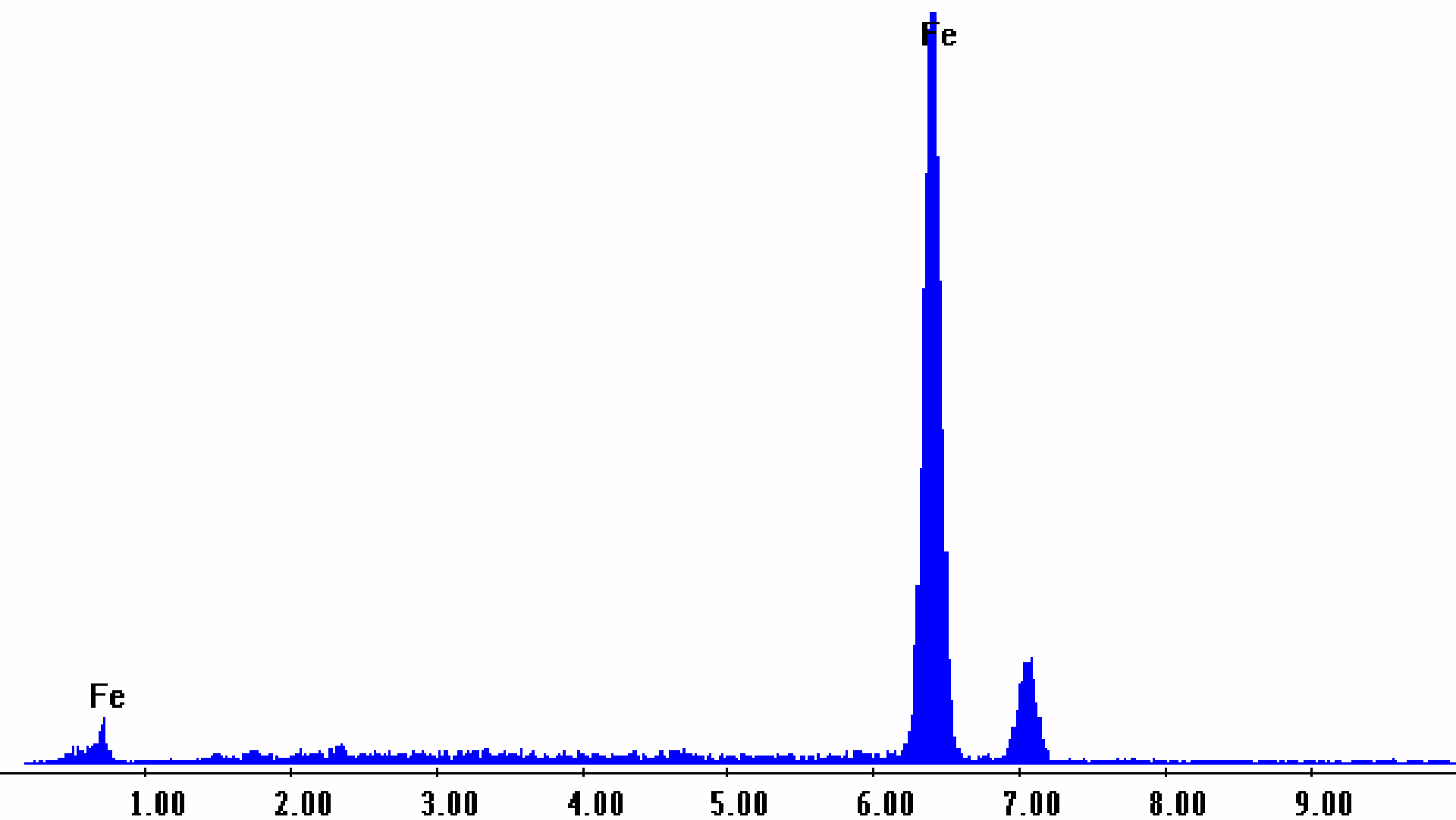
Acc.V Spot Magn Det WD |-----| 50 μ m
30.00 kV 4.0 500x SE 8.3

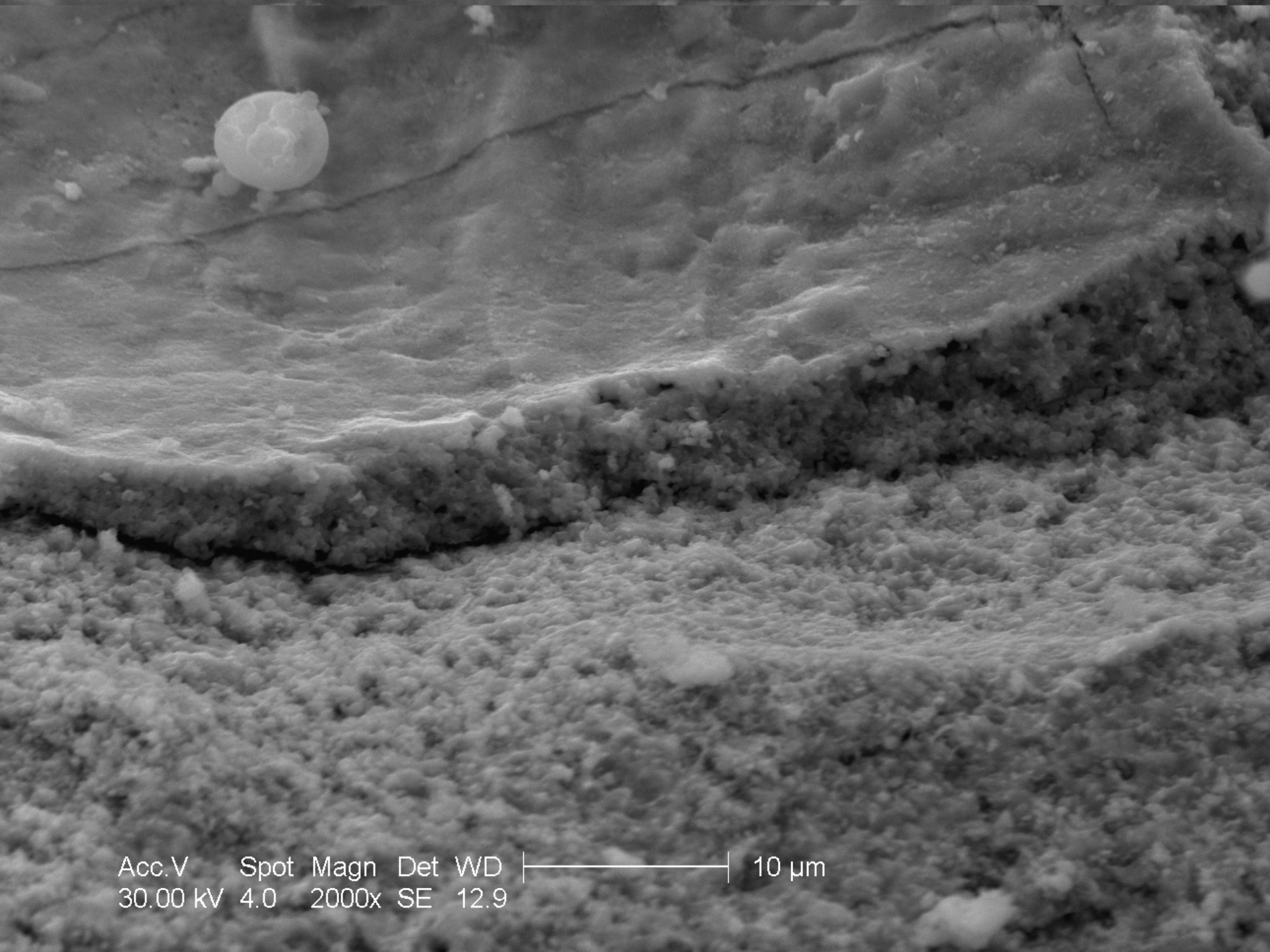
SEM Image of Waterwall Coal #2 Area 2

Label A:

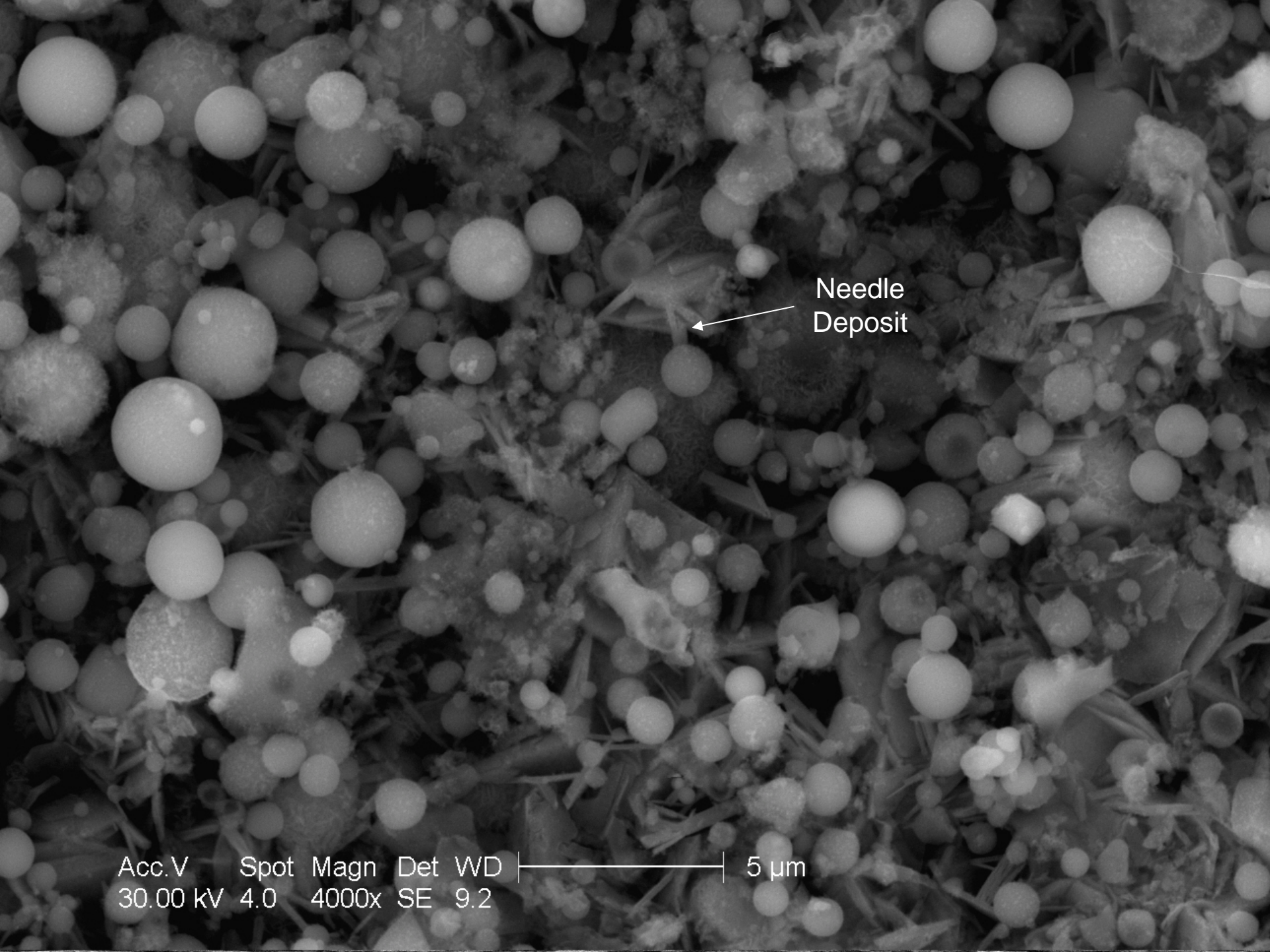


Label A:





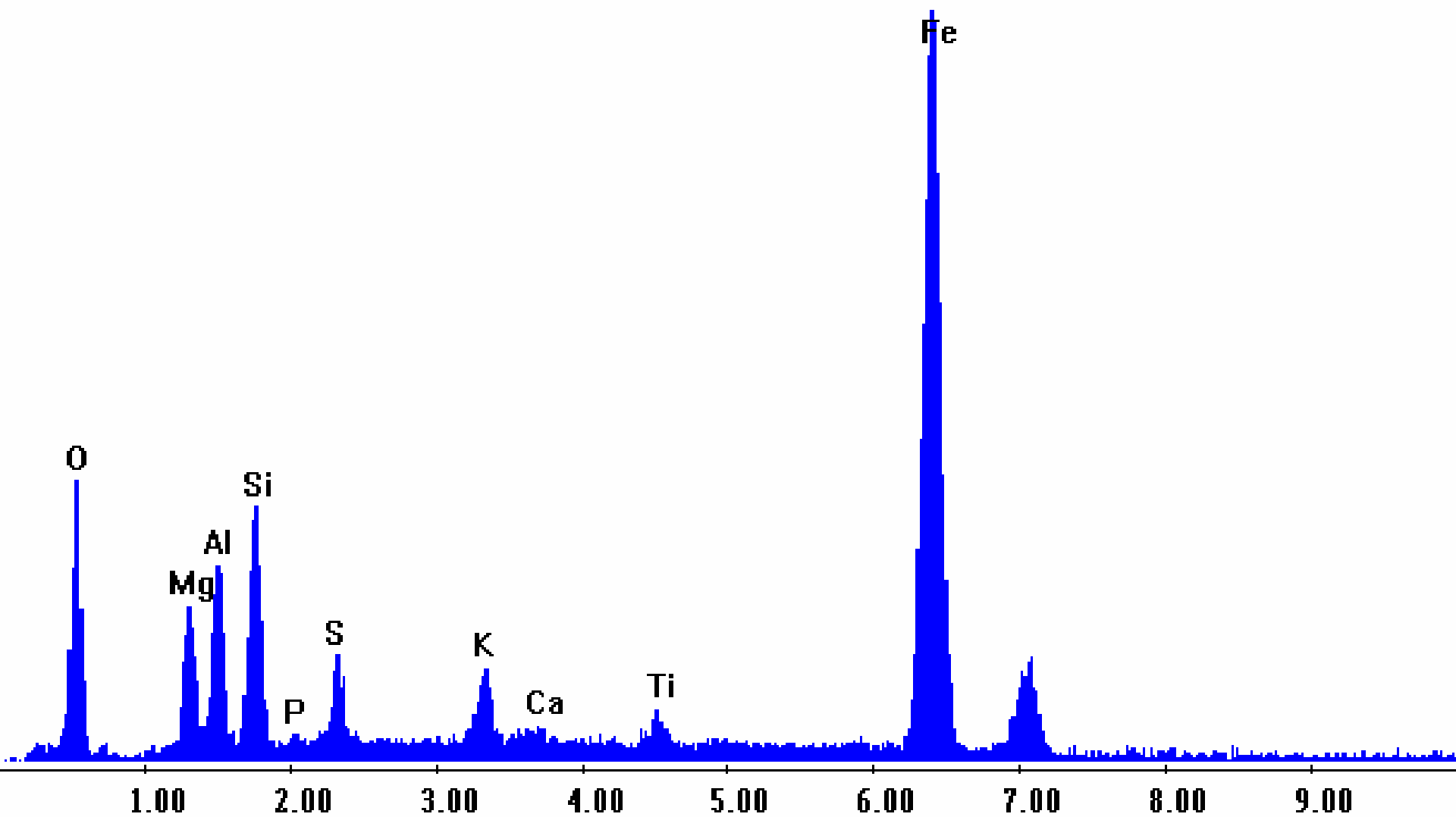
Acc.V Spot Magn Det WD |-----| 10 μ m
30.00 kV 4.0 2000x SE 12.9

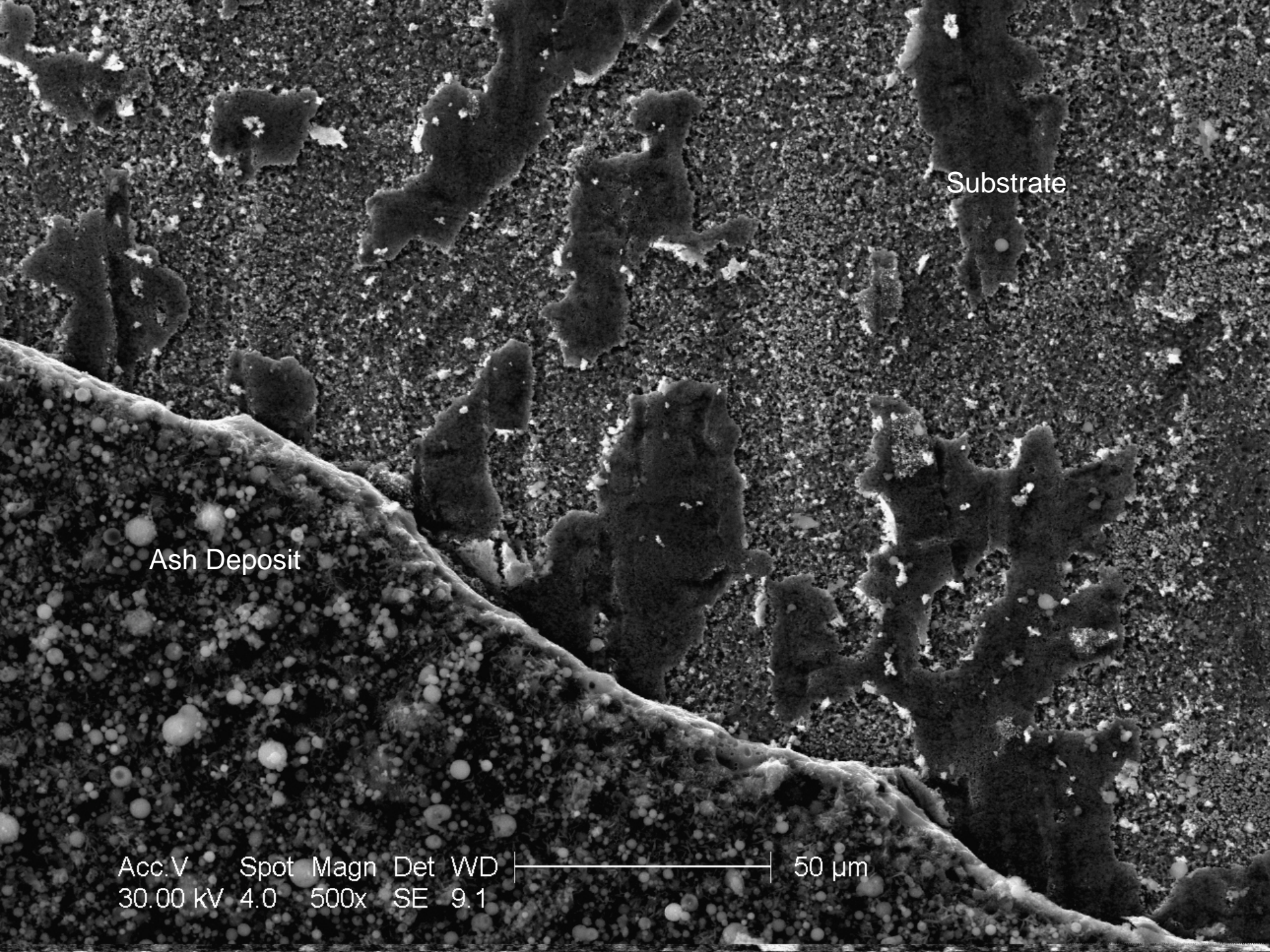


Needle
Deposit

Acc.V Spot Magn Det WD |-----| 5 μ m
30.00 kV 4.0 4000x SE 9.2

Label A:



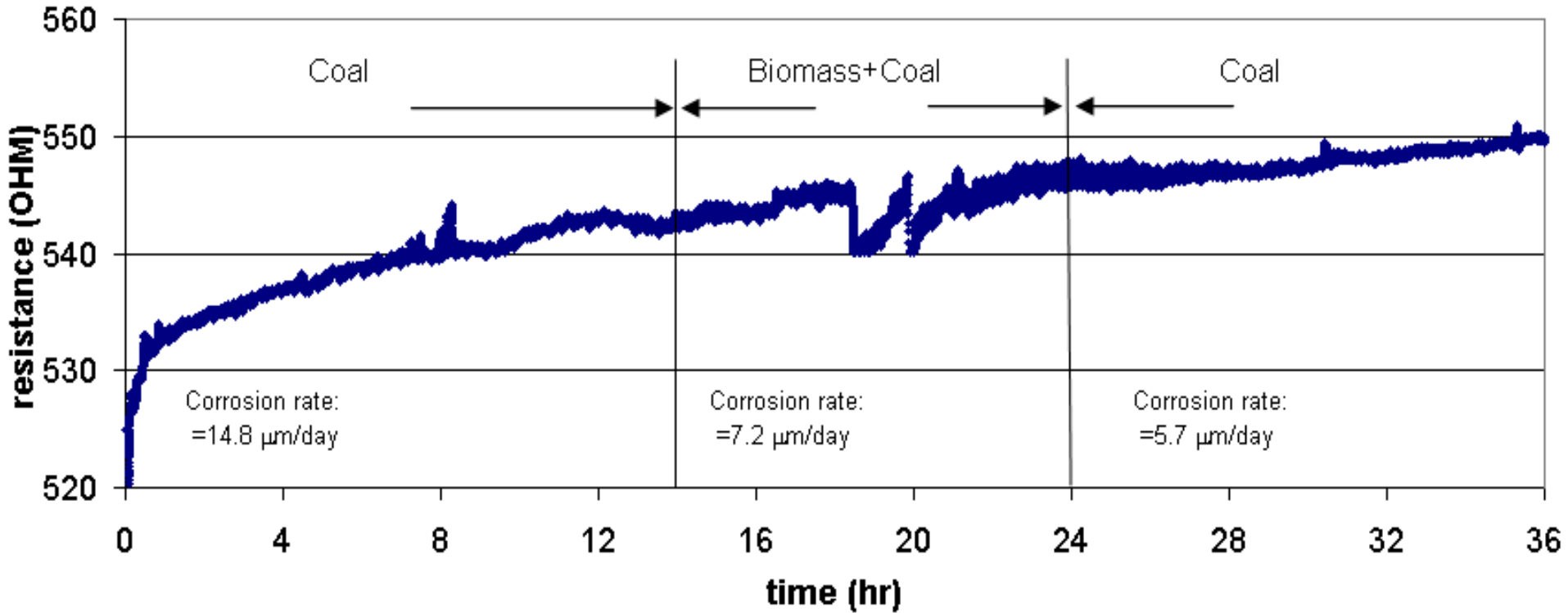


Substrate

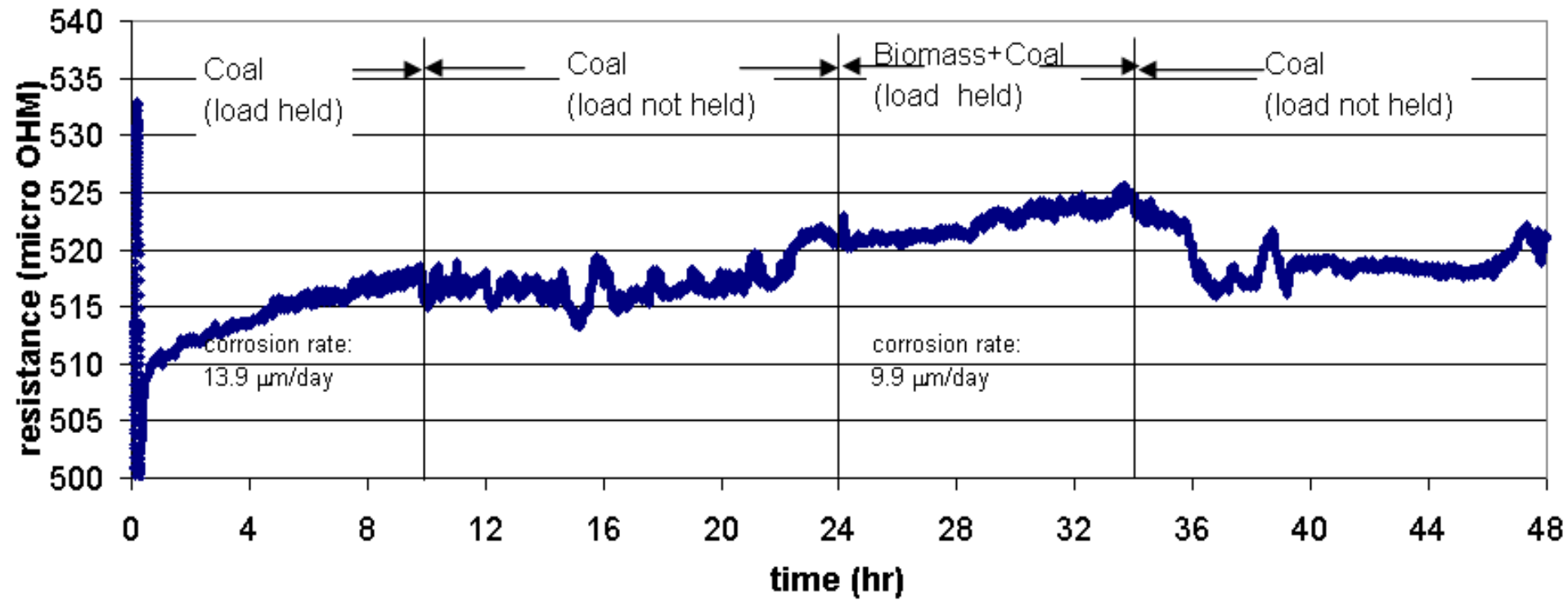
Ash Deposit

Acc.V Spot Magn Det WD |-----| 50 μ m
30.00 kV 4.0 500x SE 9.1

Sensor Resistance Data



Repeat Run



Result Summary

Location	Fuel sequence	Steam (lb/h)	Corrosion rate ($\mu\text{m}/\text{day}$)	
			100% Coal	Biomass
Superheater	100% coal Biomass+coal 100% coal	530,000	14 (0-10 hr)	9.9 (24-34 hr)
Superheater	100% coal Biomass+coal 100% coal	530,000	15 (0-14 hr) 5.7 (24-40 hr)	7.2 (14-24 hr)
Superheater	Biomass+coal	530,000		27 (1-6.5 hr)
Superheater	Biomass+coal	530,000		28 (1-7hr)
Waterwall	100% coal	320,000	7.2 (0-20hr)	
Waterwall	Biomass+coal 100% coal	530,000	9.1 (10-24 hr)	
Waterwall	100% coal Biomass+coal 100% coal	530,000	17* (0-14 hr) 11(32-72 hr)	

Conclusions

- The ER probe can be used to determine corrosion in short measurement period.
- The corrosion rates for biomass co-firing and coal were measured.
- The differences between biomass and coal corrosion are still to be understood.
- More testing is needed to validate data.

Questions?

E. C. Gaston Steam Plant

